AD-A128 941 MAGNETOFERROELECTRICS DIVERTABLE FERROELECTRICS AND PYROELECTRIC GLASS CE..(U) PENNSYLVANIA STATE UNIV UNIVERSITY PARK MATERIALS RESEARCH LA.. 1/1

UNCLASSIFIED A G HALLIYAL ET AL. 28 FEB 83 F/G 20/3. NL

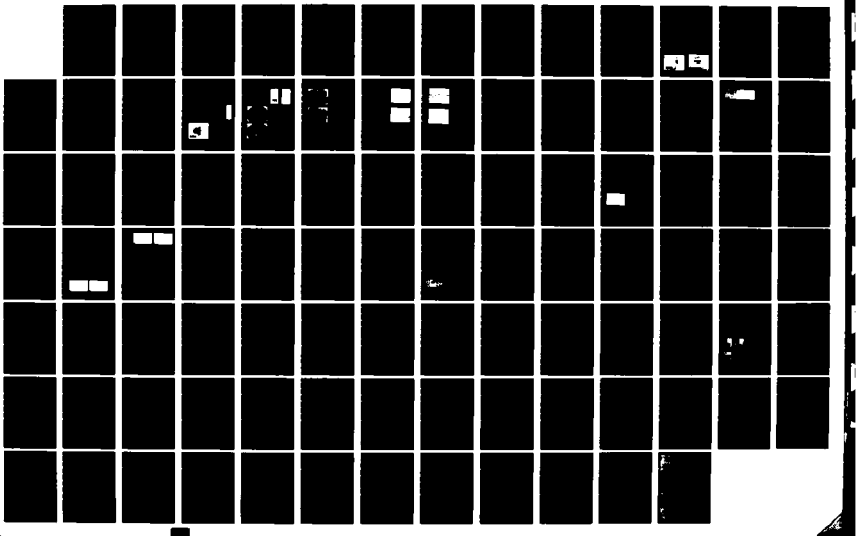

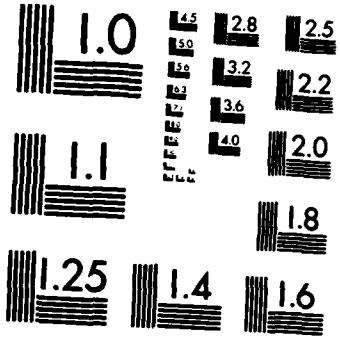

Magnetoferroelectrics, Divertable Ferroelectrics and Pyroelectric Glass-Ceramics

Final Report

A. G. Halliyal, R. E. Newnham, L. E. Cross and A. S. Bhalla

February 28, 1983

U. S. Army Research Office

Contract No. DAAG29-80-C-0008

Materials Research Laboratory
The Pennsylvania State University
University Park, Pennsylvania 16802

THE MATERIALS RESEARCH LABORATORY

THE PENNSYLVANIA STATE UNIVERSITY

UNIVERSITY PARK, PENNSYLVANIA

SECURITY CLASSIFICATION OF THIS PAGE *(When Data Entered)*

REPORT DOCUMENTATION PAGE

READ INSTRUCTIONS BEFORE COMPLETING FORM

1. REPORT NUMBER	2. GOVT ACCESSION NO. AD-A128 941 / 3. RECIPIENT'S CATALOG NUMBER
4. TITLE *(and Subtitle)* Magnetoferroelectrics, Divertable Ferroelectrics and Pyroelectric Glass-Ceramics	5. TYPE OF REPORT & PERIOD COVERED Final 6. PERFORMING ORG. REPORT NUMBER
7. AUTHOR(s) A. G. Halliyal, R. E. Newnham, L. E. Cross, A. S. Bhalla	8. CONTRACT OR GRANT NUMBER(s) DAAG29-80-C-0008
9. PERFORMING ORGANIZATION NAME AND ADDRESS Materials Research Laboratory The Pennsylvania State University University Park, Pennsylvania 16802	10. PROGRAM ELEMENT, PROJECT, TASK AREA & WORK UNIT NUMBERS
11. CONTROLLING OFFICE NAME AND ADDRESS U.S. Army Research Office Post Office Box 12211 Research Triangle Park, NC 27709	12. REPORT DATE February 28, 1983 13. NUMBER OF PAGES
14. MONITORING AGENCY NAME & ADDRESS*(if different from Controlling Office)*	15. SECURITY CLASS. *(of this report)* 15a. DECLASSIFICATION/DOWNGRADING SCHEDULE

16. DISTRIBUTION STATEMENT *(of this Report)*

Approved for public release; distribution unlimited.

17. DISTRIBUTION STATEMENT *(of the abstract entered in Block 20, if different from Report)*

18. SUPPLEMENTARY NOTES

THE VIEW, OPINIONS, AND/OR FINDINGS CONTAINED IN THIS REPORT ARE THOSE OF THE AUTHOR(S) AND SHOULD NOT BE CONSTRUED AS AN OFFICIAL DEPARTMENT OF THE ARMY POSITION, POLICY, OR DECISION, UNLESS SO DESIGNATED BY OTHER DOCUMENTATION.

19. KEY WORDS *(Continue on reverse side if necessary and identify by block number)*

Magnetoferroelectric, Piezoelectrics, Glass-Ceramics, Shape Memory, Pyroelectricity.

20. ABSTRACT *(Continue on reverse side if necessary and identify by block number)*

During the past three years the major topics on which work was carried out under the above contract are (1) grain oriented glass-ceramics for piezoelectric and pyroelectric devices; (2) shape memory effect in PLZT ceramics, and (3) magnetoferroelectric effect.

Several glass-ceramic compositions were developed which showed a high figure of merit for application in pyroelectric devices. They are also good

DD FORM 1 JAN 73 1473 EDITION OF 1 NOV 65 IS OBSOLETE

SECURITY CLASSIFICATION OF THIS PAGE *(When Data Entered)*

candidate materials for piezoelectric resonators, and surface acoustic wave devices. In the report, the compositions, processing methods and advantages of glass-ceramics over single cyrstals for use in devices are classified at length. A connectivity model was developed for the prediction of piezoelectric and pyroelectric properties of multicomponent glass-ceramics.

Shape-memory effect in metals and alloys is a well known phenomenon. It is the recovery of a plastically deformed material to its original shape by heating. Under the above program, shape-memory effect in PLZT ceramics was investigated.

Another highlight of the past three years was the discovery of a new class of ferroelectric materials possessing a magnetically induced ferroelectricity called 'magnetoferroelectricity'. A magnetoferroelectric develops a reversible spontaneous electric polarization on passing through a magnetic phase transition. The effect was demonstrated in chromium chrysoberyl Cr_2BeO_4.

Table of Contents

A

1. Introduction

This report documents work carried out over the period July 1, 1979 to February 28, 1983, in the Materials Research Laboratory of the Pennsylvania State University under Contract No. DAAG29-80-C-0008. Our major accomplishments during the above contract period were:

(1) Development of a new family of grain oriented glass-ceramics with interesting piezoelectric and pyroelectric properties (Appendices 1 to 8).

(2) Investigation of shape memory effect in PLZT ceramic samples (Appendices 9 to 10).

(3) Discovery of a new type of ferroelectricity, called magnetoferroelectricity and demonstration of the effect on Cr_2BeO_4.

A brief description of work on these topics is given below highlighting the more important features of the work. A full description of the work can be found in appendices which comprises of published or submitted papers on the above topics.

2. Polar Glass-Ceramics

During this program, several glass-ceramic compositions have been developed with useful piezoelectric and pyroelectric properties. All the glass-ceramics selected for the present study were non-ferroelectric. Major effort was devoted to optimizing the composition and processing variables to obtain glass-ceramics with reproducible properties and good mechanical strength. Appendices 1 to 8 contain the work done on piezoelectric and pyroelectric properties of these polar glass-ceramics.

These glass-ceramics with oriented crystallites were prepared by crystallizing glasses of suitable composition in a strong temperature gradient.

Initially x-ray diffraction and microstructure studies were performed to evaluate the degree of preferred orientation of the crystalline phases in the recrystallized glass-ceramic samples.

Our initial work showed the possibility of obtaining a glass-ceramic containing oriented crystallites of $Li_2Si_2O_5$ crystalline phase, by surface crystallization of Li_2O-$2SiO_2$ glasses. These samples showed encouraging pyroelectric response. However, mechanical strength and physical integrity of the samples was a problem with glass-ceramics belonging to Li_2O-SiO_2 system. Efforts were made to improve the properties of glass-ceramics in this system by adding modifying oxides such as ZnO or B_2O_3. We succeeded in obtaining glass-ceramics with both good physical properties and improved pyroelectric and piezoelectric properties. In particular lithium borosilicate glass-ceramics gave excellent results (Appendix 7).

During the later part of the program, several compositions of fresnoite ($Ba_2TiSi_2O_8$), its germanium analogue ($Ba_2TiGe_2O_8$) and their modifications were studied. Several substituents were tried for Ba and Ti sites.

For application in pyroelectric detectors, a commonly-used figure of merit is p/K where p is the pyroelectric coefficient and K is dielectric constant. The pyroelectric coefficient of lithium borosilicate and fresnoite glass-ceramics are in the range 8-12 $\mu C/m^2{}^\circ K$ and dielectric constants are in the range 5-15. Hence, a high value of p/K can be achieved even though the pyroelectric coefficients are relatively low compared to ferroelectric materials. The figure of merit of glass-ceramics giving the best regults to date are 50% of that of widely-used pyroelectric materials such as $LiTaO_3$.

Glass-ceramics with similar compositions were also found to be good candidate materials for piezoelectric resonators. The piezoelectric and electromechanical properties of these glass-ceramics are summarized in Appendix 5.

From the present study it is clear that a wide range of piezoelectric properties can be realized by appropriate modification of the composition of glasses.

A connectivity model was developed for the prediction of piezoelectric and pyroelectric properties of multicomponent glass-ceramics containing crystallites of several crystalline phases. The possibility of tailoring both the piezoelectric and pyroelectric properties has been explored by modifying the composition of parent glasses (Appendix 8). Lithium borosilicate and fresnoite glass-ceramics look to be promising materials for surface acoustic wave devices. Several industries have already expressed interest in carrying out further tests on the glass-ceramics for SAW devices.

In summary, our present work on polar non-ferroelectric glass-ceramics shows that these materials are potential candidate materials for both pyroelectric detectors and piezoelectric resonators. In device applications glass-ceramics offer several advantages over single crystal materials. Large area targets can be prepared at much lower cost. The problem of depoling and aging commonly encountered in all ferroelectric materials will be avoided in these materials since they are not ferroelectric. The pyroelectric and piezoelectric properties of these materials extend to very high temperatures.

3. Shape-Memory Effect

The recovery of a plastically deformed material to its original shape by heating is called shape-memory effect. This effect has been extensively studied in metallic alloys and is generally associated with martensitic phase transformations. Phase transformations in ferroelectric materials are not martensitic, but apparently similar effects have been observed in PLZT ceramics as part of this contract.

In order to understand the mechanisms responsible for shape-memory effect in PLZT ceramics more detailed studies have been carried out. In the present

study, the shape-memory effect in PLZT (Lead Lanthanum Zirconate Titanate) ceramics with composition x/65/35 ($4.0 \leq x \leq 8.0$) was investigated using bending experiments and temperature cycling. Relationships between load and the degree of bending, together with their temperature dependence, were determined, and characteristic temperatures associated with the onset and disappearance of the pseudo-plastic shape change were compared with the observed dielectric anomalies. Effects of mechanical stress and electric field on the shape-memory temperatures and the magnitude of strain were investigated. From these studies it was concluded that domain alignment and the temperature-dependence of spontaneous strain are important factors governing the shape-memory effect in ferroelectrics. Preferred-orientation effects were confirmed by X-ray diffraction analysis. Appendices 9 and 10 summarize the work on shape-memory effect, done during the present period.

4. Magnetoferroelectrics

One of the accomplishments during this period has been the discovery of a new class of ferroelectric material possessing a magnetically induced ferroelectricity which has been called 'magnetoferroelectric'. This effect was predicted on the basis of symmetry arguments and was experimentally confirmed in chromium chrysoberyl Cr_2BeO_4 (Appendix 11).

A magnetoferroelectric develops a reversible spontaneous electric polarization on passing through a magnetic phase transition. This effect was demonstrated in Cr_2BeO_4 which undergoes a phase transition from a centric paramagnetic state to a complex antiferromagnetic state at 28°K. It was shown that ceramic samples can be poled electrically below the transition temperature to a remnant polarization about five orders of magnitude smaller than $BaTiO_3$. No ferroelectric anomaly is observed at Tc, but both the remnant polarization and the pyroelectric coefficient can be reversed in sign with a poling field.

Appendix 1

Pyroelectric Glass-Ceramics

G. J. Gardopee, R. E. Newnham, A. G. Halliyal. and A. S. Bhalla

Pyroelectric glass-ceramics

G. J. Gardopee, R. E. Newnham, A. G. Halliyal, and A. S. Bhalla
Materials Research Laboratory, The Pennsylvania State University, University Park, Pennsylvania 16802

(Received 18 February 1980; accepted for publication 4 March 1980)

Highly oriented surface layers of lithium disilicate crystals were grown by crystallizing glasses of composition $Li_2Si_2O_5$ in a temperature gradient. The polar *c* axes of the crystallites were oriented parallel to the temperature gradient and perpendicular to the sample surface. The pyroelectric response of the glass-ceramic crystallized in a thermal gradient was approximately four times larger than that of a touramaline crystal of similar dimensions. The time dependence of the pyroelectric signal obeys the thin-film equivalent circuit model developed by Chynoweth.

PACS numbers: 77.70. + a

In several glass systems where the crystallization processes of devitrification have been extensively studied, the crystalline phases have symmetries consistent with both pyroelectricity and piezoelectricity.[1-4] Electro-optic properties[2] and switching behavior[3] have been reported for glass-ceramics containing ferroelectric microcrystals of $BaTiO_3$, $NaNbO_3$, and $LiTaO_3$. Pyroelectricity in a ferroelectric sodium cadmium niobate glass-ceramics has recently been described by Layton and Smith.[5]

However, except for ferroelectric glass-ceramics, where piezoelectricity and pyroelectricity are induced by electric poling of the domain structure, little attention appears to have been given to other techniques for inducing a polar orientation texture. This study is concerned with lithium disilicate glass composition for which the equivalent crystalline forms are pyroelectric, but *not* ferroelectric. The glass-ceramic samples prepared in temperature gradients gave strong pyroelectric response and are, to the best of our knowledge, the first examples of nonferroelectric polar glass-ceramics.

For this study the stoichiometric composition $Li_2O{\cdot}2SiO_2$ (lithium disilicate) was selected. According to x-ray structure analysis,[6] crystalline $Li_2Si_2O_5$ belongs to orthorhombic space group *Ccc*2 (point group *mm*2). In the polar [001] direction, the crystals have a dielectric constant of about 7, and are not ferroelectric.

Rindone[7,8] has studied the crystallization of lithium disilicate glasses under isothermal conditions and observed a tendency for the crystallographic *c* axis to align perpendicular to the surface. The degree of orientation of the crystallites was assessed from x-ray diffraction patterns.

In our studies, glasses of composition $Li_2Si_2O_5$ were prepared by mixing reagent-grade silicic acid (J. T. Baker Chem. Co., Phillipsburg, NJ) and lithium carbonate (Fisher Scientific Co., Fair Lawn, NJ), followed by melting in a globar furnace. The melt was maintained at 1400 °C for 24 h for fining and homogenization. Transparent samples were obtained by pouring the melt into a graphite mold, after which the samples were annealed for 12 h at 400 °C. Polished samples in the form of thick disks were used for the crystallization studies. Crystallization was carried out in two ways: (i) Isothermal crystallization, in which the entire sample was uniformly heated to the crystallization temperature, typically 600 °C, and maintained at that temperature for one hour; and (ii) Thermal gradient crystallization, in which a temperature gradient was maintained across the sample. In this method the sample was placed on a hot stage and heated to 600 °C within five minutes, and the temperature increased slowly to 800 °C at a rate of 3 °C/min, followed by rapid cooling to room temperature.

The x-ray diffraction patterns of the samples crystal-

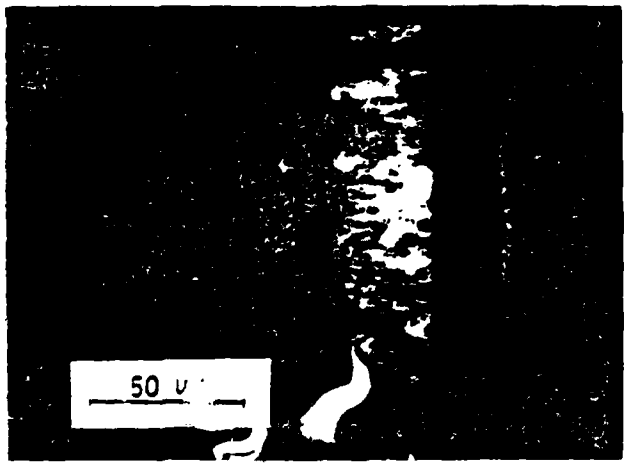

FIG. 1. Optical photomicrograph of sample crystallized by isothermal method (× 500).

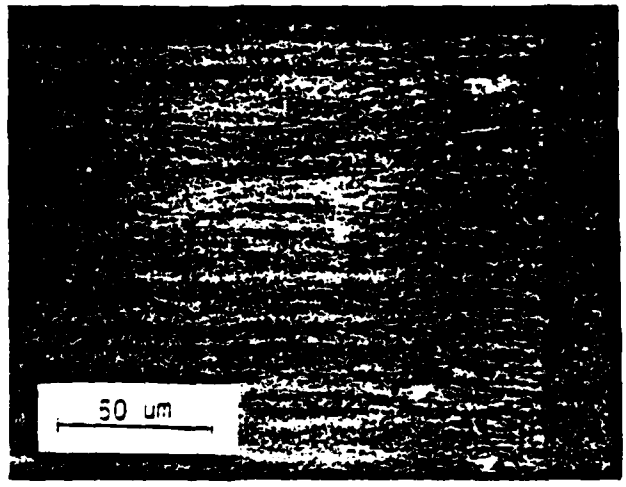

FIG. 2. Optical photomicrograph of sample crystallized by thermal gradient method (× 500).

 0003-6951/80/100817-02$00.50

lized by both methods showed highly oriented growth of crystallites at the surfaces, with the polar c axis perpendicular to the sample surface. The degree of orientation was almost perfect in the thermal gradient samples. Optical photomicrographs (Figs. 1 and 2) of polished cross sections showed that needlelike $Li_2Si_2O_5$ crystals form at the surface of the sample, prior to nucleation and crystallization of spherulites in the interior. The thickness of the oriented surface layers can be controlled by varying the preparation conditions and thermal treatment. Optimum thicknesses were obtained in samples crystallized under a thermal gradient.

Pyroelectric response of these samples was studied by the Chynoweth method.[9] The voltage response was measured at room temperature with a chopping frequency of 5 Hz. Carefully prepared samples with highly oriented surface layers 200–600 μ thick were studied. A large pyroelectric response was measured from the samples crystallized under thermal gradient. The pyroelectric signal measured by the Chynoweth experiment is indicative of the figure of merit $p/\epsilon\rho c$, where p is the pyroelectric coefficient, ϵ the dielectric permittivity, ρ the density, and c the specific heat of the sample. Using identical sample sizes and experimental conditions, the signals were compared with those obtained from tourmaline, which has similar ϵ, c, and ρ values. Tourmaline has a pyroelectric coefficient of about $4\,\mu C/m^2\,^\circ C$. The pyroelectric figure of merit of the lithium disilicate glass-ceramics were four times larger than tourmaline, but about an order of magnitude weaker than such commercial pyroelectrics as lithium tantalate ($p = 190\,\mu C/m^2\,^\circ C$).

The response from isothermally prepared samples was about ten times smaller than thermal gradient samples, reflecting the enhanced polarity of the samples prepared in a thermal gradient. Further improvement in the pyroelectric response is anticipated by reducing the thickness to very thin platelet form. The mechanical fragility of the specimens makes this somewhat difficult.

The waveforms of the pyroelectric response of lithium disilicate and lithium tantalate were studied at chopping frequencies of 5 and 0.5 Hz. In both cases, it was observed that the voltage rises to a maximum when the light was turned on and begins to decay with time. The voltage reverses when the light is turned off and again decays. The measured time dependence of the glass-ceramic pyroelectric responses obeys the thin-layer equivalent circuit model developed by Chynoweth.[10] In this model it is assumed that the pyroelectric signal originates in a thin layer adjacent to the surface, and that the signal is capacitively coupled through the nonpyroelectric bulk of the sample. Reasonably good agreement between this model and the observed behavior confirms that the pyroelectric signals in lithium disilicate originate in the highly oriented surface layers.

Although the magnitude of the signals generated by the $Li_2Si_2O_5$ glass-ceramics are small compared to currently used ferroelectric pyroelectric detector materials, these samples are the first example of a nonferroelectric pyroelectric glass-ceramic. The process for making these new pyroelectric materials is amenable to mass production.

We wish to thank our colleagues at the Materials Research Laboratory for their advice and assistance. This work was sponsored by Defense Advanced Research Projects Agency (Contract DARPA Project No. P-15124-MS) and by the U. S. Army Office of Research and Development (Contract Grant No. DAAG29-78-0033).

[1] A. Herzog, J. Am. Ceram. Soc. 47, 107 (1964).
[2] N. F. Borrelli and M. M. Layton, J. Non Cryst. Solids. 6, 197 (1971).
[3] N. F. Borrelli and M. M. Layton, IEEE Trans. Electron. Devices ED-16, 511 (1969).
[4] A. M. Glass, M. E. Lines, K. Nassau, and J. W. Shiever, Appl. Phys. Lett. 31, 4 (1977).
[5] M. M. Layton and J. W. Smith, J. Am. Ceram. Soc. 58, 435 (1975).
[6] F. Liebau, Acta Crystallogr. 14, 389 (1961).
[7] G. E. Rindone, in *Proceedings of the Symposium on Nucleation and Crystallization in Glasses and Melts*, edited by M. K. Roser, G. Smith, and H. Insley (American Ceramic Society, Columbus, O., 1962), pp. 63–69.
[8] G. E. Rindone, J. Am. Ceram. Soc. 45, 7 (1962).
[9] A. G. Chynoweth, J. Appl. Phys. 27, 78 (1956).
[10] A. G. Chynoweth, Phys. Rev. 102, 705 (1956).

Appendix 2

Pyroelectric $Li_2Si_2O_5$ Glass-Ceramics

G. J. Gardopee, R. E. Newnham and A. S. Bhalla

PYROELECTRIC $Li_2Si_2O_5$ GLASS-CERAMICS

G. J. GARDOPEE†, R. E. NEWNHAM and A. S. BHALLA

Materials Research Laboratory, The Pennsylvania State University, University Park, Pennsylvania 16802

(Received August 6, 1980; in final form January 6, 1981)

Highly oriented surface layers of lithium disilicate crystals were grown by crystallizing glasses of the composition Li_2O: SiO_2. The thickness of the oriented layer was a function of the thermal treatment. The crystallites in these layers were oriented with their *c*-axes perpendicular to the sample surface. These layers were found to be pyroelectric as determined by the Chynoweth technique. The pyroelectric responses of the glass-ceramics crystallized in a thermal gradient were approximately four times larger than that of a tourmaline crystal of similar dimensions.

1 INTRODUCTION

The improvement of existing pyroelectric materials and the development of new pyroelectric materials with properties that are superior to those materials which are currently used, have been the goal of much of the research in the field of pyroelectrics. In the area of vidicon targets, these efforts have led to the development of deuterated triglycine fluoroberyllate (DTGFB). The ferroelectric crystals such as TGS and DTGFB require careful preparation and are subject to performance degradation due to depoling. The object of the present work was to crystallize a non-ferroelectric pyroelectric phase from a relatively simple oxide glass in a manner which would yield a composite with a pyroelectric response of a useful magnitude.

The concept of crystallizing an electrically active phase from an oxide glass has been employed in the past by the electronic materials industry. Extensive research at Corning Glass Works was directed towards developing a glass system from which $BaTiO_3$ could be crystallized to yield a high permittivity glass ceramic.[1]

Electro-optic effects have been reported in glass-ceramics containing sodium niobate.[2] The optical properties of glasses containing crystallites of both sodium potassium niobate and barium titanate were studied for possible use as optical switching elements.[3]

Layton and Smith[4] reported pyroelectricity in glass-ceramics in which the crystalline phase was ferroelectric. In this study, glasses containing crystals of $Na_{0.9}Cd_{0.5}NbO_3$ were poled. Reversible polarization and pyroelectricity were measured in their samples.

Reversible pyroelectricity has been reported in lithium niobate and lithium tantalate glasses.[5] This effect was explained as the result of ferroelectricity in the glassy state, but the possibility of contributions from electrets could not be eliminated.

In the present work, lithium disilicate crystals were crystallized from glasses which had the composition of 33.3 mole % Li_2O and 66.6 mole % SiO_2.

1.1 The System Li_2O-SiO_2

The system Li_2O-SiO_2 was selected for study for a number of reasons. The crystallization behavior of these glasses is well known and has been thoroughly reported.[6]

Of the crystalline products in the glass-forming region, lithium disilicate was selected for study. Liebau reports the structure of lithium disilicate to be monoclinic in space group Cc and to have a strong orthorhombic pseudosymmetry. Unit cell dimensions with respect to the orthorhombic unit cell are $a = 5.82$ Å, $b = 14.66$ Å, and $c = 4.79$ Å. Liebau determined that the structure consists of corrugated Si_2O_5 layers held together by lithium ions. Projections of the tetrahedra onto the three orthogonal planes appear in Figure 1. The orthorhombic *c*-axis is the polar axis. A projection of the crystal structure onto the (100) plane is presented in Figure 2. These diagrams clearly show the acentric, polar nature of the structure along the *c*-axis.

† Present address: Perkin Elmer Corporation, 100 Wooster Heights Road, Danbury, CT 06810.

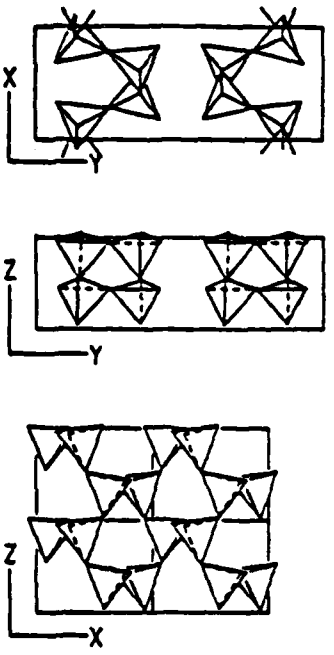

FIGURE 1 Arrangement of $(SiO_4)^{-4}$ tetrahedra in $Li_2Si_2O_5$.

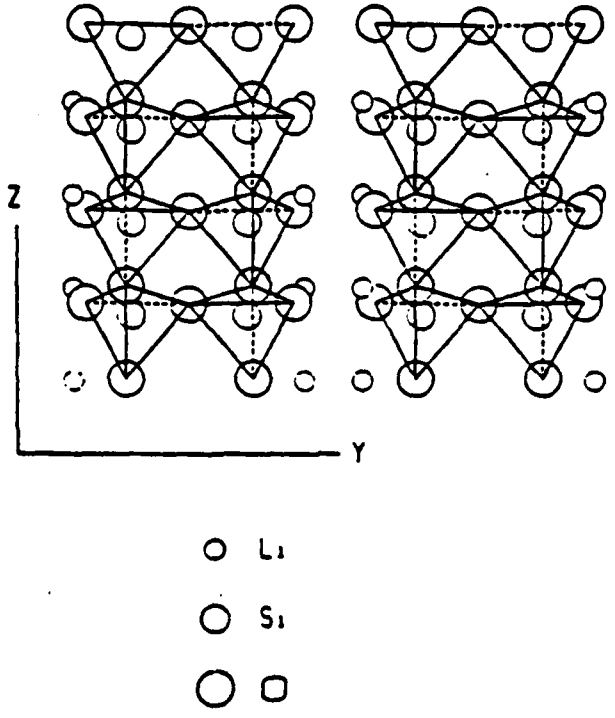

FIGURE 2 Projection of the structure of $Li_2Si_2O_5$ onto the (100) plane.

Single crystals of lithium disilicate would be expected to be both pyroelectric and piezoelectric in the *c*-direction. Attempts at growing single crystals have been made. These efforts result in bundles of needle-like crystals oriented with the *c*-axis parallel to the long direction of the crystallites. Optical examination shows that the crystallites are twinned on a very fine scale. Neither of the two possible polar directions of the *c*-axis is favored.[8] Because of the compensating effects of this extensive twinning, little or no pyroelectricity or piezoelectricity can be detected.

Crystals of lithium disilicate grown in glasses in the Li_2O-SiO_2 system have been shown to be highly oriented in thin layers near the surface of the glass.[9,10] These workers reported that the crystals in a thin layer near the surface have their *c*-axes perpendicular to the sample surface. The intention of the present work was to take advantage of this orientation phenomenon to produce a glass-ceramic in which the polar *c*-axis is aligned perpendicular to the sample surface. The mechanical interaction between the glass matrix and the crystallites might enhance the pyroelectric properties through the secondary effect.

2 EXPERIMENTAL

2.1 Sample Preparation

Reagent-grade acid and lithium carbonate were mixed in the proportions necessary to form glasses of composition $Li_2O:2SiO_2$. The mixture was melted in a platinum crucible in an electric furnace at temperatures in the range from 1400 to 1450°C for at least 24 hours. The fined glass was poured into graphite molds. The large residual stress from the rapid cooling was partially relieved by annealing for 12 hours at 400°C. Glass disks of varying thicknesses were produced by grinding and polishing the glass cylinders. Sample thicknesses ranged from approximately 130 micrometers to 5 millimeters.

Two general types of crystallization treatments were used. The treatment in which the entire sample was uniformly heated to the crystallization temperature will be termed "isothermal". Crystallization in which a thermal gradient is maintained in the samples will be termed "gradient" crystallization. The isothermally crystallized samples were crystallized in a small electric tube furnace. The samples were quickly heated to 600°C and held at that temperature for one hour. All samples were

cooled to room temperature from the crystallization temperature at a rate of approximately 100°C/minute.

The thermal gradient samples were prepared by polishing one end of a glass cylinder. The polished surface was placed on the heating element of a microscope hot stage. A small piece of platinum foil was placed between the heating element and the glass sample. The hot stage was heated to 600°C within 5 minutes to establish a thermal gradient across the sample. The temperature of the stage was increased to 800°C at the rate of 200°C/hour. The thermal gradient was estimated to be approximately 300°C/cm.

After cooling, the thermal gradient samples were thinned by grinding and polishing the cold end of the cylinders. X-ray and Chynoweth measurements were performed on the thin crystallized layer at the hot face of these samples.

At least one sample from each batch of glass was isothermally crystallized at 600°C and was ground to a powder. X-ray diffraction analyses were performed on a Picker diffractometer using CuK_α radiation. The patterns obtained were compared to standard patterns for phase identification.

To determine the degree of crystallite orientation in the samples, x-ray diffraction was performed on the as-crystallized surfaces. The relative peak heights from the crystallized samples were compared to the relative peak heights of the standard powder pattern to qualitatively evaluate the degree of orientation.

2.2 *Pyroelectric measurements*

The pyroelectric responses were determined at room temperature using a method described by Chynoweth.[11] Sputtered gold electrodes were applied to both sides of the sample. Fine gold wires were attached to the electrodes using an air-drying silver paste. Radiation from a light source is chopped at a set frequency. The voltage developed across the sample is amplified and measured by a phase-sensitive detector. All measurements were compared with the signal from a sample of single crystals of lithium tantalate and tourmaline. The lithium tantalate standard also provided a means to standardize the various equipment parameters to obtain reproducible results.

The circuit shown in Figure 2 was employed to view the wave form generated by the samples. The signal from the FET amplifier was filtered to remove the 60 Hz and high frequency noise and the filtered signal was displayed on the oscilloscope. For the 5 Hz wave forms, the signal was first processed through a notch filter to remove the 60 Hz component. The signal was then processed through a bandpass filter to remove the high and low frequency noise. For the 0.5 Hz signal the 60 Hz noise was amplified, inverted, and added to the original signal to cancel out the noise by destructive interference. Photographs were taken of the image of the wave forms as displayed by a storage oscilloscope.

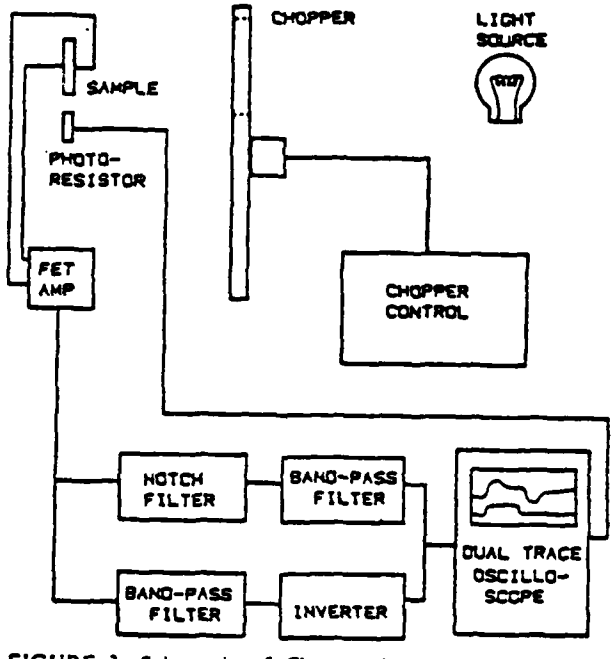

FIGURE 3 Schematic of Chynoweth apparatus for wave form display.

3 RESULTS AND DISCUSSION

The powder x-ray diffraction powder patterns for these glass-ceramics indicated that the only crystallization phase present in detectable quantities was lithium disilicate. No attempt was made to determine the stoichiometry of these samples from the x-ray patterns.

3.1 *Isothermal crystallization*

Soaking times at the crystallization temperature were varied from one hour or more down to ten minutes. The samples crystallized for longer times, regardless of the presence or absence of an applied field, were completely opaque. Those

samples crystallized for shorter times were either translucent or slightly opalescent in appearance. In these samples, no bulk spherulitic crystallite growth could be observed with the unaided eye. These observations correspond to those made using the microscope hot stage. Surface crystallization occurs relatively quickly, but the nucleation and growth of the spherulites is a slower process. The short crystallization times result in surface crystallization but little or no visible crystallization of the bulk of the samples.

3.1.1 X-ray diffraction In general, the x-ray diffraction patterns of the isothermally crystallized glass-ceramics showed that the sample surfaces contained highly oriented crystallites. As in the work of Rindone, the strong (002) reflection indicates that the crystallographic *c*-axis is perpendicular to the sample surface.[9] The degree of orientation was estimated by calculating the ratio of the peak heights of the (002) to the (040) reflections. For random polycrystalline or powdered samples, this ratio is about 1:7. A higher ratio than this would indicate that the *c*-axis is preferentially aligned perpendicular to the sample surface. For the isothermally crystallized samples, this ratio was typically 100:1. Ratios as high as 300:1 were measured. Because of the high degree of orientation in many of these samples, it was often impossible to resolve the (130), (040), and (111) peaks. In these cases, this ratio was calculated on the basis of the height of the next highest peak in the range from 23 to 25 degrees 2-theta.

The ratios obtained from the diffraction patterns agree well with those obtained by Rindone for $Li_2Si_2O_5$ crystals in $Li_2O:4SiO_2$ glass.[9] He reported ratios as high as 500:1 for glasses crystallized without the addition of platinum nuclei.

The degree of orientation was dependent only on the quality of the surface finish. A sample which had been ground but not polished yielded an x-ray pattern very similar to that of a powdered sample. No enhancement of the 002:040 peak height ratio occurred unless the sample surfaces were highly polished prior to crystallization.

3.1.2 Microstructure Microscopic examination of all the samples was made. Etching the samples revealed the oriented surface crystallization detected by the diffractometer. Figure 4 is an optical photomicrograph of a typical layer. Figures 5-a and

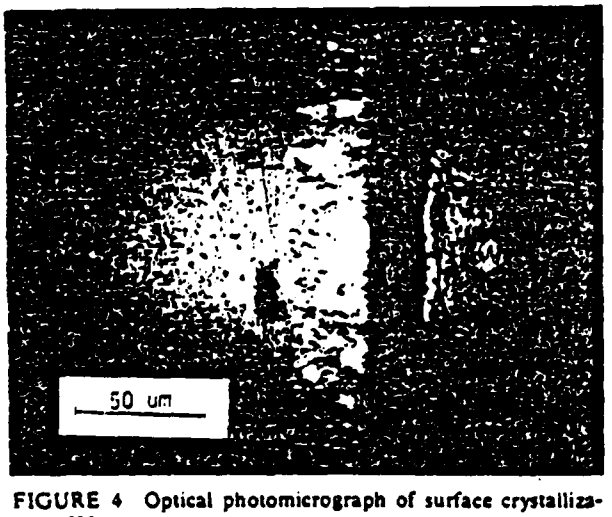

FIGURE 4 Optical photomicrograph of surface crystallization (500×).

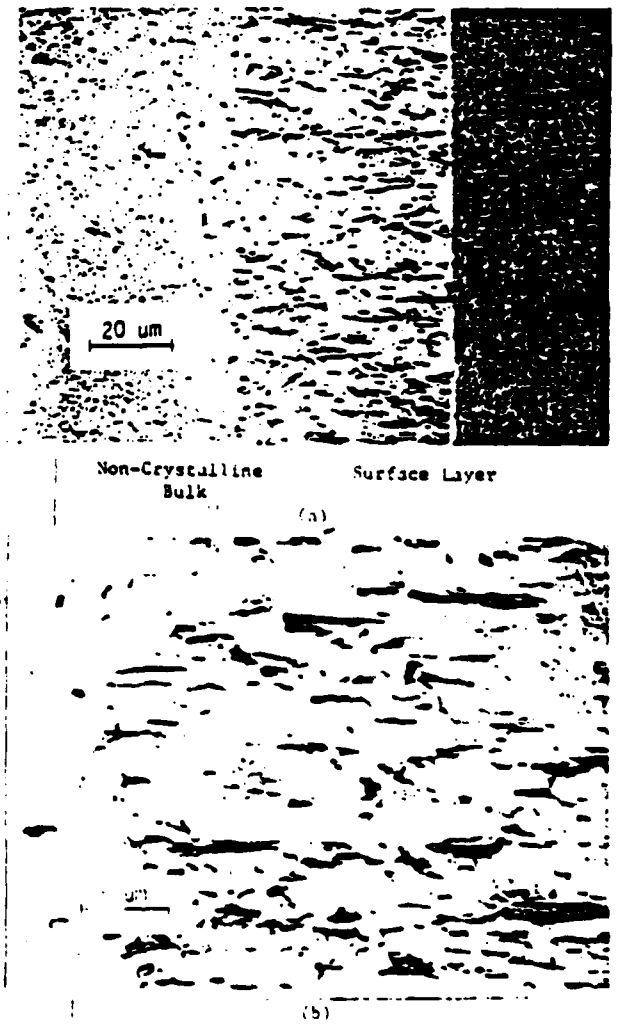

FIGURE 5 SEM photomicrograph of oriented, crystallized surface layer: (a) 700×; (b) 3000×.

5-b are SEM photomicrographs which show the needle-like lithium disilicate crystals in these samples. The depth of the oriented layer in the isothermally crystallized samples varied from as little as 20 μm up to 250 μm. The depth of this layer was related to the length of time at the crystallization temperature. Those samples crystallized for short periods of time generally had thinner oriented layers. The bulk crystallization is spherulitic (and thus not oriented) in nature. The surface crystallization will grow into the sample until it encounters these spherulites. In the thicker samples the combination of oriented surface crystallization and the bulk spherulitic crystallization resulted in a sandwich structure. Figures 6-a and 6-b are optical photomicrographs of an isothermally crystallized sample which was approximately 0.08 cm thick.

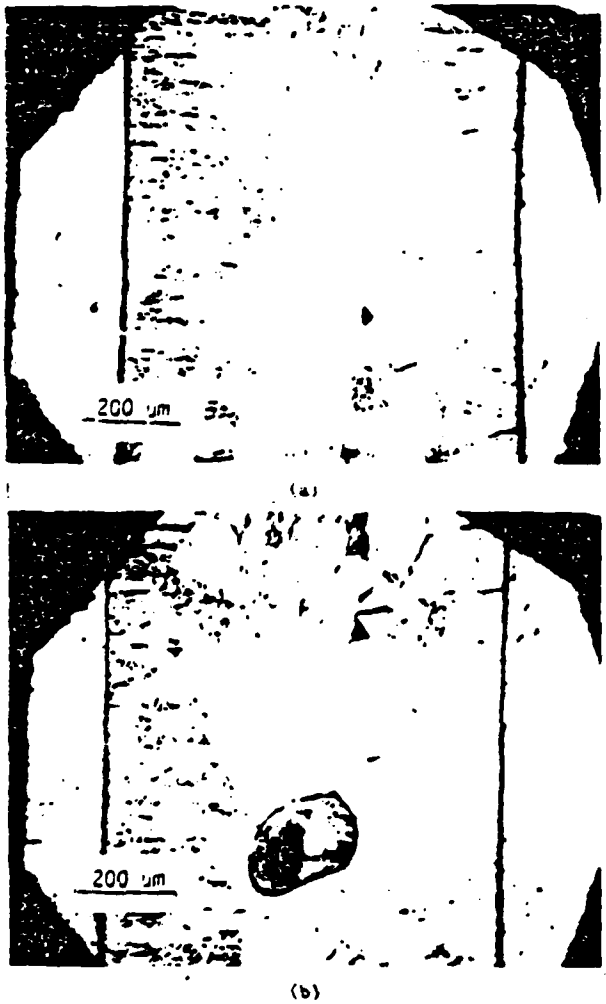

FIGURE 6 Optical photomicrographs of isothermally crystallized glass-ceramic (100×).

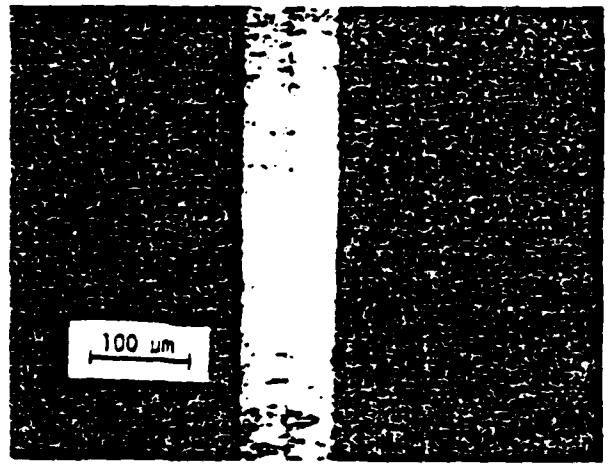

FIGURE 7 Optical photomicrograph of isothermally crystallized glass-ceramic (200×).

The thinner samples consisted of the two layers of oriented crystallites extending inward from the surfaces but with no intervening layer of spherulitic growth. Figure 7 is a photomicrograph of a 0.013 cm sample. The two layers have apparently grown inwards towards the centerline of the sample faster than the rate of formation of the spherulitic crystallites. The thickness of the oriented layers is approximately 60 to 90 μm in these samples.

3.2 Thermal gradient crystallization

Macroscopically, the thermal gradient samples appeared to be crystallized on the hot surface to a depth of about two millimeters. The bulk of the sample remained non-crystalline with the exception of a few spherulites in the center of the sample.

3.2.1 X-ray diffraction X-ray diffraction was performed on the crystallized surface. Peak height ratios (002:040) as high as 200:1 were measured. The degree of orientation was once again determined to be a function of surface finish only.

3.2.2 Microstructure The depth of the oriented layer was as much as 1 mm, or at least four times greater than the layers in any of the isothermally crystallized samples. Figures 8-a and 8-b are photomicrographs of a typical thermal gradient sample showing the oriented layer of crystallites.

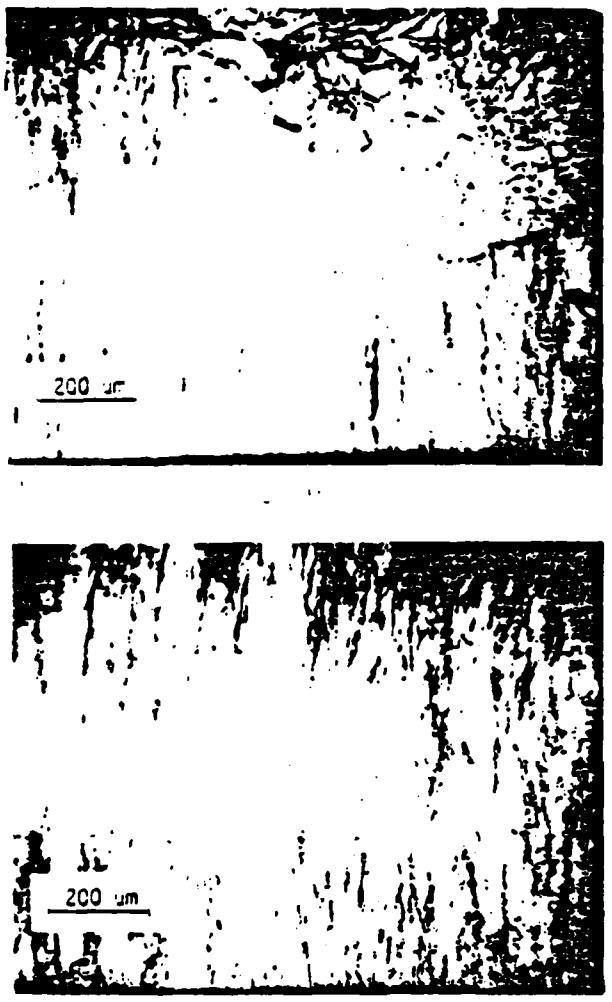

(b)

FIGURE 8 Optical photomicrographs of oriented layer in thermal gradient sample (100×).

This technique enabled the preparation of samples in which a single oriented layer of lithium disilicate crystals could be grown to a substantial thickness.

3.3 Pyroelectric measurements

Table I contains the results of the pyroelectric measurements on several of these samples. The voltage recorded in Table I is the voltage after amplification. All measurements were made at a frequency of 5 Hz.

The lithium tantalate sample used to standardize the equipment had the largest signal. The signals generated in the lithium disilicate samples were much smaller. The inverse relationship between the sample thickness and the magnitude of the signal was exhibited by the isothermally crystallized glass-ceramics.

The thermal gradient sample produced the largest signal of the glass-ceramics. For the purposes of comparison, a sample of single crystal tourmaline was ground and polished to a thickness close to that of the thermal gradient sample. Under identical conditions, the thermal gradient sample produced a signal which was approximately a factor of four larger than that produced by the tourmaline crystal.

It might be argued that the voltage signal in these samples may be related to effects other than pyroelectricity. There is, however, substantial evidence that pyroelectricity, whether primary or secondary due to mechanical interaction with the piezoelectric properties, is responsible for the signal.

First, the AC Chynoweth method eliminates

TABLE I

Pyroelectric responses of $Li_2Si_2O_5$ glass-ceramics, lithium tantalate, and tourmaline

Material	Sample Thickness	Crystallization	Amplified Voltage (mV)	V Sample / V $LiTaO_3$	Sample Capacitance at 1 K	Tan δ
$LiTaO_3$	130 μm	Single crystal	350	1.0	74 pf	.005
$Li_2Si_2O_5$	800 μm	Isothermal	0.1	2.9×10^{-4}	.2 pf	~.007
$Li_2Si_2O_5$	100 μm	Isothermal	1.9	5.4×10^{-3}	1.6 pf	~.007
$Li_2Si_2O_5$	470 μm	Thermal gradient	11	3.1×10^{-2}	.4 pf	~.007
Tourmaline	450 μm	Single crystal	2.7	7.7×10^{-3}	.4 pf	~.006

Note: Amplifier input capacitance = 1 pf
Gain = 100:1

many of the DC effects that are often measured as a material is heated. Thermoelectricity can contribute to the DC current, but the voltage generated during the time the light is on would rise to an equilibrium value and would not decay with time. The thermoelectric voltage would not change sign on cooling. Photoconduction and the trapping of charge carriers may result in the decay of the signal with time, but the sample would not recover to its original condition during the dark cycle.[11]

The frequency dependence of the pyroelectric voltage response has been described by Putley.[12] For a true pyroelectric material, the log of the voltage should be a linear function of the log of the chopping frequency provided that the chopping frequency is greater than $1/\tau$, where τ is the electrical time constant for the detector-amplifier circuit. This frequency dependence has been plotted in Figure 9 for both the lithium tantalate standard and a glass-ceramic sample. Note the linearity of both functions in this frequency range. This indicates that the frequency dependence of the signal in the lithium disilicate glass-ceramics follows the predictions of the pyroelectric theory.

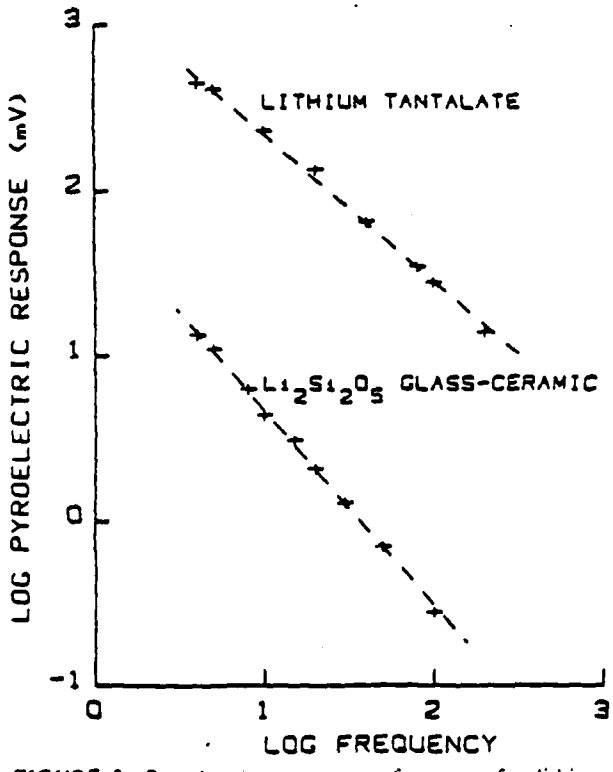

FIGURE 9 Pyroelectric response vs frequency for lithium tantalate standard and lithium disilicate glass-ceramic.

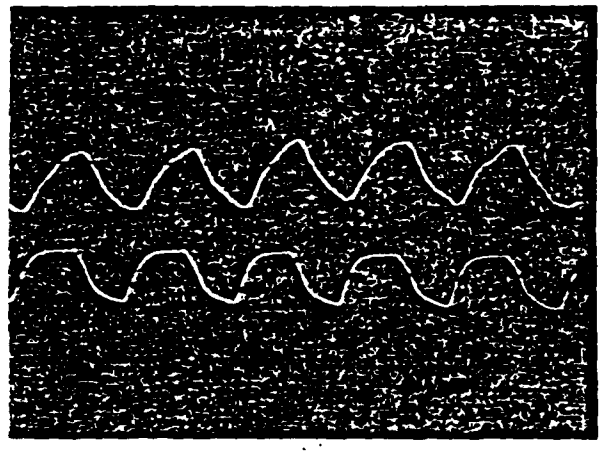

(a)

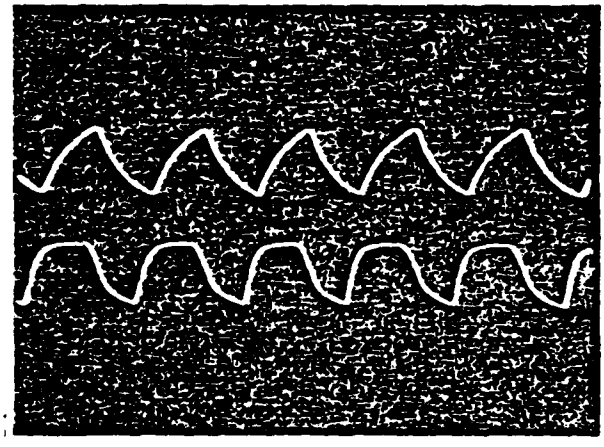

(b)

FIGURE 10 Wave forms of Chynoweth responses at 5 Hz: (a) $Li_2Si_2O_5$ glass-ceramic; (b) $LiTaO_3$ single crystal.

The wave forms of the samples of lithium disilicate and lithium tantalate at chopping frequencies of about 5 Hz and 0.5 Hz, respectively, appear in Figures 10 and 11. The lower trace in the two photographs is the voltage drop across the photoresistor. The voltage of both samples rises to a maximum when the light is turned on and begins to decay with time. The voltage reverses when the light is turned off and again decays towards the baseline.

Given the tendency of the lithium disilicate crystals to twin on a very fine scale, the existence of pyroelectricity in these glass-ceramics is unexpected. In order for pyroelectricity to be detected in the oriented layers, the polarities of the crystal-

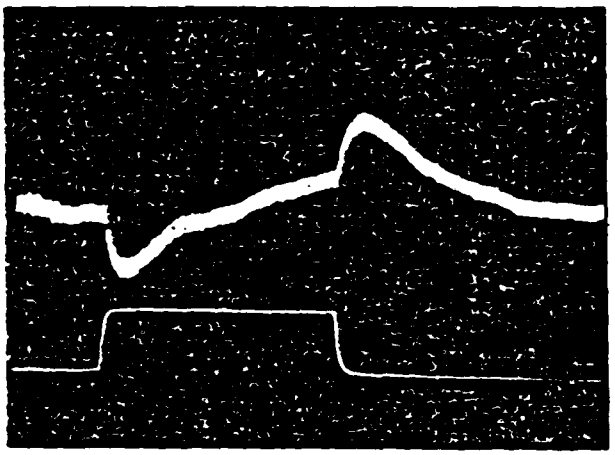

(a)

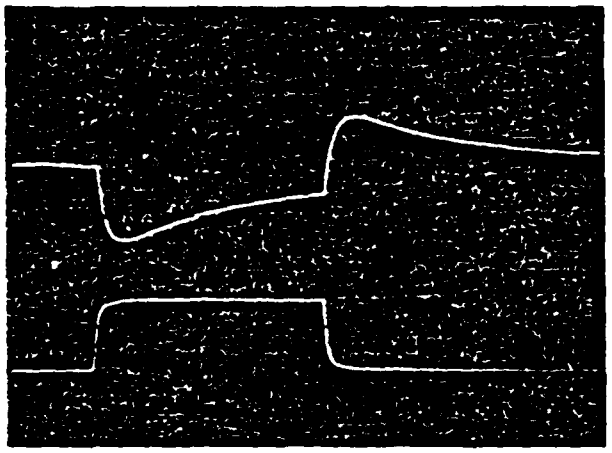

(b)

FIGURE 11 Wave forms of Chynoweth responses at 0.5 Hz: (a) $Li_2Si_2O_5$ glass-ceramic; (b) $LiTaO_3$ single crystal.

lites cannot be randomly arranged. There must be some mechanism operating during crystallization which favors one polar sense of the *c*-axis over the other.

One possible mechanism involves the migration of alkali ions to the surface during heating. The explanation of the orientation effect in the surface layers of these glasses is based on the observation that the surface of an alkali-containing glass is higher in alkali concentration than is the bulk.[10] In a glass containing lithium, silicon, and oxygen, a high lithium concentration at the surface, if uncompensated by negative surface charges, must create an electric field within the glass. The surface of the glass would be expected to be positive with respect to the bulk. If lithium ion migration occurs prior to nucleation and crystallization, the electric field due to ion migration may influence the polar orientation of the crystallites within the oriented layer.

An alternative explanation based on lithium ion migration would be that the high lithium ion concentration at the surface favors the nucleation and growth of one of the two possible orientations through some mechanism not involving the electric field created by the ion migration.

If the migration of lithium ions towards the sample surfaces is held responsible for the favoring of one sense of the *c*-axis polarity over the other, then it must be true that the polarity of the two layers of oriented crystallites in the isothermally crystallized samples must be opposite to each other.

The accuracy of this statement can be tested by examining the phase relations between the light pulses heating the sample and the resultant voltage. For a single crystal such as the lithium tantalate standard, the polarity of the electrodes is independent of which surface is exposed to the light pulses. If the sample is inverted with respect to the light source, the sign of the detected voltage will not reverse.

This experiment was performed on the lithium disilicate samples. The samples which consisted of two oriented layers of crystallites separated by a spherulitic region did appear to reverse the sign of the voltage when inverted with respect to the light source. It was determined that the surface of the sample which is facing the light source was always positive with respect to the opposite surface. The samples behaved as if they consisted of two pyroelectric single crystals joined together such that the polar sense of the crystals opposed each other. This measurement indicated that the polarities of the oriented layers were in agreement with the proposed mechanism.

A further check was performed on samples which consisted of only a single oriented layer. Measurements of these samples showed that they behaved like single crystals. One surface always became positive regardless of which surface was exposed to the light pulses.

From these measurements it was concluded that the polarity of the crystallites in the oriented layers was not random. Some mechanism, probably related to the migration of lithium ions, was responsible for the favoring of one polar orientation

over the other. The signal detected by the Chynoweth apparatus originates in the oriented layers. In those samples which consisted of two oriented layers separated by a random, spherulitic region, only the layer facing the light source contributes to the signal. The voltage induced across this layer by the temperature change is capacitively coupled to the opposite surface.

This explanation accounts for the relative magnitude of the signals generated by the glass-ceramics. In the thicker, isothermally crystallized samples, the signal originates in the oriented surface layer closest to the light source. The intervening spherulitic layer does not contribute to the response. The thinner isothermally crystallized samples give larger signals because of the reduced mass (and thus larger temperature change) but only one layer can contribute to the signal. If the temperature of the second layer changes, it will tend to oppose the signal of the first layer. There is no opposing oriented layer in the thermal gradient samples to reduce the magnitude of the signal. These samples produced larger signals than the two-layer isothermally crystallized glass-ceramics.

4 CONCLUSIONS

Glass-ceramics containing highly oriented layers of $Li_2Si_2O_5$ crystallites have been made from glasses having the composition $Li_2O:4SiO_2$. The nucleation and crystallization behavior of this glass was found to be identical to the behavior of similar glasses as described in the literature. The highly oriented layers form at the surfaces of the samples prior to the nucleation and crystallization of spherulites in the interior of the samples. The degree of orientation was found to be dependent on the sample surface finish only.

Microscopic examination of the crystallized glasses showed that the oriented layers consisted of needle- or lath-like crystals oriented with their long axes perpendicular to the sample surface. The thickness of the oriented layers could be varied by varying the sample preparation and thermal treatment. Optimum layer thicknesses were obtained in samples which were crystallized by the application of a thermal gradient.

Pyroelectricity was detected in the crystallized glasses using the Chynoweth technique.

The existence of pyroelectricity in these glass-ceramics is evidence that there is a preferred orientation for the polar direction of the *c*-axes during crystallization of the oriented layer.

Although the absolute magnitude of the signals generated by these glass-ceramics is small compared to currently used pyroelectric detector materials, these samples represent the first reported non-ferroelectric pyroelectric glass-ceramics. The techniques and processes developed in this study may be applied to other systems to develop a new class of pyroelectric materials.

ACKNOWLEDGEMENT

This work was sponsored by the Advanced Research Projects Agency (MDA903-78-C-0306) and by the U.S. Army Research Office (DAAG29-76-G-0145).

REFERENCES

1. A. Herzog, *IEEE Trans.*, PHP-9, 247 (1973).
2. N. F. Borrelli, *J. Appl. Phys.*, 38, 4243 (1967).
3. N. F. Borrelli and M. M. Layton, *IEEE Trans.*, ED-16, 511 (1969).
4. M. M. Layton and J. W. Smith, *J. Amer. Ceram. Soc.*, 58, 435 (1975).
5. A. M. Glass *et al.*, *Appl. Phys. Lett.*, 31, 4 (1977).
6. F. C. Kracek, *J. Phys. Chem.*, 34, 2641 (1930).
7. V. F. Liebau, *Acta Cryst.*, 14, 389 (1961).
8. A. Bhalla, Private communication (1979).
9. G. E. Rindone, Symposium on Nucleation and Crystallization in Glasses and Melts, The American Ceramic Society, Columbus, Ohio, 1962.
10. C. L. Booth and G. E. Rindone, *J. Amer. Ceram. Soc.*, 47, 25 (1964).
11. A. G. Chynoweth, *J. Appl. Phys.*, 27, 78 (1956).
12. E. H. Putley, *Semicond. Semimetals*, Volume 5 (Academic Press, NY 1970) p. 259.

Appendix 3

Polar Glass Ceramics

A. Halliyal, A. S. Bhalla, R. E. Newnham, L. E. Cross

Ferroelectrics, 1981, Vol. 38, pp. 781-784
0015-0193/81/3801-0781/$06.50/0

POLAR GLASS CERAMICS

A. HALLIYAL, A.S. BHALLA, R.E. NEWNHAM, L.E. CROSS
Materials Research Laboratory, The Pennsylvania State University, University Park, PA 16802, USA

Abstract—Pyroelectric-piezoelectric glass ceramics of polar materials like $Li_2Si_2O_5$, $Ba_2TiGe_2O_8$, $Ba_2TiSi_2O_8$, and various compositions in the systems Li_2O-B_2O_3, Li_2O-SiO_2-ZnO, Li_2O-SiO_2-B_2O_3 have been prepared by oriented recrystallization of the glasses under a strong temperature gradient, providing a simple inexpensive process for preparing piezoelectric and pyroelectric materials. High pyroelectric responses were observed in these glass-ceramics. Values of piezoelectric d_{33} coefficients, frequency constants, electromechanical coupling coefficients and dielectric properties of glass-ceramics were in close agreement with the values of respective single crystals.

INTRODUCTION

In recent years there has been a growing interest in the study of ferroelectricity in glassy state and recrystallized ferroelectric glasses[1-10]. Dielectric and pyroelectric measurements have been reported in glasses of stoichiometric compositions of $LiTaO_3$, $LiNbO_3$, $Pb_5Ge_3O_{11}$ and $PbTiO_3$[1-3].

Electro-optic properties, dielectric and pyroelectric measurements and switching behavior have been reported for glass ceramics containing ferroelectric microcrystals of $BaTiO_3$, $NaNbO_3$, $LiTaO_3$, $PbTiO_3$, $Pb_5Ge_3O_{11}$ and several other materials in a silica or borate rich glass matrix[4-10]. Effect of heat treatment process on porosity, grain size and on ferroelectric properties of the recrystallized glasses has been studied. All these studies on glass ceramics are limited to the ferroelectric glass ceramics where piezoelectric and pyroelectric properties are induced by electric poling of the domain structure of the microcrystals. Not much attention has been given to studies for inducing polar orientation in the microcrystals in nonferroelectric glass ceramics. Recently it has been shown that by controlled crystallization of glasses having compositions of pyroelectric-piezoelectric materials in a strong normal temperature gradient it is possible to obtain glass ceramics with both crystallographic and polar orientations[11,12]. This paper describes the piezoelectric and pyroelectric measurements done on several glass-ceramic compositions. Advantages of glass ceramics for various device applications are discussed.

EXPERIMENTAL DETAILS

Glasses of compositions $Ba_2TiGe_2O_8$, $Ba_2TiSi_2O_8$, Li_2O-$2SiO_2$ and several compositions in the systems Li_2O-B_2O_3, Li_2O-SiO_2-ZnO and Li_2O-SiO_2-B_2O_3 were prepared by mixing reagent grade chemicals in the desired molar ratios and melting in a globar furnace. The compositions of the glasses and the crystallization temperatures determined from DTA runs are given in Table 1. Crystallization of glasses was carried out in a temperature

TABLE 1

Properties of Glass-Ceramic Samples Prepared in a Temperature Gradient

	ϵ_r	T_{cr}(°C)[a]	Crystalline Phases[b]	Piezo[c] d_{33} pC/N	Chynoweth response[d] pyro mV
$2BaO-2GeO_2-TiO_2$	15	800	B_2TG_2	+6	(-) 20
$BaO-1.8SiO_2-TiO_2$	12	860	B_2TS_2+Q	+3	(+) 35
$Li_2O-2SiO_2$		585	LS_2	-1	(-) 20
$Li_2O-2SiO_2-0.1ZnO$	5	570	LS_2+LSZ+Q	-3	(-) 70
$Li_2O-2SiO_2-0.2ZnO$	6	580	LS_2+LSZ+Q	-4	(-)100
$Li_2O-2SiO_2-0.25ZnO$		585	LS_2+LSZ+Q	-4	(-) 80
$Li_2O-2SiO_2-0.4ZnO$	8	590	LS_2+LSZ+Q	0	(-) 4
$Li_2O-3B_2O_3$		580	LB_2+LB_3	+3	(-) 70
$Li_2O-1.8SiO_2-0.2B_2O_3$	8	605,680	LS_2+LB_2+LS	+6	(-)200
$Li_2O-1.33SiO_2-0-66B_2O_3$	8	670	LS_2+LB_2+LS	+3	(-) 85
$Li_2O-1.8SiO_2-0.1ZnO-0.1B_2O_3$	7	580,670	LS_2+LSZ	-2	(-) 20

[a] T_{cr} is the crystallization temperature determined from DTA runs.

[b] Abbreviation for phases.

B_2TG_2 = $Ba_2TiGe_2O_8$ — LSZ = Li_2ZnSiO_4

B_2TS_2 = $Ba_2TiSi_2O_8$ — LS = Li_2SiO_3

Q = SiO_2 (quartz) — LB_2 = $Li_2B_4O_7$

LS_2 = $Li_2Si_2O_5$ — LB_3 = $Li_2B_6O_{10}$

[c] Measured on the surface facing the higher temperature end of the temperature gradient axis.

[d] (±) indicates the sign of pyroelectric coefficient p.

gradient by placing the polished glass samples, in the form of thick disks, on a microscope hot stage (E. Leitz, Inc.). A detailed procedure for the preparation of glass-ceramic samples can be found in references 11-14. The crystalline phases in the glass-ceramic samples were identified from x-ray powder patterns. The piezoelectric constants were measured using a d_{33} meter. For resonance studies, samples in the shape of circular disks were prepared, polished and gold electrodes were sputtered. Measurements were made both in the radial and the thickness mode of resonance by resonance and antiresonance method using a Hewlett Packard 3585A spectrum analyzer[14]. Pyroelectric responses from thin samples (250 μm) were measured by the dynamic Chynoweth technique[15] at a modulating frequency of 4 Hz.

MICROSTRUCTURE OF RECRYSTALLIZED SAMPLES

Glass-ceramics prepared from recrystallization of the glasses in a temperature gradient showed a high degree of crystallographic orientation. Studies on the degree of preferred orientation of the crystallites as a function of depth from the hot face revealed that the oriented crystallites region extends deep in the glass-ceramic samples and then tapers off (Figure 1). Needle-like crystals grow from the hot face into the sample along the direction of the temperature gradient. The depth of the oriented region was 400 to 600 μm. The width of the crystallites estimated from the optical microscope is in the range 2-5 μm.

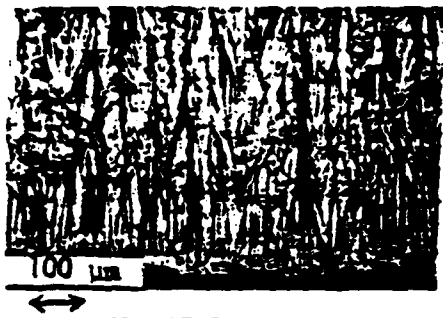

FIGURE 1

Fig. 1.
Optical photomicrograph of oriented crystallized region in Li_2O-$2SiO_2$-0.2ZnO glass-ceramics (x100).

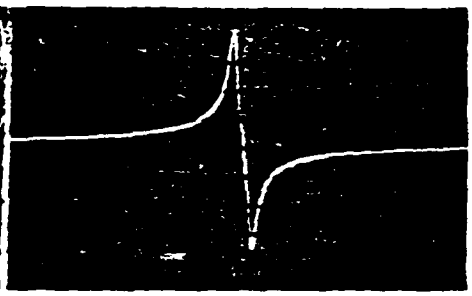

FIGURE 2

Fig. 2.
Resonance spectrum for Li_2O-$1.8SiO_2$-$0.2B_2O_3$ glass-ceramic (horizontal scale = 6.8 kHz; vertical scale = 5 dB).

PIEZOELECTRIC PROPERTIES

The piezoelectric d33 coefficients and their signs measured on the surface facing the higher temperature gradient end are given in Table 1. For $Ba_2TiGe_2O_8$ and $Ba_2TiSi_2O_8$ glass-ceramics, the sign of d33 was positive. For $Li_2Si_2O_5$ the sign of d33 was negative and remained the same in samples containing small amounts of ZnO in the composition. However, the magnitude of d33 increased for compositions containing even a small amount of ZnO. Addition of small amounts of B_2O_3 in $Li_2Si_2O_5$ reversed the sign and increased the magnitude of d33. This indicated that both the crystallization behavior and the polar orientation were influenced strongly by the various ionic species present in the parent glass.

A typical resonance spectrum observed in glass-ceramic samples is shown in Fig. 2. The electromechanical properties of some of the glass-ceramic compositions are given in Table 2.[14,16] The coupling coefficients k_p and k_t of $Ba_2TiGe_2O_8$ glass-ceramics are comparable to the corresponding values of single crystals. The values for mechanical quality factor Q are comparatively higher. The TCR values for Li_2O-SiO_2-B_2O_3 glass-ceramics are comparable to the values of commonly used piezoelectric materials like $LiTaO_3$ and $LiNbO_3$. In this system, the strong dependence of TCR on the composition of the parent glass suggests that it might be possible to reduce TCR further by a suitable choice of the composition of the parent glass. In addition, by employing proper heat treatment cycles for crystallization, it is possible to prepare glass ceramics with oriented crystallites of more than one phase from the glass matrix. Hence, in such glass-ceramic systems, composition and processing parameters are the extra controlling factors, which can be exploited to tailor the properties of piezoelectric resonators.

TABLE 2

Electromechanical Properties of Glass Ceramics

Composition	N_p m-Hz	N_t m-Hz	k_p %	k_t %	Q	TCR ppm/°C
$2BaO$-$2GeO_2$-TiO_2	3100	2500	4.4	7.5	700	95 (0°-100°C)
$Ba_2TiGe_2O_8$ (single crystal)	2900	2150	6.2	10.0	650	50 (0°-100°C)
Li_2O-$1.8SiO_2$-$0.2B_2O_3$	4500	--	14	--	1000	60 (0°-100°C)
Li_2O-$1.33SiO_2$-$0.66b_2O_3$	4200	--	9	--	400	30 (30°-60°C)

PYROELECTRIC PROPERTIES

The pyroelectric voltage response of the samples measured by the Chynoweth technique are given in Table 1. Pyroelectric responses from grain oriented glass-ceramics were typically 50% of the responses from the corresponding single crystals. Lithium borosilicate glass-ceramics seem very promising for pyroelectric applications. A strong pyroelectric response was measured from glass ceramics of composition Li_2O-1.8SiO_2-0.2B_2O_3 and was comparable to the signal from a commercial pyroelectric such as $LiTaO_3$.

For pyroelectric detectors and vidicon, the figure of merit is given by $P/\varepsilon\rho C_p K$ where p is the pyroelectric coefficient, ε the dielectric constant, ρ the density, C_p the specific heat and K is the thermal conductivity of the material. The dielectric constants of the glass-ceramics listed in Table 1 are in the range 5 to 10 and the densities are about 2-3 gms/cc. A high figure of merit could be possible in glass-ceramic pyroelectric detectors.

SUMMARY

Several piezoelectric and pyroelectric materials can be prepared in the glassy phase, and it is possible to prepare large area, inexpensive polar glass ceramics by recrystallizing the glasses under a strong normal temperature gradient. Electrical properties of glass ceramics are less sensitive to the chemical impurities and the defects in the samples. The piezoelectric and pyroelectric properties of the glass ceramics can be tailored to the desired requirements by recrystallizing the multicomponentglasses using a proper temperature cycle. Pyroelectric and electromechanical properties of glass ceramics are comparable to their properties in the single crystal form. Such composite elements may be useful for device applications based on flexural resonance mode, in pyroelectric detectors, for resonators, and in SAW devices. The process for preparing glass ceramics is amenable to mass production.

ACKNOWLEDGMENTS

This work was sponsored by the U.S. Army Research Office (DAAG 29-80-C-0008) and the Advanced Research Project Agency (DARPA Project No. P-15124-MS).

REFERENCES

1. A.M. Glass, M.E. Lines, K. Nassau, J.W. Shiever, Appl. Phys. Lett. 31, 249 (1977).
2. A.M. Glass, K. Nassau, J.W. Shiever, J. Appl. Phys. 48, 5213 (1977).
3. M. Takashiege, T. Mitsui, T. Makagura, Y. Aikawa, M. Jang, Jpn. J. Appl. Phys. 20, L159 (1981).
4. A. Herzog, J. Amer. Ceram. Soc. 47, 107 (1964).
5. N.F. Borrelli, J. Appl. Phys. 38, 4243 (1967).
6. M.E. Lines, Phys. Rev. B15, 388 (1977).
7. T. Kokubi, H. Nagao, M. Tashiro, Yogyo-Kyokai-shi 77, 293 (1969).
8. C.G. Bergeron and C.K. Russell, J. Amer. Ceram. Soc. 48, 115 (1965).
9. K.Takahashi, L.E. Cross, R.E. Newnham, Mat. Res. Bull. 10, 599 (1975).
10. M.M. Layton, J.W. Smith, J. Amer. Ceram. Soc.58, 435 (1975).
11. G.J. Gardopee, R.E. Newnham, A.G. Halliyal, A.S. Bhalla, Appl. Phys. Lett. 36, 817 (1980).
12. G.J. Gardopee, R.E. Newnham, A.S. Bhalla, Ferroelectrics 33 (1981) (accepted).
13. A. Halliyal, A.S. Bhalla, R.E. Newnham, L.E. Cross, J. Mater. Sci. 16, 1023 (1981).
14. A. Halliyal, A.S. Bhalla, R.E. Newnham, L.E. Cross, J. Mater. Sci. (accepted).
15. A.G. Chynoweth, J. Appl. Phys. 27, 78 (1956).
16. A. Halliyal, A.S. Bhalla, R.E. Newnham, L.E. Cross, J. Appl. Phys. (submitted).

Appendix 4

$Ba_2TiGe_2O_8$ and $Ba_2TiSi_2O_8$ Pyroelectric Glass-Ceramics

A. Halliyal, A. S. Bhalla, R. E. Newnham, L. E. Cross

JOURNAL OF MATERIALS SCIENCE 16 (1981) 1023–1028

$Ba_2TiGe_2O_8$ and $Ba_2TiSi_2O_8$ pyroelectric glass-ceramics

A. HALLIYAL, A. S. BHALLA, R. E. NEWNHAM, L. E. CROSS
Materials Research Laboratory, The Pennsylvania State University, University Park, Pennsylvania 16802, USA

Pyroelectric glass-ceramics of composition $Ba_2TiGe_2O_8$ and $Ba_2TiSi_2O_8$ were prepred by crystallizing the glasses in a temperature gradient. High pyroelectric responses up to 50% of the single-crystal values were observed because of the high degree of orientation of the crystallites in the glass-ceramic samples. The piezoelectric and dielectric properties of the glasses and the glass-ceramics are also consistent with the properties of the single crystals.

1. Introduction

Pyroelectric lithium disilicate glass-ceramics have recently been prepared by growing highly orientated surface layers of lithium disilicate crystals by crystallizing the glasses of stoichiometric glass compositions $Li_2O \cdot 2SiO_2$ in a temperature gradient [1]. This technique provides a method of fabricating large and inexpensive pyroelectric devices. However, one difficulty encountered in working with the lithium disilicate pyroelectric glass-ceramic was that thin targets (of thickness, $d < 200\,\mu m$) cut perpendicular to the growth direction (the polar c-axis of $Li_2Si_2O_5$) were extremely fragile and could not be prepared routinely.

In this study pyroelectric glass-ceramics of barium titatnium silicate (BTS: $Ba_2TiSi_2O_8$ or fresnoite) and barium titanium germanate (BTG: $Ba_2TiGe_2O_8$) are described, the physical properties of which are superior to $Li_2Si_2O_5$. Thin sections of these glass-ceramics, less than $100\,\mu m$ in thickness, can easily be prepared since they are mechanically much stronger. Glass-ceramics of BTG and BTS were prepared by crystallizing glasses of stoichiometric compositions of BTG and a silica-rich composition ($64SiO_2-36BaTiO_3$) of BTS in a thermal gradient. The dielectric and pyroelectric properties were measured and compared with the properties of single crystals.

In the single-crystal form fresnoite belongs to the crystallographic point group 4mm and is pyroelectric [2]. $Ba_2TiGe_2O_8$ is reported to be a ferroelastic [3, 4] below 810° C and belongs to the orthorhombic polar point group mm2. In the paraelastic phase above the transition temperature, T_c, BTG also belongs to the tetragonal point group 4mm.

Glass-ceramics in the $BaTiO_3-SiO_2$ system have been previously investigated. Herczog [5] studied the crystallization of $BaTiO_3$ in a silicate glass matrix. Dielectric and electro-optic measurements on transparent glass-ceramics containing ferroelectric $BaTiO_3$ in a glass matrix have also been reported [6]. However, the primary interest in these materials has been concerned with the dielectric and electro-optic properties of the glass-ceramics, and in the ferroelectric nature of $BaTiO_3$ crystallites surrounded by a glass matrix. In these studies no efforts have been made to develop glass-ceramics containing orientated crystallites. The present study describes the preparation and characterization of glass-ceramics containing orientated crystallites of the pyroelectric (but non-ferroelectric) BTS and BTG phases.

2. Experimental details

Glasses of composition $64SiO_2 \cdot 36BaO \cdot 36TiO_2$ were prepared by mixing reagent-grade silicic acid*, barium carbonate† and titanic oxide‡.

*J. T. Baker Chemical Co., Phillipsburg, NJ, USA.
†Fisher Scientific Co., Phillipsburg, NJ, USA.
‡Eagle–Picher Industries, Inc., Quapaw, Oklahoma, USA.

0022–2461/81/041023–06$02.60/0

followed by melting in a globar furnace. Fresnoite has a high melting point (1400° C) and thus, it was difficult to obtain bubble-free glasses of the stoichiometric composition. To avoid this problem, a composition was selected which lies near the eutectic point on the silica-rich side of the $BaTiO_3$–SiO_2 binary phase diagram [7]. This composition lies well within the range of glass formation in the $BaTiO_3$–SiO_2 system.

In the case of BTG, reagent-grade barium carbonate, germanium oxide* and titanic oxide were mixed and melted in the furnace. In both cases, the melts were maintained at 1375° C for 24 hours for fining and homogenization. Transparent samples were obtained by pouring the melt into a graphite mould. The samples which crystallized during pouring of the melt were remelted and poured again into the graphite mould in order to ensure transparent glass samples. All the glass samples were annealed at 600° C for 12 hours and then cut and polished in the form of thick disks in preparation for the crystallization studies. To determine the crystallization temperatures of the glass compositions, differential thermal analysis (DTA) measurements were performed on the glass samples. Exothermic peaks were observed at 860° C in the case of BTS and at 800° C in the case of BTG, as shown in Fig. 1.

Crystalization was carried out in a temperature gradient by placing the polished glass samples, in the form of thick disks, on a microscope hot stage.† The temperature gradient near the hottest temperature zone was perpendicular to the surface of the sample and it was estimated to be about 100° C mm^{-1}. Typical heating cycles used for glass crystallization are shown in Fig. 2. The heating cycle consisted of an initial rapid rise in temperature to minimize volume nucleation, followed by a slow increase in temperature at a rate of about 3° C min^{-1}. After reaching the maximum crystallization temperature (1100° C for BTS and 1000° C for BTG), the samples were held at this temperature for 24 hours. The temperature was then decreased rapidly to room temperature. The thicknesses of the crystallized portions of the glasses ranged from 1 to 2 mm, depending on the heating cycle.

The degree of preferred orientation of the

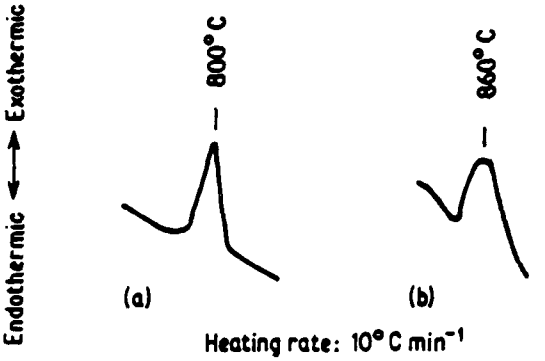

Figure 1 DTA heating curves of (a) BTG and (b) BTS glasses.

glass-ceramic was evaluated from X-ray diffractometer patterns. X-ray diffraction (XRD) patterns were recorded on surfaces normal to the direction of the temperature gradient (Fig. 3). The XRD patterns were compared with the standard powder diffraction patterns to determine the relative degree of orientation. The dielectric constants of glass and glass-ceramic disks were measured with a capacitance bridge. The piezoelectric behaviour parallel to the crystallization direction was studied using a d_{33}-meter.‡ The samples were thinned down to about 200 μm in thickness and the pyroelectric response was measured by the dynamic Chynoweth technique [8] at a modulating frequency of 4 Hz. The pyroelectric signals on glass-ceramics were compared with the responses from single crystals of the BTG and BTS. The densities of BTG, BTS glasses and glass-ceramic samples were determined by a mercury porosimeter§ and compared with the densities of single crystals.

3. Results and discussion

Table I summarizes the data for the glass and glass-ceramic samples. Single-crystal values are also listed for comparison.

X-ray powder diffraction patterns of the crystallized samples showed that the principal crystallized phases were fresnoite in the BTS glass-ceramics and $Ba_2Ge_2TiO_8$ in the BTG glass-ceramic samples. A few low-intensity peaks of an unidentified phase were observed in the powder diffraction patterns of both compositions. The samples showed highly orientated crystal growth

*Eagle–Picher Industries, Inc., Quapaw, Oklahoma, USA.
†Model No. 493, manufactured by E. Leitz, Inc., Rockleigh, NJ, USA.
‡Model CPDT 3300, manufactured by Channel Products, Chesterland, OH, USA.
§Model JS-7146, manufactured by American Instrument Co., Silver Spring, MD, USA.

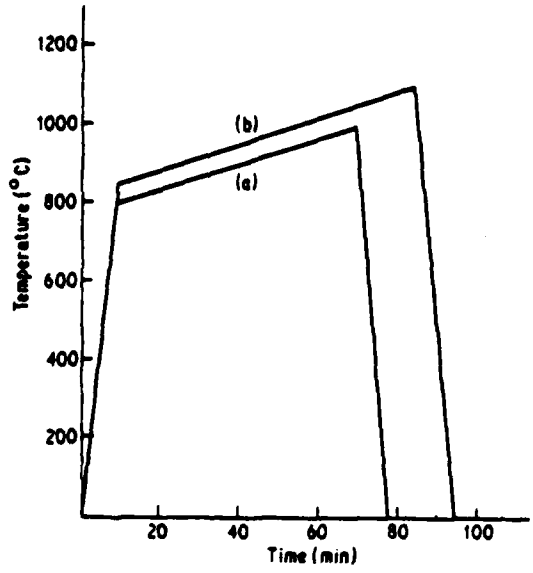

Figure 2 Heating cycles used for crystallizing (a) BTG and (b) BTS glasses.

in a direction parallel to the temperature gradient, with the polar *c*-axis perpendicular to the hot surface of the sample. As shown in Fig. 4, the 0 0 2 reflection was the strongest in the X-ray patterns of the crystallized surfaces. The ratio of the intensity of the 0 0 2 peak to that of the 2 1 1 peak was taken as a measure of the relative degree of orientation. The intensity ratios are given in Table I. Comparison of the intensity ratios in the glass-ceramic samples with the intensity ratios of a standard powder pattern, showed a high degree of orientation of the crystallites in the glass-ceramics. An even higher degree of orientation was obtained in the samples with good surface finish.

The degree of preferred orientation in crystallized samples of BTS and BTG was similar to that observed previously [1] in $Li_2Si_2O_5$. It was observed that the degree of orientation of the crystallites in the isothermally crystallized glass-ceramics was poor compared to the samples crystallized in a temperature gradient. In addition, detailed studies of the microstructure of the crystallized samples showed that the thickness of the well-orientated region was larger in the case of samples crystallized in a temperature gradient, indicating that thermal gradient crystallization is preferable for obtaining well orientated glass-ceramics.

The main reason for the orientation of the crystallites is surface-nucleated crystallization which takes place in both the isothermal and temperature-gradient crystallization. A higher degree of electrical and crystallographic orientation is obtained in the temperature-gradient crystallization method due to the absence of volume nucleation; however, in the case of isothermal crystallization, the orientation of the crystallites is limited to a layer only a few micrometers thick due to the simultaneous occurrence of volume nucleation. Atkinson and McMillan [9] attempted to produce a $Li_2Si_2O_5$ glass-ceramic with an aligned microstructure by a hot-extrusion method. They were partially successful in obtaining glass-ceramic samples with the disilicate crystal crystallographically-aligned parallel to the extrusion axis. However, the degree of orientation of the crystallites was less than that obtained in glass-ceramic samples prepared by crystallizing the glasses in a temperature gradient [1].

The density of BTG glass was about the same as

TABLE I Summary of data for glass and glass-ceramic samples

Sample	X-ray intensities, $\frac{I(0\,0\,2)}{I(2\,1\,1)}$	Dielectric constant, ϵ^*	Dissipation factor*	Density ($g\,cm^{-3}$)	d_{33} ($\times 10^{12}\,C\,N^{-1}$)	Pyroelectric response
BTG glass	—	17	0.003	4.74	—	50% to 60% of single-crystal value
BTG glass-ceramic	85	15.0	0.002	4.56	5 to 7	
$Ba_2Ge_2TiO_8$ single crystal	0.2 (standard powder pattern)	$\epsilon_{11} = 20$ $\epsilon_{22} = 20$ $\epsilon_{33} = 13$	0.003	4.84	8	
BTS glass	—	15	0.002	4.01	—	50% to 60% of single-crystal value
BTS glass-ceramic	15	12.5	0.002	3.90	2 to 3	
$Ba_2Si_2TiO_8$ single crystal	0.2 (standard powder pattern)	$\epsilon_{11} = \epsilon_{22} = 15$ $\epsilon_{33} = 11$	0.003	4.45	3.8	

*Measurements were made at 1 MHz for the glass and glass-ceramic and at 1 kHz for single crystals.

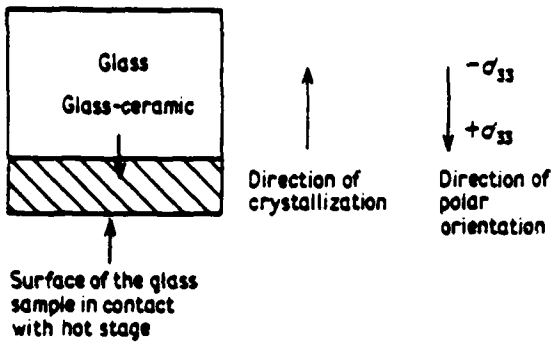

Figure 3 The direction of polar orientation in glass-ceramic samples.

the single-crystal form (Table I), while that of BTS glass was slightly lower than the density of fresnoite single crystals because of the excess silica used in the BTS composition. Only a small decrease in density occurred on crystallization of the glass phases, indicating a low concentration of voids in the glass-ceramic samples. Samples as thin as 100 μm could be prepared without difficulty because of the absence of pores and cracks.

The dielectric constants of BTS and BTG glasses measured at 1 MHz are very close to the mean dielectric constant, $(\epsilon_{11} + \epsilon_{22} + \epsilon_{33})/3$, of the corresponding crystalline phases. On crystal-

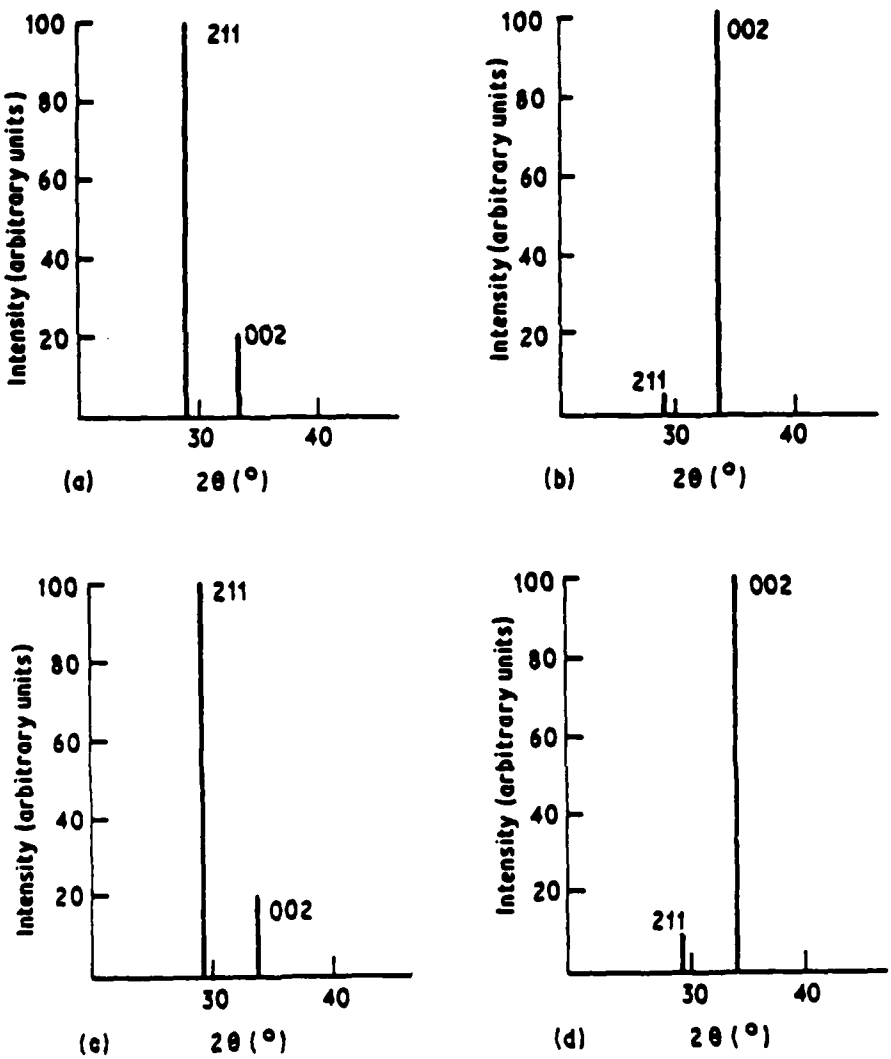

Figure 4 X-ray diffraction patterns of (a) Ba_2GeTiO_6 standard powder diffraction pattern, (b) BTG glass-ceramic, (c) $Ba_2TiSi_2O_8$ standard powder diffraction pattern, and (d) BTS glass-ceramic.

lization, the dielectric constants of the glass-ceramic samples show a slight decrease; the dielectric constant measured in the crystallization direction is closer to the ϵ_3-values of the single crystals. This is consistent with the fact that the c-axis is the preferred orientation direction in the glass-ceramic, as indicated by X-ray diffraction analysis.

The loss tangent factors of the glass-ceramics were similar to those measured on single crystals.

Piezoelectric coefficients, d_{33}, measured in the crystallization direction in glass-ceramics were comparable to the single-crystal d_{33} coefficient values reported [2–4] for BTS and BTG. Opposite faces of the sample gave opposite signs for the piezoelectric constant. The large magnitude of d_{33}-values and its sign reversal suggest that the crystallites in the glass-ceramics are not only orientated along the c-axis in the crystallization direction, but that most of the crystallites have the same polarity as well. The fact that the d_{33}-values remained constant over the entire surface of the glass-ceramic testifies to the uniformity and the homogeneity of the samples.

As in the previous study of lithium disilicate [1], it was observed that the temperature gradient dictated both the electrical and crystallographic alignment. In all samples the polar orientation was antiparallel to the direction in which crystallization proceeds into the glass, with the positive end of the dipole pointing toward the high-temperature end of the sample, as depicted in Fig. 3. There may be several causes for the polar alignment of the crystallites. One possible cause is the existence of high local electric fields resulting from surface pyroelectric charges [10]. These local electric fields might dictate the orientation of the dipoles as crystallization proceeds into the glass. A second possible cause is the nature of the surface chemistry. It is known that low charge cations such as Li^+ or Ba^{2+} migrate to the surface upon heating [11]. This higher surface concentration of cations could influence the nature of both the crystallization and polar orientation. It is possible that as the crystallization proceeds into the bulk of the glass, starting from a cation-rich surface, the positive end of the dipole moments in the crystallites will be directed toward the hot surface.

The pyroelectric response on the glass ceramics was studied by the dynamic Chynoweth method. Pyroelectric voltage responses of between 50 and 60% of the single-crystal values were obtained reproducibly with the glass-ceramic samples. The sign of the pyroelectric coefficient is negative for BTG single crystals and positive for BTS. A similar difference in sign was observed with glass-ceramics. For a simple pyroelectric detector, the figure of merit is given by p/ϵ, where p is the pyroelectric coefficient and ϵ is the dielectric permittivity. The pyroelectric coefficients of single crystals of $Ba_2TiGe_2O_8$ and $Ba_2TiSi_2O_8$ are 3 and $10\,\mu C\,m^{-2}\,°C^{-1}$, respectively [12]. Since the dielectric constants of the glass-ceramics are comparable with those of single crystals, it can be concluded that the pyroelectric coefficients of the glass-ceramics are of the same order of magnitude as those of the single crystals. Specimens of 100 to $500\,\mu m$ in thickness were studied during pyroelectric tests. Samples of large surface area and less than $100\,\mu m$ in thickness were mechanically strong and gave reproducible results, suggesting their use as pyroelectric detectors.

4. Conclusions

Glass-ceramics of composition $Ba_2TiGe_2O_8$ and $Ba_2TiSi_2O_8$ were prepared by crystallizing the glasses in a temperature gradient. The glass-ceramics show preferred orientation, with the polar c-axis parallel to the temperature gradient. Pyroelectric responses up to 50% of the single-crystal values were observed on these glass-ceramic samples. Measurement of the density, dielectric constant, and piezoelectric constant gave results comparable to the reported single-crystal properties.

Acknowledgement

We wish to thank our colleagues at the Materials Research Laboratory for their advice and assistance. This work was sponsored by the U.S. Army Office of Research and Development (Contract Grant No. DAAG29-78-0033) and by Defense Advanced Research Projects Agency (Contract DARPA Project No. P-15124-MS).

References

1. G. J. GARDOPEE, R. E. NEWNHAM, A. G. HALLIYAL and A. S. BHALLA, *Appl. Phys. Lett.* 36 (1980) 817.
2. M. KIMURA, Y. FUGINO and T. KAWAMURA, *ibid.* 29 (1976) 227.
3. M. KIMURA, K. DOI, S. NANAMATSU and T. KAWAMURA, *ibid.* 23 (1973) 531.
4. M. KIMURA, K. UTSUMI and S. NANAMATSU, *ibid.* 47 (1976) 2249.

5. A. HERCZOG, *J. Amer. Ceram. Soc.* 47 (1964) 107.
6. N. F. BORRELLI and M. M. LAYTON, *J. Non-Cryst. Sol.* 6 (1971) 197.
7. D. E. RASE and R. ROY, *J. Amer. Ceram. Soc.* 38 (1955) 393.
8. A. G. CHYNOWETH, *J. Appl. Phys.* 27 (1956) 78.
9. D. I. H. ATKINSON and P. W. McMILLAN, *J. Mater. Sci.* 12 (1977) 443.
10. P. E. BLOOMFIELD, I. LEFKOWITZ and A. D. ARONOFF, *Phys. Rev. B* 4 (1971) 974.
11. G. E. RINDONE, in Proceedings of the Symposium on Nucleation and Crystallization in Glasses and Melts, edited by M. K. Roser, G. Smith and H. Insley (American Ceramic Society, Columbus, Ohio, 1962) pp. 63–69.
12. A. S. BHALLA, unpublished work.

Received 4 July and accepted 22 September 1980.

Appendix 5

Piezoelectric and Elastic Properties of Barium Germanium Titanate and Lithium Borosilicate Glass-Ceramics

A. Halliyal, A. S. Bhalla, R. E. Newnham, and L. E. Cross

PIEZOELECTRIC AND ELASTIC PROPERTIES OF BARIUM GERMANIUM TITANATE AND LITHIUM BOROSILICATE GLASS-CERAMICS

A. Halliyal, A.S. Bhalla, R.E. Newnham, and L.E. Cross

Materials Research Laboratory
The Pennsylvania State University
University Park, PA 16802

Abstract

Piezoelectric barium germanium titanate and lithium borosilicate glass-ceramics were prepared by crystallizing the glasses in a temperature gradient. The piezoelectric constants electromechanical coupling factors and elastic constants of the glass-ceramics were measured by the resonance method. Some of the glass-ceramics exhibit high electromechanical coupling factors and low temperature coefficient of resonance making them of interest as temperature compensated resonators.

Introduction

Several nonferroelectric polar glass-ceramics have been studied from the point of view of their application in piezoelectric devices and pyroelectric detectors[1-5]. It has been shown that it is possible to prepare glass-ceramics with good crystallographic and polar orientation by crystallizing the glasses in a temperature gradient resulting in glass ceramics with reasonably good piezoelectric properties. Detailed studies of the piezoelectric properties of barium germanium titanate[3] and lithium borosilicate[4] glass ceramics showed that the piezoelectric properties of these glass-ceramics are comparable to those of commonly used piezoelectric materials. Some glass ceramics in the Li_2O-SiO_2-B_2O_3 system showed high electromechanical coupling coefficients and low temperature coefficient of resonance (TCR)[4]. It has been suggested that because of their good electromechanical properties and a high degree of crystallographic orientation near the glass-ceramic surfaces, lithium borosilicate glass-ceramics might find an application in SAW devices[4].

Glass ceramic piezoelectrics can be easily fabricated in large sizes and their properties can be optimized by adjusting the glass composition and processing parameters.

In the present paper we report elastic and piezoelectric measurements on fresnoite ($Ba_2Si_2TiO_8$) glass ceramics and a few compositions in the Li_2O-SiO_2-B_2O_3 system. Piezoelectric, elastic and electromechanical coefficients of glass ceramics of composition $Ba_2Ge_2TiO_8$ (BGT), $Ba_2Ge_2TiO_8$-$Ba_2Si_2TiO_8$ solid solution (BGST) with excess silica, and Li_2O-$(2-x)SiO_2$-xB_2O_3 glass-ceramics here investigated by resonance methods. The measured values are compared with the reported properties of $Ba_2Ge_2TiO_8$ and $Ba_2Si_2TiO_8$ single crystals.

Experimental Procedure

The procedure followed for preparing glass-ceramics with oriented crystallites is essentially the same as that reported in earlier studies[2,3]. The glass samples were prepared by mixing reagent grade chemicals in the desired molar ratio and melting in a platinum crucible, using a globar furnace. The glass samples were crystallized in a temperature gradient by placing polished glass disks on a microscope hot stage*. Details concerning the heating cycles employed during crystallization of the glasses can be found in references 1-3. The crystalline phases in the glass-ceramic samples were identified from x-ray powder diffraction patterns.

Piezoelectric constant d_{33} parallel to the crystallization direction was measured using a d_{33}-meter**. For resonance studies, samples were prepared in the form of circular disks 8 mm in diameter and 0.3 to 0.6 mm in thickness. Gold electrodes were sputtered on the polished surfaces. Resonance behavior in the thickness mode and planar mode were investigated using a spectrum analyzer†. The resonance frequency constants, electromechanical coupling factors and mechanical quality factor Q were determined by measuring the resonance and anti resonance frequencies. From these values, some of the elastic and piezoelectric coefficients were calculated. The temperature coefficient of resonance (TCR) was evaluated by measuring the resonance frequency as a function of temperature at intervals of 5° in the temperature range -20 to 100°C.

Results and Discussion

The crystalline phases identified from the x-ray powder diffraction patterns are listed in Table 1, along with the densities and dielectric constants. All the crystalline phases belong to polar point groups, and hence the piezoelectric properties of the glass-ceramic are not diluted by inactive phases. The densities and dielectric constants of BGT and BGST glass-ceramics are in close agreement with those of $Ba_2Ge_2TiO_8$ and $Ba_2Si_2TiO_8$ single crystals.

*E. Leitz, Inc., Rochleigh, NJ, Model No. 493.
**Channel Products, Chesterland, OH, Model CPDT 3300
†Hewlett-Packard, Loveland, CO, Model 3585A.

0090-5607/81/0000-0315 $00.75 © 1981 IEEE

Table 1.

Physical Properties of Glass-Ceramics

Composition	Crystalline* Phases	Dielectric constant ϵ_{33}/ϵ_o	ρ gm/cm^3
$2BaO-2GeO_2-TiO_2$ (BGT)	B_2TG_2	15	4.8
$2BaO-2SiO_2-GeO_2-TiO_2$ (BGST)	$B_2TG_2 + B_2TS_2$ (solid solution)	10.3	4.3
$Li_2O-1.8SiO_2-0.2B_2O_3$	$LS_2 + LB_2 + LS$	9	2.3
$Li_2O-1.33SiO_2-0.66B_2O_3$	$LS_2 + LB_2 + LS$	8	2.3
$Ba_2Ge_2TiO_8$ (Single crystal)	-----	13	4.84
$Ba_2Si_2TiO_8$ (single crystal)	-----	11	4.45

*Abbreviation for Phases: $B_2TG_2 = Ba_2Ge_2TiO_8$, $B_2TS_2 = Ba_2Si_2TiO_8$, $LS_2 = Li_2O \cdot 2SiO_2$, $LB_2 = Li_2O \cdot 2B_2O_3$, $LS = Li_2O \cdot SiO_2$.

As mentioned earlier, the glass-ceramics prepared by crystallizing the glasses in a temperature gradient show a high degree of crystallographic orientation parallel to the temperature gradient. Needle-like crystallites grow from the hot face deep into the sample along the direction of the temperature gradient[1-3]. The c-axes of the crystallites show preferred orientation but the a or b do not. The alignment of the polar c-axes is responsible for the pyroelectric and piezoelectric properties of the glass ceramics. The properties of the glass ceramics are isotropic in the plane perpendicular to the c-axes of the crystallites.

A ferroelectric ceramic material prepared by conventional sintering methods is non-piezoelectric even though the individual crystals may be strongly piezoelectric. To convert the ceramic into a piezoelectric, it is necessary to pole the ceramic with an external electric field[6].

Thus the symmetry of a poled ceramic body is ∞m and for piezoelectric and elastic phenomena this is equivalent to hexagonal symmetry 6 mm. Since the polar glass-ceramics with oriented crystallites and the poled ceramics both have only one polar direction, the symmetries are the same (∞m). The independent, non-zero elastic, piezoelectric and dielectric constants for this symmetry are s_{11}, s_{12}, s_{13}, s_{33}, s_{55}, d_{31}, d_{33}, d_{15}; ϵ_{11} and ϵ_{33}. Additional non zero coefficients are related to these by symmetry relations.

The values of piezoelectric d coefficients, the elastic constants and the electromechanical coupling coefficients of the glass-ceramics are given in Table 2. The values of piezoelectric d coefficients and elastic coefficients of BGT and BGST glass-ceramics are comparable to the values of $Ba_2Ge_2TiO_8$ and $Ba_2Si_2TiO_8$ single crystals, from which we conclude that there are no substantial differences in the elastic behavior of the glass and crystalline phases in the glass-ceramics.

The electromechanical coupling coefficients k_t and k_p of BGT glass-ceramics are lower than the corresponding values of $Ba_2Ge_2TiO_8$ single crystal[3], but those of BGST glass-ceramics are slightly higher. The planar coupling k_p of $Li_2O-1.8SiO_2-0.2B_2O_3$ glass ceramic[4] is higher than $LiTaO_3$ and other commonly used piezoelectric materials. The mechanical quality factors Q are surprisingly high for the glass-ceramics (300-1000).

A typical resonance spectrum observed in glass-ceramic samples is shown in Figure 1, and plot of relative resonance frequency Δf_R as a function of temperature is shown in Figure 2, where

$$\Delta f_R = \frac{f_T - f_{RT}}{f_{RT}} .$$

Here, f_T is the resonance frequency at temperature T and f_{RT} is the resonance frequency at room temperature. The temperature coefficients of resonance (TCR), calculated from the slopes of Δf_R vs T plots are listed in Table 2.

The TCR values of BGT and BGST glass-ceramics are larger than those of either $Ba_2Ge_2TiO_8$ and $Ba_2Si_2TiO_8$ single crystals. For lithium borosilicate glass ceramics the TCR values are comparable to the values of commonly used piezoelectric single crystals[4]. TCR of $Li_2O-1.33SiO_2-0.66-B_2O_3$ glass-ceramic is 30 ppm/°C in the temperature range 20-60°C (Fig. 2), the useful operating range for most piezoelectric devices.

The strong dependence of the electromechanical coupling coefficients and TCR on the composition of the parent glass suggests that further improvements in the properties are possible by suitably modifying the composition. In addition, the amount and orientation of the different crystalline phases can be controlled by emplying suitable heat treatment cycles providing another controlling factor to tailor the properties of glass-ceramics.

Summary

The piezoelectric coefficients and elastic constants of several piezoelectric glass-ceramics were measured by resonance methods. It is possib to fabricate large inexpensive glass-ceramic piezoelectric devices with substantial electromechanical coupling factors and low TCR. The

Table 2.

Piezoelectric and Elastic Constants

Property	$Ba_2Ge_2TiO_8$ Glass-Ceramic	BGST Glass-Ceramic	$Ba_2Ge_2TiO_8$ Single Crystal	$Ba_2Si_2TiO_8$ Single Crystal	Li_2O-1.8SiO_2-0.2B_2O_3	Li_2O-1.33SiO_2-0.66B_2O_3
d_{33}x10^{-12}C/N	6	6	8	3.8	6	3
d_{31}x10^{-12}C/N	1.2	2.1	2.0	2.7	2.4	1.5
s_{11}x10^{-12}m^2/N	9.2	9.0	8.8	7.6	9.5	11
s_{12}x10^{-12}m^2/N	-1.9	-2.3	-1.9	-1.6	-2.4	-2.8
s_{66}x10^{-12}m^2/N	22	22	21	17	24	27
c_{33}x10^{12}N/m^2	0.13	0.12	0.09	0.08	---	---
N_t(mt. Hz)	2500	2600	2150	---	---	---
N_p(mt. Hz)	3100	3500	2900	---	4500	4200
k_t	0.075	0.15	0.10	---	---	---
k_p	0.045	0.12	0.10	---	0.14	0.09
k_{31}	0.04	0.07	0.06	0.10	0.09	0.05
Q	700	300	---	650	1000	400
TCR ppm/°C (0-100°C) z-cut	95	>100	48	51	60	30 (20-60°C)

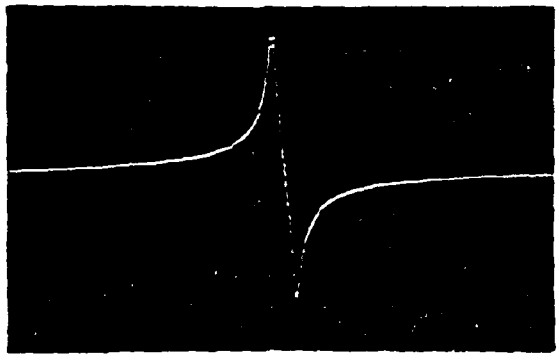

Figure 1. Resonance spectrum for Li_2O-1.8SiO_2-0.2B_2O_3 (horizontal scale = 6.8 kHz vertical = 5 dB).

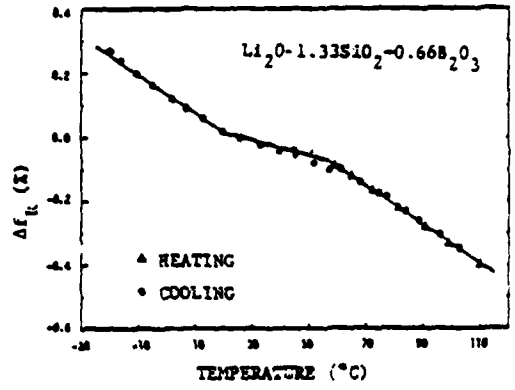

Figure 2. Relative resonance frequency as a function of temperature for Li_2O-1.33SiO_2-0.66B_2O_3.

piezoelectric properties of the glass-ceramics are comparable to those of single crystals, and can be optimized by proper choice of composition and heat treatment. The glass-ceramic piezoelectric materials may be useful in temperature compensated bulk resonators, in SAW devices and in flexural mode resonators.

Acknowledgment

This work was sponsored by the U.S. Army Research Office (DAAG29-80-C-0006).

References

1. G.J. Gardopee, R.E. Newnham, A.S. Bhalla, Ferroelectrics 33, 155 (1981).
2. A. Halliyal, A.S. Bhalla, R.E. Newnham, L.E. Cross, J. Mater. Sci. 16, 1023 (1981).
3. A. Halliyal, A.S. Bhalla, R.E. Newnham, L.E. Cross, and T.R. Gururaja, J. Mater. Sci. (accepted).
4. A. Halliyal, A.S. Bhalla, R.E. Newnham, L.E. Cross, J. Appl. Phys. (accepted).
5. A. Halliyal, A.S. Bhalla, R.E. Newnham, L.E. Cross, Ferroelectrics (1981) (accepted).
6. B. Jaffe, W.R. Cook, Jr., and H. Jaffee, Piezoelectric Ceramics, Academic Press, London and NY (1971).

Appendix 6

Study of the Piezoelectric Properties of $Ba_2Ge_2TiO_8$ Glass-Ceramic and Single Crystals

A. Halliyal, A. S. Bhalla, R. E. Newnham, L. E. Cross, T. R. Gururaja

JOURNAL OF MATERIALS SCIENCE 17 (1982) 295–300

Study of the piezoelectric properties of $Ba_2Ge_2TiO_8$ glass-ceramic and single crystals

A. HALLIYAL, A. S. BHALLA, R. E. NEWNHAM,
L. E. CROSS, T R. GURURAJA
Materials Research Laboratory, The Pennsylvania State University, University Park, PA 16802, USA

Glass-ceramics of composition $Ba_2Ge_2TiO_8$ with oriented crystallites were prepared by crystallizing the glasses in a temperature gradient. The degree of preferred orientation of the crystallites as a function of depth was studied. Piezoelectric resonance properties of both the glass-ceramics and the single crystals were studied. The piezoelectric d_{33} coefficient, the frequency constants and the electromechanical coupling coefficients of the glass-ceramic were comparable to the single-crystal values.

1. Introduction

A technique for fabricating glass-ceramics of lithium disilicate ($Li_2O \cdot 2SiO_2$) and barium germanium titanate ($Ba_2Ge_2TiO_8$; BGT) has been reported in our earlier studies [1–3]. It was observed that the crystallization behaviour of glass-ceramics is influenced strongly by the heating cycle employed during the crystallization of the glasses. Two kinds of heat treatments were investigated: (a) heating under uniform isothermal environment and (b) heating with temperature gradients across the sample. Detailed studies of the microstructure and X-ray diffractometer patterns of the crystallized samples showed a considerable degree of crystallographoc orientation, in both cases. However, the piezoelectric d_{33} values and the pyroelectric responses of BGT glass-ceramics prepared under the temperature gradient were much higher than the respective properties of the samples prepared in isothermal conditions, indicating a strong polar orientation in the samples prepared by the former method. In addition, the d_{33} value of the BGT glass-ceramic was comparable to that of single crystals. These facts led us to investigate the piezoelectric properties of BGT glass-ceramic in greater detail.

Barium germanium titanate is a non-ferroelectric–ferroelastic [4] below 810° C, belonging to the orthorhombic polar points group mm2. In the paraelectric phase above 810° C it is in tetragonal point group 4 mm. Some of the elastic and piezoelectric properties of BGT single crystals have been reported [4–5], but detailed investigations of the piezoelectric properties have not been carried out. Single crystals of BGT have been grown by Czochralski and Bridgman techniques. However, the Bridgman technique yields a poor quality crystal, and Czochralski-grown crystals often contain a small cloudy core, perhaps associated with radial microcracks. Frequently the crystals contain microtwin domains. Hence, it was felt that it might be useful to investigate the piezoelectric properties of BGT glass-ceramics. In the case of several piezoelectric materials, which can be prepared easily in the form of glass, it is possible that simple glass-ceramic processing techniques could be useful in making large-area non-ferroelectric–piezoelectric resonant elements.

Since the thickness of the highly oriented region in the glass-ceramic depends on the heating cycle employed for crystallization, a systematic study to obtain well-oriented samples of desired thickness has been carried out. Also, in the present study, the piezoelectric resonance properties of BGT glass-ceramic and single crystal are compared. To our knowledge this is the first time that the resonance properties of non-ferroelectric–piezoelectric glass-ceramics have been reported.

2. Experimental details

The procedure for preparing BGT glass-ceramic with oriented crystallites is essentially the same

0022–2461/82/010295–06$02.60/0

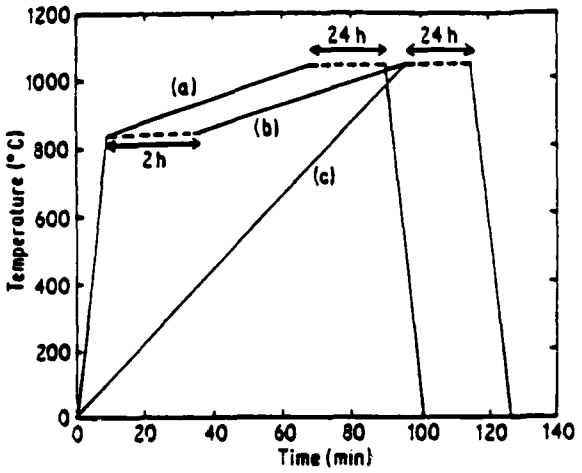

Figure 1 Heating cycles for crystallizing BGT glasses.

as reported in the previous study [3]. The glass samples were prepared by mixing reagent grade chemicals in the required stoichiometric proportion and melting in a globar furnace. Differential thermal analysis (DTA) measurements indicated that the crystallization temperature of the glass was 800° C. The glass samples were crystallized in a temperature gradient by placing the polished glass samples in the form of thick discs on a microscopic hot stage.* An alumina substrate (0.5 mm thick) was placed below the glass samples to provide a uniform temperature gradient in the vertical direction. Heating cycles slightly different from the previous study [1] were used to compensate for the reduction in temperature near the hot face due to the alumina substrate. Three types of heating cycles were used, as shown in Fig. 1. The heating cycle (a) consisted of an initial rapid rise in temperature to minimize volume nucleation, followed by a slow increase in temperature at a rate of about 3° C min^{-1}. After reaching the maximum temperature (1040° C), the samples were held at this temperature for 24 h. The temperature was then decreased rapidly to room temperature. Cycle (b) was the same as Cycle (a), except that it included a two-hour nucleation step at 840° C. Cycle (c) represents isothermal crystallization carried out in a furnace, with no temperature gradient. The thickness of the crystallized portions of the glasses ranged from 1 to 2 mm in the case of heating cycles (a) and (b).

The degree of preferred orientation of the glass-ceramic was evaluated from X-ray diffractometer patterns, recorded on surfaces normal to the direction of the temperature gradient [3]. The X-ray diffraction patterns of the glass-ceramics prepared by following the above three types of heating cycles were compared with the standard powder patterns to determine the relative degree of orientation.

The piezoelectric constant d_{33} parallel to the crystallization direction was determined using a d_{33}-meter.† For resonance studies, samples in the shape of circular discs of dimensions approximately 2.5 to 3 mm diameter and 0.5 to 0.75 mm in thickness were prepared. From single-crystal samples grown by Czochralski-pulling along the c-axis, circular discs were prepared in a similar way, with the c-axis perpendicular to the major faces. Gold electrodes were sputtered onto the polished surfaces. Resonance behaviour in the pure thickness mode and planar modes was studied by the resonance and anti-resonance method using a spectrum analyser.‡ The resonance frequency constants, the electromechanical coupling factors and the mechanical quality factor Q were determined both for the glass-ceramic and the single-crystal samples by measuring the resonance (f_r) and anti-resonance (f_a) frequencies. The temperature coefficient of the resonance frequency in a thickness mode was studied by measuring the resonance frequency at intervals of 5° C.

3. Results and discussion

3.1. Crystallization behaviour

The glass-ceramic samples showed highly oriented growth of crystallites in a direction parallel to the temperature gradient, with the polar c-axis perpendicular to the hot surface of the sample [3]. The 0 0 2 reflection was the strongest in the X-ray diffraction patterns of the crystallized surfaces. The ratio of the intensity of the 0 0 2 peak to that of the 2 1 1 peak was taken as a measure of the relative degree of orientation. The intensity ratios were measured for glass-ceramic samples at various depths from the surface facing the hotter temperature zone by polishing-off successive layers. Fig. 2 shows the variation of I_{002}/I_{211} as a function of depth for the glass-ceramic samples prepared by following the three different heating cycles mentioned earlier. In general, a high degree of orien-

*E. Leitz, Inc., Rockleigh, New Jersey, USA: Model No. 493.
†Channel Products, Chesterland, Ohio, USA: Model CPDT 3300.
‡Hewlett-Packard, Loveland, Columbia, USA: Model 3585 A.

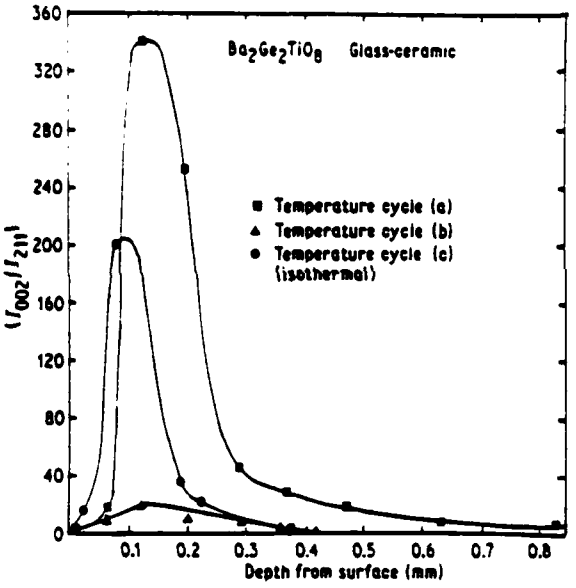

Figure 2 The degree of preferred orientation as a function of depth for different heating cycles.

tation is observed in all the cases, at a depth of about 100 μm from the high-temperature face. In all three cases it was observed that the flatness of the glass surface was lost after crystallization. Hence, it is possible that the apparent reduction in the degree of orientation observed near the high-temperature face is due to the unevenness of the glass-ceramic surface after crystallization rather than to the actual misorientation of the crystallites near the hot face. This was evident from the fact that the I_{002}/I_{211} ratio showed a maximum value at a depth where the surface of the glass-ceramic became completely flat after polishing. As is to be expected, the samples prepared by following the Cycle (b), which included a nucleation step also, showed a poor degree of orientation compared to the samples prepared by following the Cycles (a) or (c).

Even though the samples crystallized isothermally (Cycle c) exhibited crystallographic orientation to a certain extent, these samples had a lower d_{33} (3 to 4 x 10^{-12} C N^{-1}) compared to the samples crystallized in a temperature gradient (5 to 7 x 10^{-12} C N^{-1}) (Cycle a), indicating that crystallization in a temperature gradient leads to a better polar orientation also. However, the highest degree of orientation was observed in the case of samples prepared by following Cycle (a), which did not include the intermediate nucleation step. Also, the depth of oriented region was much greater in this case.

Hence, for studying the piezoelectric properties of the glass-ceramics, the samples were prepared by crystallizing the glasses according to the Cycle (a). All the piezoelectric properties of the glass-ceramic samples mentioned in this paper refer to the glass-ceramic samples prepared by following Cycle (a).

3.2. Piezoelectric properties

Resonance spectra for the thickness mode are shown in Fig. 3 for both the glass-ceramic and single-crystal samples. Resonance in the planar mode was weak compared to the resonance signal in the thickness mode. Resonance spectra in the radial mode are shown in Fig. 4. The radial mode of vibration was very weak for the glass-ceramic samples. This is not surprising, since the crystallites in the glass-ceramics are oriented only along the *c*-direction, there being no preferred orientation along the *a*- or *b*-axes. In addition, there is a glassy phase surrounding the crystallites. Both these factors might be responsible for the weakening of the radial mode vibration in the glass-ceramic samples. In Table I, the measured resonance properties of the glass-ceramic and the single crystal are summarized. The reported values for

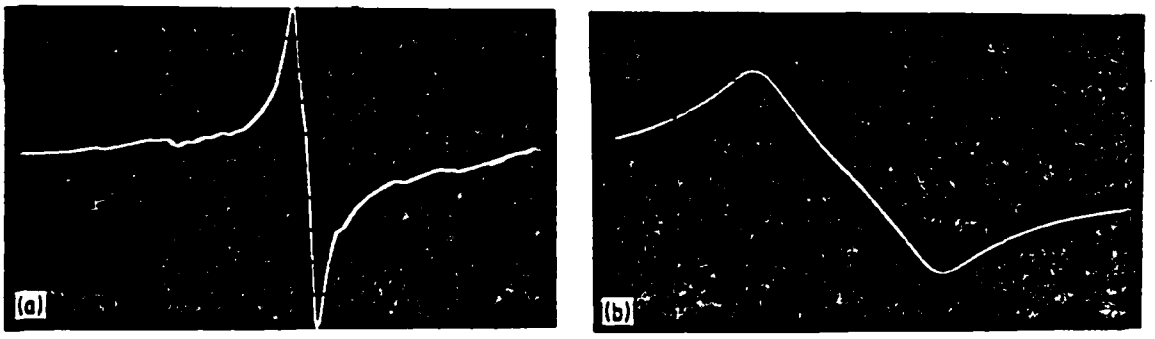

Figure 3 Resonance spectra in the thickness mode. (a) BGT glass-ceramic, horizontal scale = 31 kHz; (b) BGT single crystal, horizontal scale = 3.06 kHz.

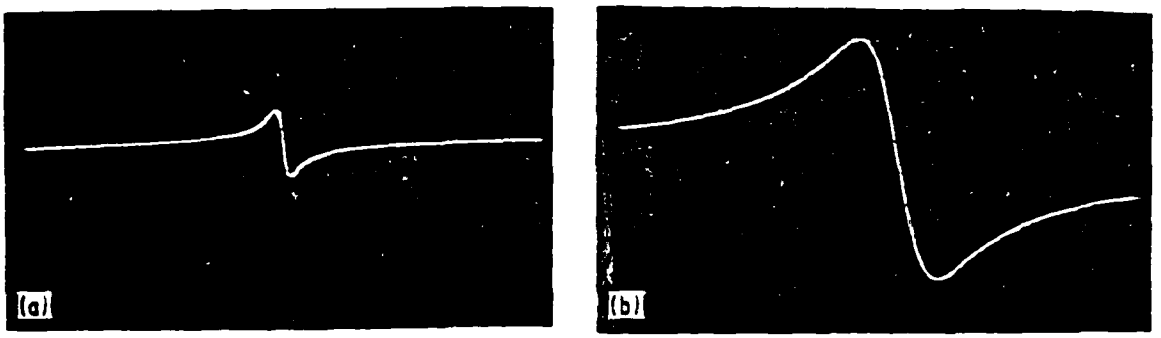

Figure 4 Resonance spectra in the radial mode. (a) BGT glass-ceramic, horizontal scale = 3 kHz; (b) BGT single crystal, horizontal scale = 1.1 kHz.

the 3–3 coupling are also given for comparison. The measured values of N_t and k_t in our single-crystal samples were higher than the reported value. This is perhaps because the Czochralski-grown crystals used in our experiments were of better quality than the crystals used in previous studies [4], which were grown by the Bridgman technique.

The variation in resonance frequency constant, N_t, with temperature was studied in the temperature range − 10 to 150° C. The relative resonance frequency Δf_R as a function of temperature for both the glass-ceramic and single crystal is plotted in Fig. 5, where

$$\Delta f_R = \frac{f_T - f_{RT}}{f_{RT}}.$$

Here f_T is the resonance frequency at temperature T and f_{RT} is the resonance frequency at room temperature. The temperature coefficients of resonance (TCR), calculated from the slopes of Δf_R against T plots are given in Table I.

The electromechanical coupling factor k_t was calculated by using the equation

$$k_t^2 = [(\pi/2) f_r/f_a] \tan [(\pi/2)\Delta f/f_a].$$

The room-temperature values of k_t are given in Table I. The temperature dependence of k_t is shown in Fig. 6. For single crystal, k_t is practically constant in the temperature range − 10 to 150° C, increasing slightly with temperature. For the glass-ceramic, k_t increases slowly with temperature.

Values of the mechanical quality factor Q are given in Table I. Difficulties were encountered in the measurement of Q, due to the small values of capacitances of the sample. Spurious resonance signals were observed with large-area glass-ceramic samples. Measurements indicated that $Ba_2Ge_2TiO_8$ has a high Q of about 700.

The temperature coefficients of resonance of some of the commonly used piezoelectric materials [7] are given in Table II for comparison. The TCR of $Ba_2Ge_2TiO_8$ single crystals is comparable to that of $Ba_2Si_2TiO_8$. It has been reported [8, 9] that $Ba_2Si_2TiO_8$ (fresnoite) is a good candidate material for surface acoustic wave (SAW) devices. The shear-mode piezoelectric surface wave of $Ba_2Si_2TiO_8$ has a coupling coefficient $k^2 = 0.0053$.

TABLE I Piezoelectric properties of $Ba_2Ge_2TiO_8$ determined by the resonance method

Property	Glass-ceramic	Single crystal	Reported values in the 3–3 mode
ϵ_{33}/ϵ_0	15	13	–
d_{33} (× 10^{-12} C N^{-1})	5–7	10	–
Frequency constant N_t (Hz m)	2500	2150	N_{33} = 1900
Thickness coupling coefficient k_t	0.075	0.10	k_{33} = 0.07 k_{15} = 0.27 k_{24} = 0.31
Mechanical quality factor Q	700	650	–
Temperature coefficient of resonance, $T_{fr} = \frac{1}{f_r}\frac{\partial f_r}{\partial T}$ (ppm/° C)	95	48	–
Frequency constant N_p (Hz m)	3100	2900	
Planar coupling coefficient k_p	0.044	0.062	

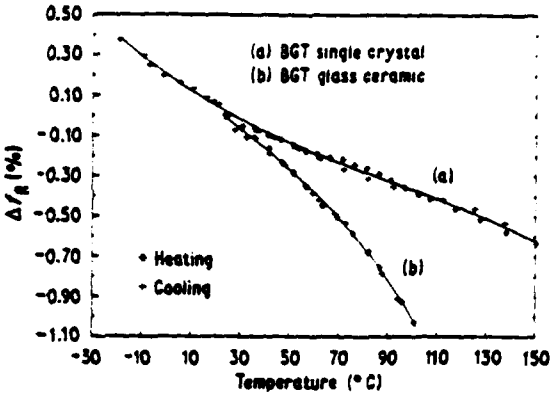

Figure 5 Relative resonance frequency as a function of temperature.

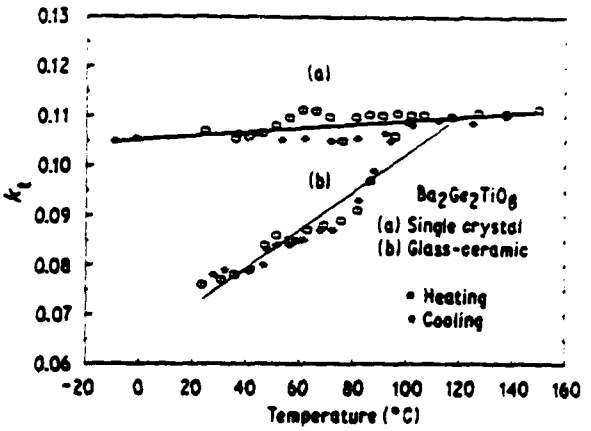

Figure 6 Variation of k_t with temperature.

which is three times larger than that of quartz ($k^2 = 0.0014$). It has a small TCR (38 ppm/° C for *X*-cut and *Y*-propagation) and a small surface velocity. The SAW characteristics of fresnoite can be further improved by partial substitution of Sr for Ba (i.e., $Ba_{2-x}Sr_xTiSi_2O_8$), with almost no change in the electromechanical coupling factor [10]. For *Z*-cuts with ⟨1 1 0⟩ propagating waves, the TCR drops from 51 to 21 ppm/° C at a Sr concentration of $x = 0.8$, which is comparable to the TCR of $LiTaO_3$. BGT also exhibits large electromechanical coupling in a pure thickness shear mode with values of $k_{15} = 0.27$ and $k_{24} = 0.31$. The SAW characteristics of $Ba_2Ge_2TiO_8$ single crystal are to be explored and this aspect needs further study.

The TCR of BGT glass-ceramics is about 95 ppm/° C, which is higher than the single-crystal value. However, further studies are necessary to explore the possibilities of fabricating BGT glass-ceramics with improved temperature compensation, by controlled crystallization of the BGT glasses, and by modifying the composition of the glasses. The present studies demonstrate the possibility of preparing glass-ceramic piezoelectric resonant elements with reasonably good piezoelectric properties from a non-ferroelectric–peizoelectric material. Piezoelectric glass-ceramics in which the crystalline component has tetragonal or higher symmetry should have a high degree of homogeneity in properties for the surface perpendicular to the polar crystallite axis and in consequence should show strong radial coupling. Such systems may have application in SAW devices.

Under controlled crystallization a desired thickness of the thin glass plate can be crystallized into a glass-ceramic layer and such composite elements may be useful for device applications based on flexural resonance modes.

4. Conclusion

Glass-ceramics of composition $Ba_2Ge_2TiO_8$ were prepared by crystallizing the glasses in a temperature gradient. The glass-ceramics show preferred orientation, with the polar *c*-axis parallel to the temperature gradient. The depth of the oriented region depends on the heating cycle employed. The piezoelectric resonance properties of the glass-ceramics are in agreement with the single-crystal properties. Measurement of piezoelectric d_{33} and electromechanical coupling coefficients

TABLE II TCR of some piezoelectric materials

Material	Orientation	TCR (ppm/° C)	Reference
$LiNbO_3$	*Y*-cut, *Z*-propagation	94	[7]
Quartz	ST-cut, *X*-propagation	0	[7]
$LiTaO_3$	*Y*-cut, *Z*-propagation	35	[7]
$Ba_2Si_2TiO_8$ (+ 10 to + 60° C)	*X*-cut, *Y*-propagation	38	[7]
	Z-cut, ⟨1 1 0⟩	51	[9]
$Ba_2Ge_2TiO_8$ (+ 10 to + 60° C)	*Z*-cut	48	Present data
$Ba_2Ge_2TiO_8$ (glass-ceramic, 0–60° C)	*Z*-surfaces	95	Present data
$(Ba_{1-x}Sr_x)Si_2TiO_8$ (+ 10 to + 60° C)	*Z*-cut, ⟨1 1 0⟩	21	[9]

on both the glass-ceramic and single crystals gave comparable results. We suggest that in the case of piezoelectric materials which can be prepared in the form of glass, it is possible to employ simple glass-ceramic processing techniques to produce glass-ceramics with useful piezoelectric properties.

Acknowledgement

This work was sponsored by the US Army Research Office (DAAG29-80-C-008).

References

1. G. GARDOPEE, R. E. NEWNHAM, A. HALLIYAL and A. S. BHALLA, *Appl. Phys. Lett.* 36 (1980) 817.
2. A. S. BHALLA, G. GARDOPEE and R. E. NEWNHAM, *Ferroelectrics* 27 (1980) 123.
3. A. HALLIYAL, A. S. BHALLA, R. E. NEWHAM and L. E. CROSS, *J. Mater. Sci.* 16 (1981) 1023.
4. M. KIMURA, K. DOI, S. NANAMATSU and T. KAWAMURA, *Appl. Phys. Lett.* 23 (1973) 531.
5. M. KIMURA, K. UTSUMI and S. NANAMATSU, *ibid.* 47 (1976) 2249.
6. L. DRAFALL and K. E. SPEAR, *J. Cryst. Growth* 33 (1976) 180.
7. A. J. SLOBODNIK, Jr, *Proc. IEEE* 64 (1976) 581.
8. M. KIMURA, *J. Appl. Phys.* 48 (1977) 2850.
9. H. YAMAUCHI, *ibid.* 49 (1978) 6162.
10. Y. ITO, K. NAGATSUMA and S. ASHIDA, *Appl. Phys. Lett.* 36 (1980) 894.

Received 29 May
and accepted 29 June 1981

Appendix 7

Piezoelectric Properties of Lithium Borosilicate Glass Ceramics

A. Halliyal, A. S. Bhalla, R. E. Newnham, and L. E. Cross

Piezoelectric properties of lithium borosilicate glass ceramics

A. Halliyal, A. S. Bhalla, R. E. Newnham, and L. E. Cross[a)]
Materials Research Laboratory, The Pennsylvania State University, University Park, Pennsylvania 16802

(Received 10 August 1981; accepted for publication 16 September 1981)

Glass ceramics in the system Li_2O-SiO_2-B_2O_3 with oriented crystallites were prepared by crystallizing the glasses in a temperature gradient. Piezoelectric and electromechanical properties of the glass ceramics are reported. Some of the compositions exhibit low temperature coefficient of resonance, comparable to $LiTaO_3$ single crystals. Advantages of fabricating glass-ceramic piezoelectric resonators are described and the possibility of using them in surface acoustic wave (SAW) devices is suggested.

PACS numbers: 43.88. + q, 43.35. + d, 77.60. + v, 81.20.Pe

INTRODUCTION

Glass ceramics of several polar piezoelectric materials (lithium disilicate-LS_2, barium germanium titanate-BGT and barium silicon titanate-BST) have been prepared recently by crystallizing the glasses of stoichiometric composition in a temperature gradient.[1-4] These glass ceramics showed high piezoelectric and pyroelectric responses due to the high degree of crystallographic and polar orientation. The piezoelectric resonance properties of BGT glass ceramics have been reported.[4] The piezoelectric d_{33} coefficients, the frequency constants, and the electromechanical coupling coefficients of the BGT glass ceramics were comparable to the reported single crystal values. The glass ceramic piezoelectric elements may offer several potential advantages over the respective single crystals. Glass ceramics are easier to fabricate and their properties are less sensitive to the impurities compared to their single crystal form. Large area samples can be prepared simply by crystallizing large area glass samples.

In recent years piezoelectric materials have become of increasing importance in the field of surface acoustic wave (SAW) devices.[5,6] Low temperature coefficient of surface velocities and high electromechanical coupling are desirable properties for a material to have to be ideally suitable for SAW device applications. However, an undesirable tradeoff between temperature coefficient of resonance (TCR) and electromechanial coupling factor is observed in most of the materials presently used for SAW devices. For example, *ST*-cut α-quartz exhibits zero TCR but shows weak electromechanical coupling. On the other hand, *y*-cut *z* propagating $LiNbO_3$ shows strong electomechanical coupling, but exhibits a high TCR (94 ppm/°C). Some of the other piezoelectric materials, which exhibit good piezoelectric properties for application in SAW devices, present severe crystal growth problems.[6]

It has been shown that a high degree of crystallographic orientation can be achieved on the glass-ceramic surfaces by crystallizing the glass samples in a large temperature gradient.[4,7] Since the surface waves in SAW devices are generally limited to within a few wavelengths of the surface, piezoelectric glass ceramic materials with oriented crystallites near the surface might find an application in SAW devices.

In this paper we discuss the possibility of tailoring the piezoelectric properties in a glass ceramic to produce resonance elements with low TCR. Glass ceramics in the Li_2O-SiO_2-B_2O_3 system were prepared and their piezoelectric properties were studied. The temperature coefficient of resonance of these glass ceramics was also measured. By proper selection of the glass composition and processing parameters, it is possible to prepare glass ceramics with oriented crystallites of more than one phase from the glass matrix. This provides an extra controlling factor for tailoring the crystalline phases and their piezoelectric properties. The compositions reported here are (1) Li_2O-$1.8SiO_2$-$0.2B_2O_3$ and (2) Li_2O-$1.33SiO_2$-$0.66B_2O_3$, where the proportions are molar ratios.

EXPERIMENTAL DETAILS

The detailed procedure for preparing glass ceramics with oriented crystallites is described elsewhere.[1-4] The glass samples were prepared by mixing reagent grade chemicals in the desired molar ratio and melting in a platinum crucible using a globar furnace. The glass samples were crystallized in a temperature gradient by placing the polished glass samples in the form of thick disks on a microscope hot stage (E. Leitz, Inc., Rockleigh, NJ, Model No. 493). The vertical temperature gradient normal to the surface of the sample was estimated to be about 100 °C mm^{-1} near the hottest temperature zone. Heating cycles similar to those described in the previous studies[1,4] were used. After reaching the maximum temperature (760 °C) the samples were held at that temperature for 24 h. The temperature was then slowly decreased to room temperature. The crystalline phases in the glass-ceramic samples were identified from x-ray powder patterns of crystallized samples. The piezoelectric constant d_{33} parallel to the crystallization direction was measured using a d_{33}-meter (Channel Products, Chesterland, OH, Model CPDT 3300). For resonance studies, samples in the shape of circular disks of 0.8 cm diameter and 0.3–0.6 mm in thickness were prepared. Gold electrodes were sputtered on the polished surfaces. Resonance behavior in the radial mode was studied by the resonance and antiresonance method using a spectrum analyzer (Hewlett-Packard, Loveland, CO, Model 3585A). The resonance frequency constants, the electromechanical coupling factors, and the mechanical quality

[a)]Also affiliated with the Department of Electrical Engineering.

 0021/8979/82/042871-04$02.40

TABLE I. Electromechanical properties of Li_2O-SiO_2-B_2O_3 glass ceramics.

Property	Li_2O-1.8SiO_2-0.2B_2O_3	Li_2O-1.33SiO_2-0.66B_2O_3
Crystalline phases	$Li_2Si_2O_5$ + $Li_2B_4O_7$ + Li_2SiO_3(W)	$Li_2Si_2O_5$ + $Li_2B_4O_7$ + Li_2SiO_3(W)
Density (g/cm³)	2.35	2.33
d_{33}($\times 10^{-12}$ C/N)	6	3
Frequency constant (Hz-m)	4500	4200
Coupling coefficient (k_p)	0.14	0.09
Mechanical quality (Q factor)	1000	400

factor Q were determined by measuring the resonance and antiresonance frequencies. TCR in the planar mode was determined by measuring the resonance frequency at temperature intervals of 5°.

RESULTS AND DISCUSSION

The crystalline phases determined by x-ray diffraction patterns of powdered samples are given in Table I. In the case of composition 1, the major crystalline phase was lithium disilicate ($Li_2Si_2O_5$). Small amounts of lithium metasilicate (Li_2SiO_3) and lithium tetraborate ($Li_2B_4O_7$) were also crystallized. $Li_2Si_2O_5$ phase showed a high degree of preferred orientation in a direction parallel to the temperature gradient with the polar c axis perpendicular to the hot face of the sample.[1] In the case of composition 2, the major phases were lithium discilicate and lithium tetraborate, with lithium metasilicate being the minor phase to crystallize. It is interesting to note that all three phases, Li_2SiO_3, $Li_2Si_2O_5$, and $Li_2B_4O_7$, belong to polar point groups, and hence the problem of diluting the piezoelectric or pyroelectric properties with an inactive phase does not arise. On the other hand there may be an improvement in piezoelectric and pyroelectric properties due to the additive nature of properties in the glass-ceramic composite.

Resonance spectra of the radial mode are shown for both compositions in Figs. 1 and 2. The piezoelectric d_{33} coefficient and other electromechanical properties are listed in Table I. The variation in resonance frequency (f_R) with temperature was studied in the temperature range − 20–100 °C. The relative resonance frequency Δf_R are plotted as a function of temperature in Figs. 3 and 4, where

$$\Delta f_R = \frac{f_T - f_{RT}}{f_{RT}}.$$

Here, f_T is the resonance frequency at temperature T and f_{RT} is the resonance frequency at room temperature. The temperature coefficients of resonance (TCR), calculated from the slopes of Δf_R vs T plots, are given in Table II along with the TCR values and coupling coefficients of some of the commonly used materials for SAW devices.

The piezoelectric d_{33} coefficient, the frequency constant N_p, the mechanical quality factor Q and coupling coefficient k_p were larger for composition 1 than for composition 2. The value k_p (0.14) for composition 1 is slightly higher than the value reported for $Li_2B_4O_7$ single crystals (maximum value of 0.12).

The value of TCR for composition 1 is about 60 ppm/°C in the temperature range − 20–35 °C and 70 ppm/°C in the temperature range 35–100 °C (Fig. 3). For composition 2 the variation of resonance frequency with temperature is interesting (Fig. 4). Below room temperature (below 20 °C) and at higher temperatures (above 65 °C) the value of TCR is 60 ppm/°C. Near room temperature in the temperature range 20–65 °C, which is the useful operating range for most of the

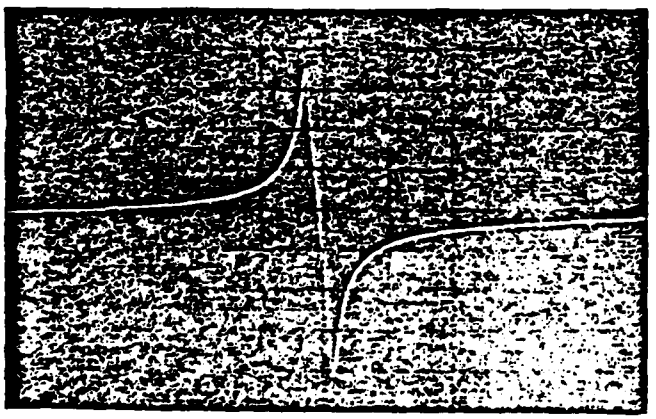

FIG. 1. Resonance spectra in the radial mode for Li_2O-1.8SiO_2-0.2B_2O_3 at room temperature (horizontal scale = 6.8 kHz; vertical scale = 5 dbl.

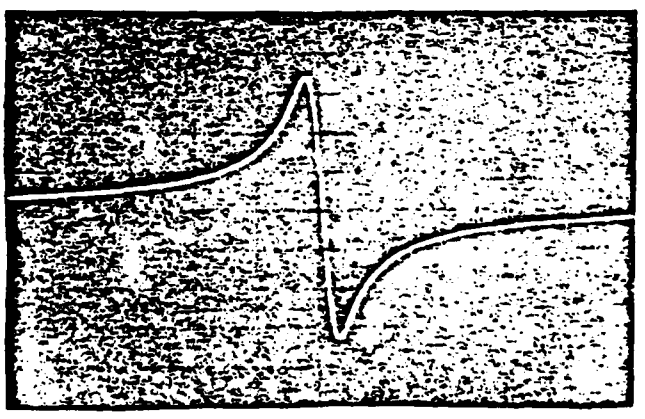

FIG. 2. Resonance spectra in the radial mode for Li_2O-1.33SiO_2-0.66B_2O_3 at room temperature (horizontal scale = 14.9 kHz; vertical scale = 2 db

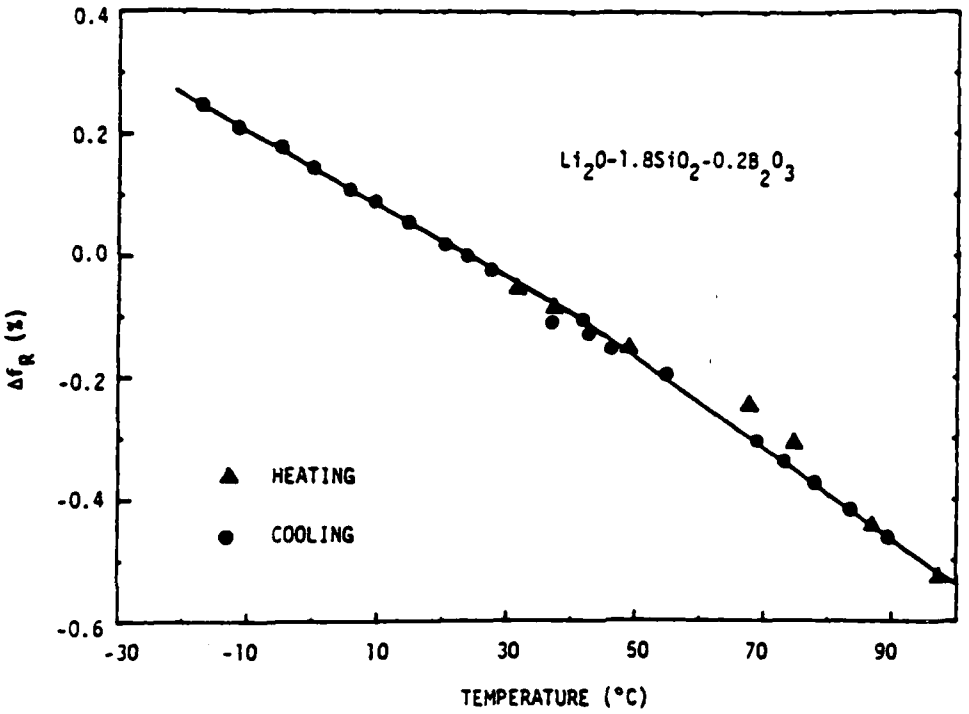

FIG. 3. Relative resonance frequency as a function of temperature for Li_2O-1.8SiO_2-0.2B_2O_3 glass ceramic.

piezoelectric devices, the TCR drops down to a low value of 30 ppm/°C, comparable to the *y*-cut TCR of $LiTaO_3$ measured along the *z* direction. The reproducibility of this behavior was verified by measuring the resonance frequencies of several samples during both the heating and cooling cycles.

The reported values of the surface-wave coupling factor k_s^2 for several single crystals and the measured values of planar coupling coefficient k_p^2 of glass ceramics are also given in Table II. In SAW devices surface-wave coupling coefficient is an important factor, indicative of large bandwidth and low insertion loss. Generally k_s is determined from surface velocity measurements, and k_p is calculated from radial mode resonance frequencies. k_s and k_p are related through the piezoelectric coefficients and dielectric and elastic constants. Materials with high values of k_p generally show good SAW electromechanical coupling.[6]

The velocity of the surface wave v_s is given by

$$v_s = \left(\frac{c}{\rho}\right)^{1/2},$$

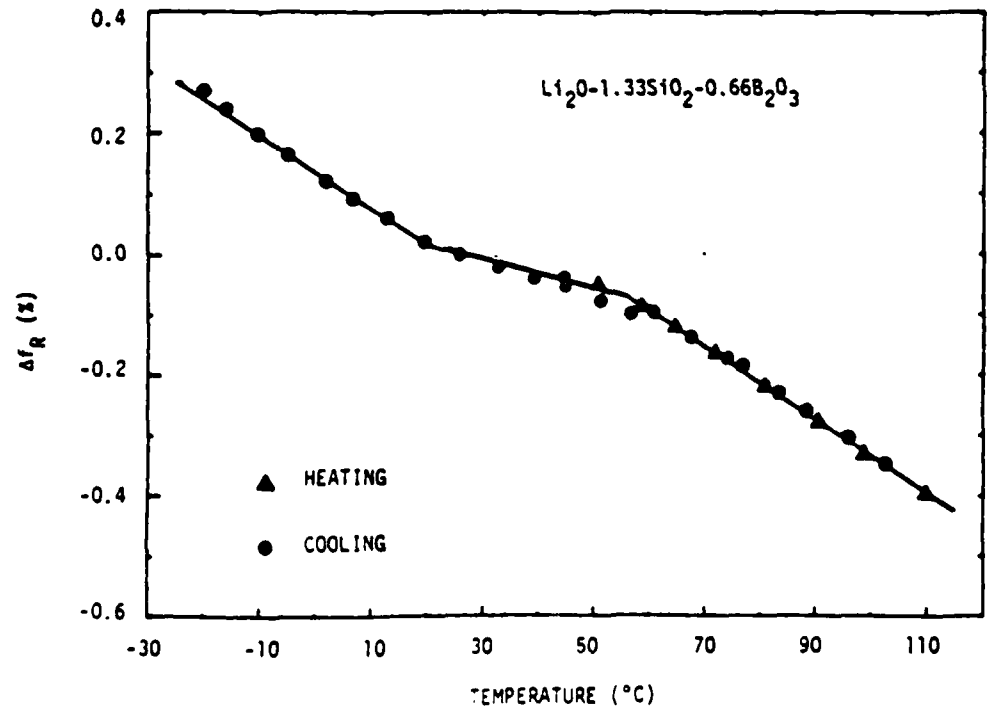

FIG. 4. Relative resonance frequency as a function of temperature for Li_2O-1.33SiO_2-0.66B_2O_3 glass ceramic.

TABLE II. Electromechanical coupling coefficient and TCR of some piezoelectric materials.

Materials	Orientation	k_t^2 or k_p^{2*}	TCR (ppm/°C)	Reference
Single crystals				
$LiNbO_3$	*y*-cut, *z* prop.	0.0486	94	9
$LiTaO_3$	*y*-cut, *z* prop.	0.0115	35	9
Quartz	*ST*-cut, *x* prop.	0.0014	0	9
$Ba_2Ge_2TiO_8$	*z*-cut	—	48	4
$Ba_2Si_2TiO_8$	*x*-cut, *y* prop.	0.0046	38	9
	z-cut, *x* prop.	0.016	51	
$(Ba_{1.2}Sr_{0.8})Si_2TiO_8$	*z*-cut, ⟨110⟩	0.015	21	10
$Li_2B_4O_7$	*z*-cut, *x* prop.	0.009	52	8
	x-cut, *z* prop.	0.012	Parabolic	8
Glass ceramics				
$Ba_2Ge_2TiO_8$	*z*-cut	—	95	4
Li_2O-1.8SiO_2-0.2B_2O_3				
(−20 to 35 °C)	*z*-surfaces	0.020	60	Present work
(35 to 100 °C)	*z*-surfaces	—	70	Present work
Li_2O-1.33SiO_2-0.66B_2O_3				
(−20 to +20 °C)	*z*-surfaces	—	60	Present work
(20 to 65 °C)	*z*-surfaces	0.008	30	Present work
(65 to 100 °C)	*z*-surfaces	—	60	Present work

*k_t^2 values for single crystals and k_p^2 values for glass ceramics.

where c is an effective elastic constant for the wave and ρ is the density. The operating frequency of the device is determined by v_s. To achieve a high operating frequency, which is desirable in many SAW devices, v_s should be high, which implies that the density of the material should be low. In this respect the lower density of glass ceramics (2.35 g/cm^3 for composition 1 and 2.33 g/cm^3 for composition 2) is an advantage.

The strong dependence of TCR on the composition of the parent glass suggests that it might be possible to reduce the TCR further by a suitable choice of the composition of the parent glass. In addition the amounts of $Li_2Si_2O_5$ and $Li_2B_4O_7$ phases in the glass ceramic can be controlled by modifying the heat treatment cycles employed for crystallization. Detailed studies on the preparation conditions, togehter with the piezoelectric and pyroelectric properties of glass ceramics in the Li_2O-SiO_2-B_2O_3 system will be reported in due course.

ACKNOWLEDGMENT

This work was sponsored by the U. S. Army Research Office (DAAG29-80-C-0008).

[1]G. Gardopee, R. E. Newnham, and A. S. Bhalla, Ferroelectrics 33, 155 (1981).
[2]G. Gardopee, R. E. Newnham, A. Halliyal, and A. S. Bhalla, Appl. Phys. Lett. 36, 817 (1980).
[3]A. Halliyal, A. S. Bhalla, R. E. Newnham, and L. E. Cross, J. Mater. Sci. 16, 1023 (1981).
[4]A. Halliyal, A. S. Bhalla, R. E. Newnham, L. E. Cross, and T. R. Gururaja, J. Mater. Sci. (to be published).
[5]R. M. White, Proc. IEEE 58, 1238 (1970).
[6]R. W. Whatmore, J. Cryst. Growth 48, 530 (1980).
[7]A. Halliyal, A. S. Bhalla, R. E. Newnham, and L. E. Cross (unpublished).
[8]R. W. Whatmore, N. M. Shorrochs, C. O'Hara, and F. W. Ainger, Electron. Lett. 17, 11 (1981).
[9]A. J. Slobodnik, Jr., Proc. IEEE 64, 581 (1976).
[10]H. Yamauchi, J. Appl. Phys. 49, 6162 (1978).

Appendix 8

Polar Glass Ceramics - A New Family of Electroceramic Materials: Tailoring the Piezoelectric and Pyroelectric Properties

A. Halliyal, A. S. Bhalla and R. E. Newnham

(Submitted for publication in Materials Research Bulletin)

POLAR GLASS CERAMICS - A NEW FAMILY OF ELECTROCERAMIC MATERIALS: TAILORING THE PIEZOELECTRIC AND PYROELECTRIC PROPERTIES

A. Halliyal, A. S. Bhalla and R. E. Newnham
Materials Research Laboratory
The Pennsylvania State University
University Park, PA 16802

ABSTRACT

Grain oriented multicomponent polar glass-ceramics have been prepared by crystallizing the glasses in a temperature gradient. Inexpensive, large area piezoelectric and pyroelectric devices can be fabricated by this method, and by adjusting the composition of the glasses and crystallization conditions, it is possible to tailor the properties to meet device requirements. Based on the growth characteristics and the connectivity pattern of the crystallites, the piezoelectric, pyroelectric and dielectric properties of glass-ceramic composites can be predicted. Two examples discussed in this paper are piezoelectric glass-ceramics which are not pyroelectric, and pyroelectric glass-ceramics which are not piezoelectric.

Introduction

In the past decade, several glass and recrystallized glass-ceramics belonging to the ferroelectric compositions such as $BaTiO_3$, $LiTaO_3$, $LiNbO_3$, $Pb_5Ge_3O_{11}$, $PbTiO_3$ and sodium cadmium niobate have been studied (1-9). The dielectric, electro-optic, piezoelectric and pyroelectric properties of these compositions have been reported. Most of these ferroelectric glass-ceramics have been prepared by crystallizing a ferroelectric phase from a silica or borate rich glass-matrix. In the devitrified glass-ceramics, it is often difficult to electrically pole the ferroelectric phase because of the low dielectric constant of the residual glassy phase, and this can be a major limitation in fabricating devices with ferroelectric glass-ceramics.

In recent years a number of glass-ceramics have been prepared in which the crystalline phase is non-ferroelectric but yet belongs to one of the polar point groups. Detailed studies of piezoelectric and pyroelectric properties of these glass-ceramics have been reported (10-15) and they appear to be interesting candidate materials for piezoelectric resonators and pyroelectric detectors.

These glass-ceramics with oriented crystallites were prepared by crystallizing glasses of suitable composition in a large temperature gradient (10-15). A high degree of crystallographic and polar (electrical) orientation were achieved during recrystallization of the glasses. Unlike ferroelectric materials (both single crystals and ceramics), the electrical domain configuration of the nonferroelectric crystalline phases in these glass-ceramics cannot be switched by an externally applied electric field. Thus both the crystallographic and polar orientation must be achieved during the nucleation stage of the devitrifiction process, and remain the same during the subsequent growth of crystallites. Hence in these nonferroelectric glass-ceramics, the temperature gradient is the vector driving force for polar orientation of the crystallites, similar to the externally applied electric field in the case of ferroelectric materials.

In many ferroelectric materials, 180° domains pose a problem. The effective piezoelectric response is reduced to $(1-2\alpha)$ of that of a single domain single crystal, where α is the fraction of the domains with opposite orientation. Many times it is either difficult or very expensive to prepare large area single domain samples for practical applications. In nonferroelectric materials there will be no aging or depoling at high temperatures, and hence polar glass-ceramics have potential high temperature applications, and are easier to handle during device fabrication where thermal processing is often required. Apart from single crystals or oriented thin films prepared by special sputtering techniques, the polar glass-ceramics are the only form in which nonferroelectric ceramics can be utilized in electronic devices. These glass-ceramics constitute a new family of electroceramic materials.

In the present paper, we describe the growth behavior of various crystalline phases in glass-ceramics of different compositions, and discuss several possible combinations of piezoelectric and pyroelectric properties in multicomponent glasses. We will illustrate the possibility of tailoring piezoelectric and pyroelectric properties of these glass-ceramics by adjusting the composition and degree of crystallinity.

Experimental

Glasses of different compositions were prepared by mixing reagent grade chemicals and melting in a platinum crucible. Glass-ceramic samples were prepared by crystallizing the glasses in a large temperature gradient normal to the surface of the glass. The details of the sample preparation technique can be found in references (10-12). Microstructure studies indicate that needle-like crystals grow from the surface into the bulk of the sample along the direction of temperature gradient. The crystalline phases in the glass-ceramic samples were identified from x-ray powder patterns. X-ray diffraction peak intensities from initial crystallizing surface were used to evaluate the degree of preferred orientation of the crystallites.

For piezoelectric and pyroelectric measurements, sections were cut normal to the temperature gradient, then polished and coated with sputtered gold electrodes. Byer-Roundy (16) and Chynoweth (17) methods were used for the pyroelectric measurements. Piezoelectric d_{33} coefficients were measured using a d_{33} meter and the electromechanical properties were determined by standard resonance techniques.

Compositions of the Glasses and Growth Habit

The composition of the glasses and their crystallization temperatures are given in Table 1, along with dielectric constants and piezoelectric d_{33} coefficients. The crystalline phases in glass-ceramics and their point group symmetries are also listed. Glass forming systems (10-15) which give glass-ceramics with desirable properties are Li_2O-SiO_2, Li_2O-B_2O_3, Li_2O-SiO_2-B_2O_3, BaO-SiO_2-TiO_2 and BaO-GeO_2-TiO_2. The crystalline phases recrystallized from the glasses within these systems are $Li_2Si_2O_5$, Li_2SiO_3, $Li_2B_4O_7$, $Ba_2TiSi_2O_8$ and $Ba_2TiGe_2O_8$. One or more crystalline phases are obtained depending on the composition of the glass. Glass compositions were optimized to obtain glass-ceramics with useful properties after recrystallization (10-12). Piezoelectric properties of the glass-ceramics were dependent both on the volume fraction and polar orientation of the crystalline phases, and in well-crystallized

TABLE 1

Compositions of Glasses and Their Properties

Composition	Tcr (°C)†	Crystalline Phases*	Dielectric Constant	Piezoelectric Coeff (d_{33}) (pC/N)
Li_2O-$2SiO_2$	585	LS_2	6	-1
Li_2O-$2SiO_2$-0.1ZnO	570	LS_2+LSZ+Q	6	-3
Li_2O-$2SiO_2$-0.2ZnO	580	LS_2+LSZ+Q	8	-3
Li_2O-$2SiO_2$-0.4ZnO	590	LS_2+LSZ+Q	10	0
Li_2O-1.8SiO_2-0.2B_2O_3	605,680	LS_2+LS+LB_2	9	+6
Li_2O-1.6SiO_2-0.4B_2O_3	625,665	LS_2+LB_2+LS	8	+3
Li_2O-1.95SiO_2-0.05 Fe_2O_3	600	LS_2+Q	--	-3
Li_2O-3B_2O_3	580	LB_2+LB_3	--	+3
Li_2O-1.8SiO_2-0.1(ZnO,B_2O_3)	580,670	LS_2+LSZ	--	-2
BaO-GeO_2-TiO_2	800	BTG	15	+7
BaO-1.8SiO_2-TiO_2	860	BST	13	+3
2BaO-3SiO_2-TiO_2	930	BST	10	+7
2BaO-2SiO_2-GeO_2-TiO_2	860	BSGT	11	+6

*Abbreviation for phases and point group symmetry.

LS_2 - $Li_2Si_2O_5$, mm2
LS - Li_2SiO_3, mm2
LB_2 - $Li_2B_4O_7$, mm2
LB_3 - $Li_2B_6O_{10}$, non-centric
LSZ - Li_2ZnSiO_4, non-centric
BTG - $Ba_2TiGe_2O_8$, mm2
BST - $Ba_2TiSi_2O_8$, 4mm
BSGT - solid solution of BTG and BST
Q - Quartz

†Temperature of exothermic peaks in DTA runs.

samples, the properties were comparable in magnitude with those of corresponding single crystals.

The sign and magnitude of the piezoelectric d_{33} coefficients measured on the surface from which crystallization commenced (which is towards the high-temperature end of temperature gradient axis) are given in Table 1. The sign of d_{33} and the polar orientation of the crystalline phases were dependent on the composition of the parent glass matrix. For the sake of the present discussion we define the growth behavior of crystalline phase on the basis of the sign of d_{33} measured on the initial crystallizing surface. (The sign of d_{33} defined in this way is different from the actual sign of d_{33} defined according to the 1949 IEEE piezoelectric convention). Here, the same sign of d_{33} for two phases means that the orientation of dipoles is similar in both the phases. In other words, both phases exhibit identical growth habit. The sign of pyroelectric coefficient is defined as follows. If on heating a pyroelectric, positive charges develop on the surface towards positive d_{33} of the crystallites, the sign of pyroelectric coefficient is positive. The above convention for the signs of piezoelectric and pyroelectric coefficients will be followed throughout the discussion in this paper.

Based on the above sign convention for d_{33}, the growth behavior of all the glass compositions listed in Table 1 can be divided into two groups as shown in Figure 1. In the case of $Ba_2TiSi_2O_8$, $Ba_2TiGe_2O_8$, Li_2O-B_2O_3 and Li_2O-SiO_2-B_2O_3 glass-ceramics the sign of d_{33} is positive, indicating that the positive end of the dipoles points toward the high temperature end of the sample. In the case of Li_2O-SiO_2, Li_2O-SiO_2-ZnO and Li_2O-SiO_2-Fe_2O_3 glass-ceramics, the sign of d_{33} is negative, indicating that the negative end of the

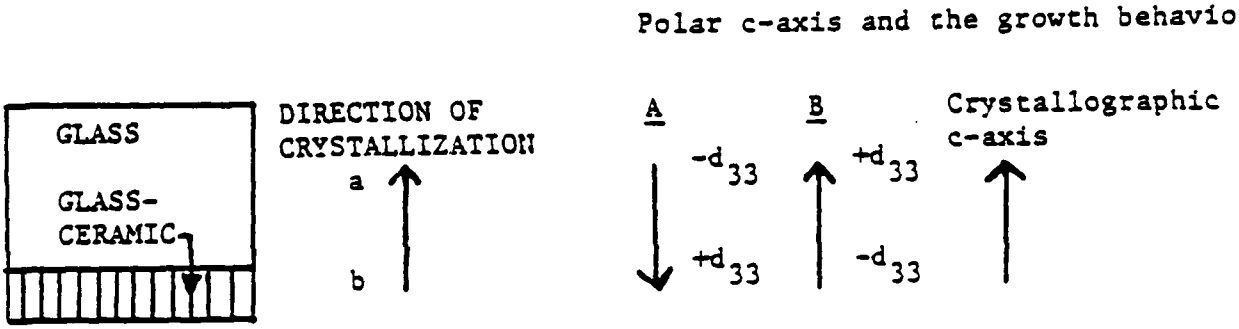

A	B
Li_2O-$(2-x)SiO_2$-xB_2O_3	$Li_2Si_2O_5$
$Ba_2TiSi_2O_8$	Li_2O-$2SiO_2$-$xZnO$
$Ba_2TiGe_2O_8$	

b is the high temperature end of temperature gradient axis.

FIG. 1

Polar Orientation - two types of growth behavior.

dipoles point toward the high temperature end. There are several possible reasons for this growth behavior or polar orientation. The presence of B_2O_3, ZnO or Fe_2O_3 appears to influence the growth habit of $Li_2Si_2O_5$ crystallite, probably by controlling the surface nucleation sites. The presence of Li_2SiO_3 or $Li_2B_4O_7$ as separate phases, which also belong to polar point groups might also be influencing the growth habit of $Li_2Si_2O_5$. In any case the present study indicates that the polar orientation of crystallites and the resulting piezoelectric and pyroelectric properties depend on the composition of the initial glass.

Diphasic Glass-Ceramic Composites

A glass-ceramic is essentially a composite of a glassy phase and one or more crystalline phases. If there is only one crystalline phase, it can be considered a diphasic system consisting of a crystalline phase embedded in an amorphous matrix. X-ray diffraction and microstructure studies of glass-ceramics indicate that the oriented region of crystallites extends deep into the sample and then tapers off (12). However, not all the crystallites extend throughout the thickness of the samples. The distribution of crystallites can be pictured as shown in Figure 2. The crystalline and glassy phases are partly in series and partly in parallel connection. As the grain orientation is improved, the length of the crystallites increases and the composite approaches pure parallel connectivity.

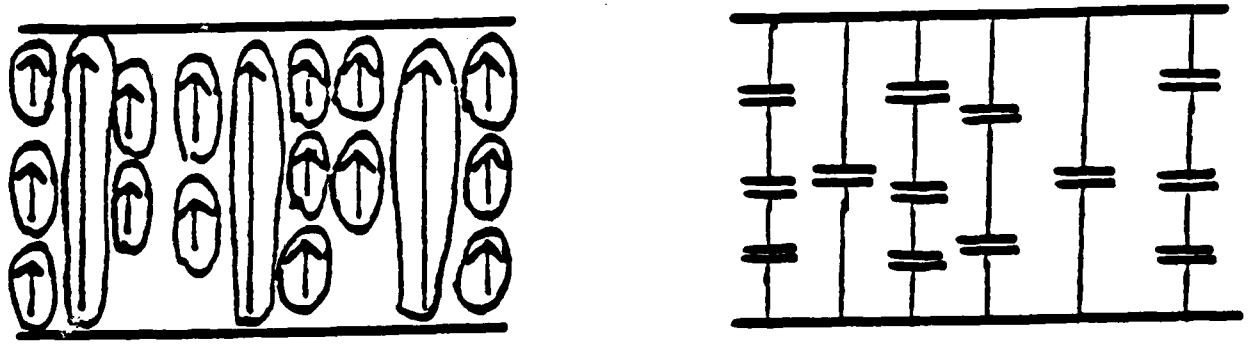

FIG. 2

Idealized microstructure of the grain-oriented glass-ceramics and its equivalent circuit.

For a composite consisting of two phases, one dimensional solutions for dielectric, piezoelectric and pyroelectric properties have been presented for both series and parallel connectivity (18,19). The results are summarized in Table 2. If the dielectric constant, piezoelectric coefficient, pyroelectric coefficient and volume fraction of the crystalline and glass phases are designated as ${}^1\varepsilon_3$, ${}^1d_{33}$, ${}^1p_3$, ${}^1v$ and ${}^2\varepsilon_3$, ${}^2d_{33}$, ${}^2p_3$, ${}^2v$, respectively, expressions for ε_3, d_{33} and p_3 of the glass-ceramic can be derived by making certain simplifying assumptions.

For the glass phase, ${}^2d_{33}$ and ${}^2p_3$ are equal to zero. In many nonferroelectric glass-ceramics, the dielectric constants of crystalline and glass phases are roughly the same. With this assumption it is obvious that the dielectric constant of the composite is the same for both series and parallel connections.

TABLE 2

Dielectric, Piezoelectric and Pyroelectric Properties of Diphasic Composites

	Series	Parallel	
Dielectric Permittivity ε_3	$\frac{{}^1\varepsilon_3\,{}^2\varepsilon_3}{{}^1v\,{}^2\varepsilon_3+{}^2v\,{}^1\varepsilon_3}$	${}^1v\,{}^1\varepsilon_3 + {}^2v\,{}^2\varepsilon_3$	(1)
Piezoelectric Coefficient d_{33}	$\frac{{}^1v\,{}^1d_{33}\,{}^2\varepsilon_3+{}^2v\,{}^2d_{33}\,{}^1\varepsilon_3}{{}^1v\,{}^2\varepsilon_3+{}^2v\,{}^1\varepsilon_3}$	$\frac{{}^1v\,{}^1d_{33}\,{}^2s_{33}+{}^2v\,{}^2d_{33}\,{}^1s_{33}}{{}^1v\,{}^2s_{33}+{}^2v\,{}^1s_{33}}$	(2)
Pyroelectric Coefficient p_3	$\frac{{}^1v\,{}^1p_3\,{}^2\varepsilon_3+{}^2v\,{}^2p_3\,{}^1\varepsilon_3}{{}^1v\,{}^2\varepsilon_3+{}^2v\,{}^1\varepsilon_3}$	${}^1v\,{}^1p_3 + {}^2v\,{}^2p_3$	(3)
Secondary Pyroelectric Effect	$\frac{2.\,{}^1v\,{}^2v({}^2\varepsilon_3\,{}^1d_{31}-{}^1\varepsilon_3\,{}^2d_{31})({}^2\alpha_1-{}^1\alpha_1)}{({}^1v\,{}^2\varepsilon_3+{}^2v\,{}^1\varepsilon_3)[{}^1v({}^2s_{11}+{}^2s_{12})+{}^2v({}^1s_{11}+{}^1s_{12})]}$ (series)		(4)
	$\frac{{}^1v\,{}^2v({}^2\alpha_3-{}^1\alpha_3)({}^1d_{33}-{}^2d_{33})}{{}^1v\,{}^2s_{33}+{}^2v\,{}^1s_{33}}$ (parallel)		(5)

where coefficients of properties of phases 1 and 2 are

${}^1p_3, {}^2p_3$ = pyroelectric coefficients

${}^1d_{33}, {}^2d_{33}$ = piezoelectric constants

${}^1\varepsilon_3, {}^2\varepsilon_3$ = dielectric permittivities

${}^1s_{33}, {}^2s_{33}, {}^1s_{11}, {}^2s_{11}, {}^1s_{12}, {}^2s_{12}$ = elastic compliances

${}^1v, {}^2v$ = volume fractions

${}^1\alpha_3, {}^2\alpha_3$ = expansion coefficients

Further, if we assume that the elastic compliance of crystalline and glassy phases are the same (${}^1s_{33} = {}^2s_{33}$), the expressions for d_{33} and p_3 in Table 2 reduce to the following expressions for both series and parallel connectivity

$$d_{33} = {}^{1}d_{33}\,{}^{1}v \qquad \text{and} \tag{6}$$

$$p_3 = {}^{1}p_3\,{}^{1}v. \tag{7}$$

The magnitudes of ${}^{1}d_{33}$ and ${}^{1}p_3$ of the crystalline phase itself depend upon the degree of both crystallographic and polar orientation of the crystallites, which is not accounted for in equations (6) and (7). We can conclude that in the ideal case of complete crystallographic and polar orientation of the crystallites, the magnitudes of d_{33} and p_3 of the composite are directly proportional to the percentage of crystalline phase, irrespective of whether the crystallites are connected in series or parallel. In addition, for this ideal case, if the glass-ceramics contain a very high percentage of crystalline phase, the values of d_{33} and p_3 approach the single crystal values of the crystalline phase. As an example, the pyroelectric coefficients of fresnoite ($Ba_2TiSi_2O_8$) are shown in Figure 3 for both single crystal and polar glass-ceramics. The lower value of pyroelectric coefficient p_3 of glass-ceramic (about 75% of the single crystal value) can be accounted for by the lack of perfect orientation of the crystallites. The piezoelectric d_{33} coefficient of the glass-ceramic is also about 75% of the single crystal value.

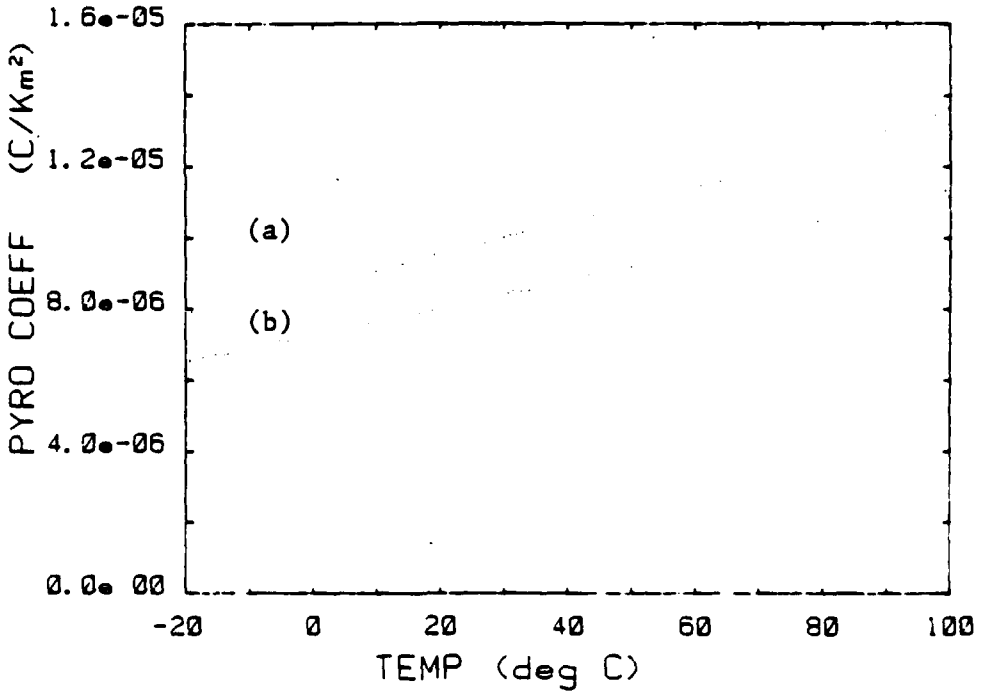

FIG. 3

Pyroelectric coefficients of (a) $Ba_2TiSi_2O_8$ single crystal and (b) $2BaO\text{-}3SiO_2\text{-}TiO_2$ glass-ceramic.

Multicomponent Glass-Ceramic Composites

Most of the glass compositions listed in Table 1 result in glass-ceramics with several crystalline phases after recrystallization. In such cases, the crystallites of more than one phase may be oriented parallel (or antiparallel) to the temperature gradient. If we assume that the crystallites of two or

more phases preserve their characteristic growth habit in relation to the direction of temperature gradient, then the piezoelectric and pyroelectric properties of polar glass-ceramic containing several phases can be predicted by the analysis discussed below. For simplicity, an analysis for glass-ceramic composites containing only two crystalline phases will be given here, recognizing however, that the analysis can be extended to more than two phases. For the signs of d_{33} and p_3, the same convention will be followed as defined in the previous section.

Consider a polar glass-ceramic consisting of two crystalline phases. Let the dielectric constant, piezoelectric coefficient, pyroelectric coefficient and the volume fraction of the two phases be ${}^1\varepsilon_3$, ${}^1d_{33}$, ${}^1p_3$, ${}^1v$ and ${}^2\varepsilon_3$, ${}^2d_{33}$, ${}^2p_3$, ${}^2v$, respectively. Let us assume that both the phases have similar elastic compliances (${}^1s_{33} = {}^2s_{33}$) and thermal expansion coefficients, thereby eliminating any secondary contributions to the pyroelectric effect (Table 2). To further simplify the analysis, let us assume that the properties of glass-ceramic are not influenced by the glassy phase (${}^3v = 0$). Irrespective of whether the crystalline phases are connected in series or parallel, we get the following equations for the properties of the composite, from equations (1), (2) and (3).

$$\varepsilon_{33} = {}^1v\,{}^1\varepsilon_3 + {}^2v\,{}^2\varepsilon_3 \tag{8}$$

$$d_{33} = {}^1v\,{}^1d_{33} \pm {}^2v\,{}^2d_{33} \tag{9}$$

$$p_3 = {}^1v\,{}^1p_3 \pm {}^2v\,{}^2p_3 \tag{10}$$

The resultant values of d_{33} and p_3 of the composite depend upon the sign and magnitude of the properties of individual phases, and also upon the volume fraction of the individual phases. Since ${}^1d_{33}$ and ${}^2d_{33}$ can be positive or negative at the growth end and ${}^1p_3$ and ${}^2p_3$ can be positive or negative, there are 16 possible cases of d_{33} and p_3, eight of which are listed in Table 3. If we consider the resulting piezoelectric and pyroelectric properties of the glass-ceramic, these 16 cases can be grouped into four classes.

The crystalline phases have the same growth behavior in the case of glass-ceramics belonging to class (a) and (b) and opposite growth behavior in cases (c) and (d). Depending on the signs of pyroelectric coefficients ${}^1p_3$ and ${}^2p_3$ of the two phases, we obtain glass-ceramic composites with completely different piezoelectric and pyroelectric properties. Glass-ceramics of class (a) are fully piezoelectric as well as pyroelectric and in the ideal case their properties can be expected to approach those of single domain single crystal materials. Glass-ceramics of class (b) are fully piezoelectric but only partially pyroelectric (or non-pyroelectric) because of the opposite signs of ${}^1p_3$ and ${}^2p_3$. Glass-ceramics of class (c) are both non-piezoelectric and non-pyroelectric and hence are not of much interest for devices. Class (d) glass-ceramics are fully pyroelectric but non-piezoelectric. Glass-ceramics of classes (b) and (d) are interesting for piezoelectric and pyroelectric device applications where the interference of the two properties may be a problem, as will be discussed below.

Examples of the Four Classes

The growth behavior of glass-ceramics of different compositions has al-

Table 3

Eight Combinations of Piezoelectric and Pyroelectric Properties

Case	Growth Habit* Sign of d_{33}		Sign of d_{33}	Sign of p_3		d_{33} of Composite	p_3 of Composite	Resultant Properties
	Phase I	Phase II		Phase I	Phase II			
a	+	+	+	+	+	$^1v^1d_{33}+^2v^3d_{33}$	$+(^1v^1p_3+^2v^2p_3)$	piezo and pyro
	+	+		-	-	$^1v^1d_{33}+^2v^2d_{33}$	$-(^1v^1p_3+^2v^2p_3)$	
b	+	+	+	+	-	$^1v^1d_{33}+^2v^2d_{33}$	$+^1v^1p_3-^2v^2p_3$	piezo but non-pyro
	+	+		-	+	$^1v^1d_{33}+^2v^2d_{33}$	$-^1v^1p_3+^2v^2p_3$	
c	+	-	+	+	+	$^1v^1d_{33}-^2v^2d_{33}$	$+^1v^1p_3-^2v^2p_3$	non piezo and non pyro
	+	-		-	-	$^1v^1d_{33}-^2v^2d_{33}$	$-^1v^1p_3+^2v^2p_3$	
d	+	-	+	+	-	$^1v^1d_{33}-^2v^2d_{33}$	$+(^1v^1p_3+^2v^2p_3)$	pyro but non-piezo
	+	-		-	+	$^1v^1d_{33}-^2v^2d_{33}$	$-(^1v^1p_3+^2v^2p_3)$	

*Sign of d_{33} measured on the initial crystallizing surface. Eight more combinations can be obtained with a negative d_{33} sign for phase I.

ready been described. This knowledge about the growth habit and the signs of pyroelectric coefficients of the crystalline phases can be exploited to design compositions which give glass-ceramics with properties of any one of the four classes described earlier.

Glass-ceramics in the systems Li_2O-SiO_2-ZnO, Li_2O-SiO_2-Fe_2O_3, and Li_2O-SiO_2-B_2O_3 have negative pyroelectric coefficient, but exhibit opposite growth behavior (case c). Compositions in the quaternary system Li_2O-SiO_2-ZnO-B_2O_3 illustrate the reduced pyroelectric and piezoelectric effect (Table 1) characteristic of glass-ceramics of class (c).

Two entirely different systems were used to prepare glass-ceramics with class (b) properties. $Ba_2TiSi_2O_8$ and $Ba_2TiGe_2O_8$ phases crystallized from glasses of composition $2BaO$-$3SiO_2$-TiO_2 and BaO-GeO_2-TiO_2 respectively showed similar growth habit, but opposite signs for pyroelectric coefficients. A glass-ceramic of composition $2BaO$-$2SiO_2$-GeO_2-TiO_2 which gave a solid solution phase after recrystallization had almost zero pyroelectric coefficient, but piezoelectric properties remained the same (Fig. 4). A similar reduction in pyroelectric coefficient of fresnoite glass was observed when a small amount of (Li_2O-$1.8SiO_2$-$0.2B_2O_3$) was incorporated in the fresnoite composition (Fig. 5). In both these cases there is no appreciable change in the piezoelectric properties, whereas the pyroelectric properties are reduced substantially over a wide temperature range. The properties of these compositions are summarized in Table 4.

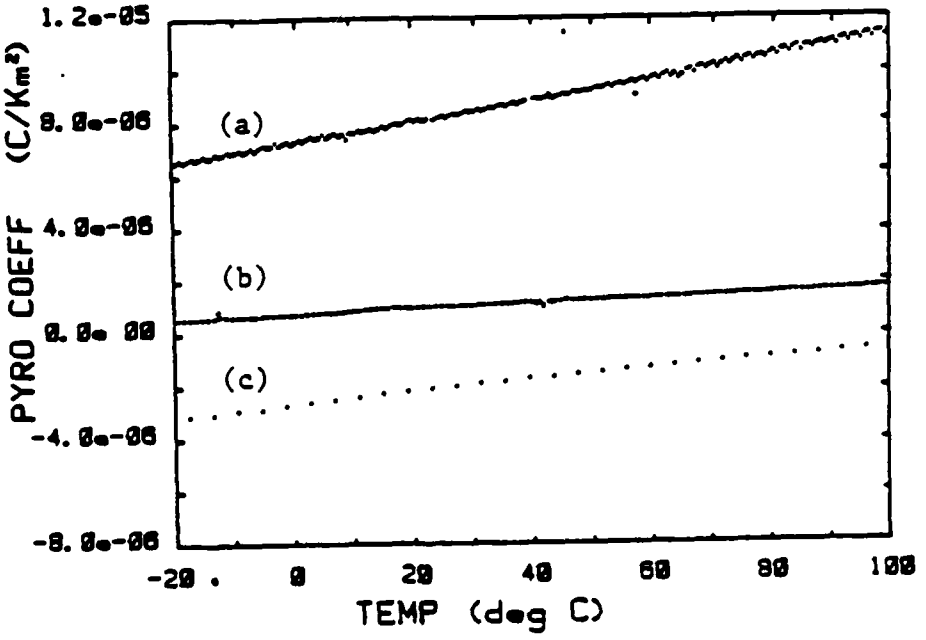

FIG. 4

Pyroelectric coefficients of glass-ceramics in the fresnoite system; (a) $2BaO$-$3SiO_2$-TiO_2, (b) $2BaO$-$2SiO_2$-GeO_2-TiO_2 and (c) BaO-GeO_2-TiO_2.

Optimizing the Piezoelectric and Pyroelectric Properties

From the examples given in the previous section, it is clear that glass-ceramics with tailored piezoelectric or pyroelectric properties can be pre-

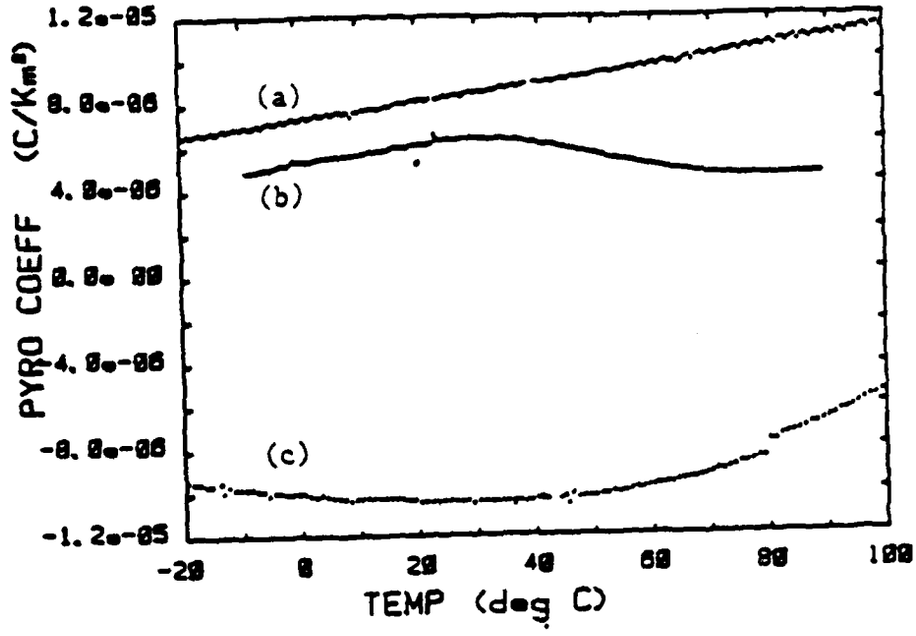

FIG. 5

Pyroelectric coefficients of fresnoite and lithium borosilicate glass-ceramics; (a) $2BaO-3SiO_2-TiO_2$, (b) $2BaO-3.8SiO_2-Li_2O-TiO_2-0.2B_2O_3$ and (c) $Li_2O-1.8SiO_2-0.2B_2O_3$.

TABLE 4

Piezoelectric and Pyroelectric Properties of Multicomponent Glass-Ceramics

COMPOSITION	P_3 ($\mu C/m^{2\circ}K$)	d_{33} ($X10^{-12}C/N$)	k_p (%)
$2BaO-3SiO_2-TiO_2$	+8	+7	14
$BaO-GeO_2-TiO_2$	-2	+6	6
$2BaO-2SiO_2-GeO_2-TiO_2$	+.8	+7	14
$2BaO-3SiO_2-TiO_2$	+8	+7	14
$Li_2O-1.8SiO_2-0.2B_2O_3$	-11	+6	14
$2BaO-3.8SiO_2-Li_2O-TiO_2-0.2B_2O_3$	+6	+7	13

pared by recrystallizing multicomponent glasses of suitable composition. The growth habit of the crystalline phases provides a means to tailor the piezoelectric and pyroelectric properties of the final glass-ceramic composite. Two of the cases discussed above look especially interesting for device applications - piezoelectric glass-ceramics which are non-pyroelectric (case b) and pyroelectric glass-ceramics which are non-piezoelectric (case d).

In piezoelectric devices used in ambient conditions, pyroelectric noise is usually undesirable. In hydrophone elements fabricated from PZT-polymer composites, for instance, such noises are reduced but only within a relatively narrow working temperature range (20).

In a similar way, piezoelectric noise interferes the high frequency IR pyroelectric signals. In some cases alternate methods are used to eliminate the interfering piezoelectric voltages developed in such devices. In the case of $LiTaO_3$ detectors, piezoelectric oscillations are damped by embedding the pyroelectric element in epoxy (21); and in PLZT detectors, piezoelectric noise is eliminated by modifying the electronics (22). Piezoelectric oscillations superimposed on the pyroelectric response have been shown to have an incubation time of 40-60 nsec, and occur after the onset of pyroelectric signals (<40 nsec). Thus the piezoelectric oscillations occur in the tail of the pyroelectric response, and hence might be cut off with proper electronics (22). Hence to avoid these problems, it may be desirable to use materials which are only piezoelectric or which are only pyroelectric. Several compositions can be formulated from Table 1, satisfying this criteria.

Piezoelectric glass-ceramics which are non-pyroelectric should satisfy the relation $\pm {}^1v^1p_3 \mp {}^2v^2p_3 = 0$ (case b). Referring to Table 4, candidate compositions can be found in the solid solution of $Ba_2Si_2TiO_8$ and $Ba_2Ge_2TiO_8$. Piezoelectric glass-ceramics which are not pyroelectric would be useful as pressure sensors that are insensitive to temperature changes. (Quartz is piezoelectric and non-pyroelectric, but cannot be used to measure pressure changes because $d_{11} + d_{22} + d_{33} = 0$. This is generally true for all piezoelectric crystals belonging to non-pyroelectric point groups).

The second case of interest is pyroelectric glass-ceramics which are not piezoelectric (case d). Here the requirement is that ${}^1v^1d_{33} - {}^2v^2d_{33} = 0$ should be satisfied. Candidate compositions may exist in the Li_2O-B_2O_3-SiO_2-ZnO quaternary system containing different amounts of ZnO and B_2O_3. Such pyroelectric materials will not be sensitive to mechanical oscillations.

Summary

Glass-ceramics of non-ferroelectric materials in which the crystalline phases belong to polar point groups were prepared by recrystallizing glasses of suitable composition in a temperature gradient. The growth behavior of the crystallites and the piezoelectric, pyroelectric and dielectric properties of multicomponent glass-ceramics have been investigated. The studies showed that

(1) In well crystallized glass-ceramics piezoelectric and pyroelectric coefficients are comparable to those of single crystals.

(2) The growth behavior of the crystalline phases was studied by measuring the sign of d_{33} on the initial crystallizing surface. The polar orientation or the growth behavior of the crystalline phases depends on the composition of the glass.

(3) It is shown that the piezoelectric and pyroelectric properties of multicomponent glasses can be predicted from the growth behavior of individual

phases and the signs of their pyroelectric coefficients. The possibility of tailoring the properties of glass-ceramics is illustrated by a number of examples. Two of the cases which look attractive for device applications are piezoelectric glass-ceramics which are non-pyroelectric and pyroelectric glass-ceramics which are non-piezoelectric.

(4) The glass-ceramic elements have several advantages over single crystals or ferroelectric materials; they are inexpensive and large area elements can be prepared. Also these materials have low dielectric constants and do not show aging or depoling, and hence are useful for high temperature applications.

Acknowledgments

It is a pleasure to thank our colleagues at the Materials Research Laboratory for their advice and encouragement. This work was supported by Army Research Office (Durham) through Contract #DAAG29-80-C-0008.

References

1. A. Herczog, J. Amer. Ceram. Soc. 47, 107 (1964).
2. N.F. Borelli, J. Appl. Phys. 38, 4243 (1967).
3. A.M. Glass, M.E. Lines, K. Nassau, J.W. Shiever, Appl. Phys. Lett. 31, 249 (1977).
4. A.M. Glass, K. Nassau, J.W. Shiever, J. Appl. Phys. 48, 5213 (1977).
5. M.M. Layton, A. Herczog, Glass Technology 10, 50 (1969).
6. M.M. Layton, J.W. Smith, J. Amer. Ceram. Soc. 58, 435 (1975).
7. M. Takashiege, T. Mitsui, T. Makagura, Y. Aikawa and M. Jang, Jpn. J. Appl. Phys. 20, L159 (1981).
8. K. Takahashi, L.E. Cross and R.E. Newnham, Mat. Res. Bull. 10, 599 (1975).
9. C.G. Bergeron and C.K. Russell, J. Amer. Ceram. Soc. 48, 115 (1965).
10. G.J. Gardopee, R.E. Newnham and A.S. Bhalla, Ferroelectrics 33, 155 (1981).
11. A. Halliyal, A.S. Bhalla, R.E. Newnham and L.E. Cross, J. Mater. Sci. 16, 1023 (1981).
12. A. Halliyal, A.S. Bhalla, R.E. Newnham, L.E. Cross and T.R. Gururaja, J. Mater. Sci. 17, 295 (1982).
13. A. Halliyal, A.S. Bhalla, R. E. Newnham and L.E. Cross, Ferroelectrics 38, 781 (1981).
14. A. Halliyal, A.S. Bhalla, R.E. Newnham and L.E. Cross, J. Appl. Phys. 53, 2871 (1982).
15. A. Halliyal, A.S. Bhalla, R.E. Newnham and L.E. Cross, IEEE Ultrasonic Symposium, 315 (1981).
16. R.L. Byer and C.B. Roundy, Ferroelectrics 3, 333 (1972).
17. A.G. Chynoweth, J. Appl. Phys. 27, 78 (1956).
18. R.E. Newnham, D.P. Skinner and L.E. Cross, Mat. Res. Bull. 13, 525 (1978).
19. D.P. Skinner, R.E. Newnham and L.E. Cross, Mat. Res. Bull. 13, 599 (1978).
20. S.Y. Lynn, M.S. Thesis, The Pennsylvania State University (1982).
21. A.M. Glass and R.L. Abrams, J. Appl. Phys. 41, 4455 (1970).
22. M. Simhony and M. Bass, Appl. Phys. Lett. 34, 426 (1979).

Appendix 9

The Shape-Memory Effect in PLZT Ceramics

V. K. Wadhawan, M. C. Kernion, T. Kimura, R. E. Newnham

Ferroelectrics. 1981. Vol. 37. pp. 575-578
0015-0193/81/3701-0575/$06.50/0

THE SHAPE-MEMORY EFFECT IN PLZT CERAMICS

V.K. WADHAWAN, M.C. KERNION, T. KIMURA, R.E. NEWNHAM
Materials Research Laboratory, The Pennsylvania State University, University Park, PA 16802, USA

Abstract—The shape-memory effect has been investigated in ferroelectric-ferroelastic PLZT ceramic samples of composition 6.5/65/35 by bending and twisting experiments and temperature cycling. The effect of an electric field on the shape memory produced by bending is also examined. During the course of these experiments some additional evidence was also obtained for the existence of a region of microdomains (quasiferroelectricity) between the normal ferroelectric and paraelectric phases of the PLZT composition investigated.

INTRODUCTION

The shape-memory effect (SME) is well known in a large class of metal thermal remanent recovery alloys[1]. A bar of such an alloy, when deformed plastically, returns to its original undeformed shape on heating to a temperature above the recovery temperature, T_f. Apart from temperature cycling, mechanical stress is the only variable influence usually employed to investigate and manipulate the SME in these materials. The SME can occur in nonmetallic systems also. Of special interest are materials which are simultaneously ferroelectric and ferroelastic. Their ferroelasticity ensures that recoverable spontaneous strain is available for contributing to the SME, and their coupled ferroelectric-ferroelastic nature implies that the spontaneous strain can be manipulated not only by applying mechanical forces, but also by electric fields. Such materials can therefore be expected to display a richer variety of SME behavior than the alloys.

$(Pb,La)(Zr,Ti)O_3$, or PLZT, is a particularly important ferroelectric-ferroelastic SME material because of its application potential. Usually the x/y/z notation is used to specify its composition, where y/z is the Zr/Ti ratio, and x denotes the atomic percentage of La^{3+} ions. Special attention has been paid to the composition of x/65/35, the ferroelastic nature of which was first demonstrated by Meitzler and O'Bryan[2]. For $x>4.5$ it displays a property known variously as penferroelectricity[3], quasiferroelectricity[4], or the β-α transition[5]. Above the Curie temperature T_c, the dielectric behavior is that of a normal paraelectric, but normal ferroelectric behavior is not observed immediately below T_c. Instead, microdomains of dimensions shorter than the wavelength of light are believed to be formed[4]. Under an external electric field, these microdomains are thought of as transforming into macrodomains, which, however, are not stable and revert to microdomains when the field is removed. The experimentally observed "slim" hysteresis loops are cited as evidence in favor of this model[4]. If the specimen is cooled well below T_c while under the action of the electric field, the macrodomains stay even when the field is switched off, and normal ferroelectric properties, in particular "fat" hysteresis loops, are observed. When the material is heated again (without a bias field), the microdomains reappear at a characteristic temperature T_p. In our experiments we have measured and correlated the characteristic temperatures associated with the SME, namely the

...tion temperature T_s and the recovery temperature T_f, with the temperatures T_p ... associated with dielectric anomalies. It is concluded that the mechanically pro... SME can be associated with the onset or disappearance of only the macrodomains, and ... the microdomains[6].

Since sufficiently large electric fields applied between temperatures T_p and T_c can change the microdomains to macrodomains, they can affect the SME in a very direct way. This was also investigated.

EXPERIMENTAL

Two types of experiments were carried out to induce the SME in PLZT ceramic samples. In the first type, about 1 cm long helices of composition 6.5/65/35 were prepared by extrusion followed by winding on a mandrel, and then sintering at 1300°C. To demonstrate the SME, the helix was first heated to 200°C, a temperature well above T_c (Figure 1.1). A compressive force of 17 gm was then applied to it along its axis, which resulted in an elastic compression of the helix (Figure 1.2). The compressive weight remained in position as the system was cooled to room temperature. Figure 1.3 shows the plastically deformed state of the helix after the weight was removed at room temperature, with about 30% decrease in height. When the helix was heated back through the phase transition, it returned to its original height (Figure 1.4), thus demonstrating dramatically the SME in a brittle ceramic.

In the second type of experiments, bending of thin bars of PLZT ceramics, supported on two knife edges, was used to produce and study the SME. Samples of composition x/65/35 were investigated for $4.0 < x < 8.0$. Details of these experiments, carried out in the absence of any applied electric fields, have been reported in one of our recent publications[6] and will not be repeated here.

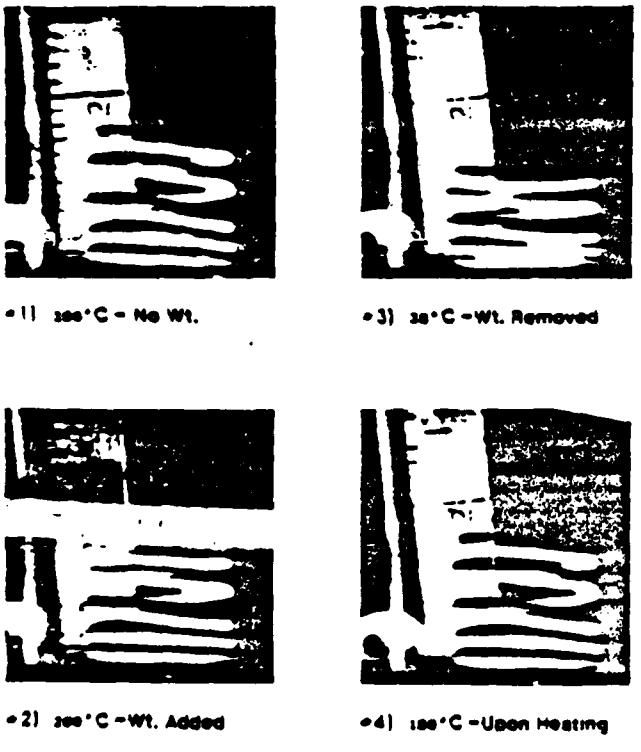

FIGURE 1. The shape-memory effect in a PLZT ceramic helix. See text for details.

In another set of experiments of the second type, samples of composition 6.5/65/35 were investigated for the effect of electric field on the SME produced by bending. A bar of the ceramic of dimensions 15x2x0.35 mm was electroded by sputtering gold on its two major faces and voltages up to 180 V were applied across these faces in different experiments. The apparatus used for monitoring the SME was essentially the same as that described in Ref.[6]. In a typical run the PLZT bar was first heated to 200°C and then cooled to room temperature (at the rate of ~2°/min) under a bending load of 49 gm. When the load was removed the bar exhibited plastic bending, which disappeared gradually on heating to temperature T_f, thus demonstrating the SME once again. The experiment was then repeated with different electric fields applied along the thickness of the sample during the heating part of the temperature cycle (Figure 2). Throughout the temprature cycling, unless an electric field was on, the major faces of the bar were kept in a short-circuited state.

RESULTS AND DISCUSSION

PLZT ceramics of composition 6.5/65/35 have polar rhombohedral crystallographic sym-

metry at room temperature when in a thermally annealed state. The polar direction coincides with the long diagonal of the unit cell[2]. When a bar of PLZT ceramic placed on two knife edges is bent mechanically by a load applied centrally from the top, the lower layers are extended and the upper layers compressed. (Similarly, in the case of a compressed helical specimen, the maximum torsional shear is experienced by the material farthest from the axis of the helix.) The longer diagonals of the unit cells (as well as the electric dipoles) align preferentially along the direction of the tensile force in the lower layers, whereas those in the upper layers align preferentially along directions perpendicular to the direction of the compressive force. When a static electric field is applied along the thickness of the bent bar, it tends to straighten the bar because, in both the lower and the upper layers, its effect is to align the dipoles preferentially along the thickness of the bar and thus annul most of the effect produced by the bending stress (Figure 2).

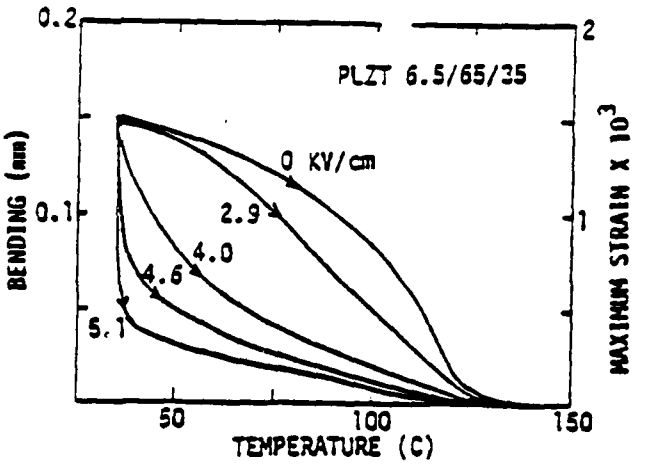

FIGURE 2. The straightening behavior of a plastically bent PLZT bar on heating under different electric fields. The electric fields were switched on at 35°C and switched off at 150°C.

In another experiment the bending load was not removed while a field of 5.1 kV/cm was applied during the heating part of the cycle (curve 2 in Figure 3). In this case not only did the straightening process slow down initially, but even the recovery temperature T_f was pushed up by ~30°C. The lower straightening effect of the electric field can be attributed partly to the opposition offered directly by the bending load and partly to the phase transition caused by the bending load[2]. The higher T_f can also be understood in terms of the new (probably tetragonal) phase resulting from the stress induced phase transition: The tetragonal phase has a higher spontaneous strain which becomes zero at a higher T_f.

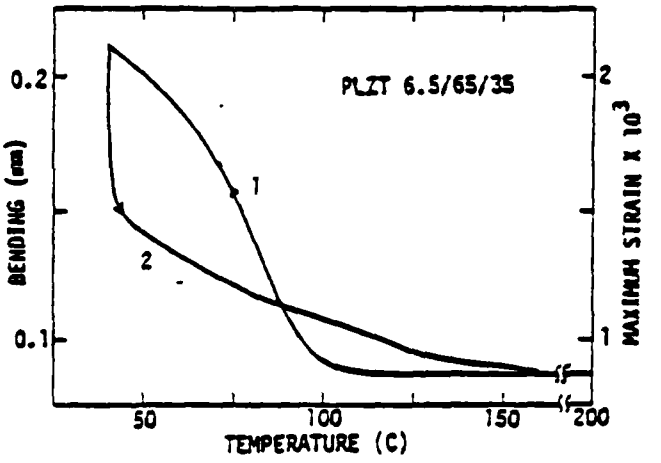

FIGURE 3. Bending and straightening behavior of a PLZT ceramic bar. Curve 1: cooling under a constant bending load. Curve 2: heating under the combined effect of the bending load and an electric field of 5.1 kV/cm. The electric field was switched off at 160°C.

For the geometry employed in the present experiments, electric field can never produce any bending of the sample. Since it opposes the effect of the bending load it may normally be expected only to reduce the bending (Figure 2). Yet in the following experiment electric field could be made to enhance the bending produced by the load in the temperature region between T_c and T_p:

The PLZT bar was heated to 200°C and the bending load was applied. The bar was then cooled at the rate of 2°/min. When the temperature fell to 130°C an electric field of 2.9 kV/cm was switched on (Figure 4). The field was switched off at 128°C and then switched on again at 126°C and so on until the temperature fell to 100°C, when it was finally switched off and the sample cooled to room temperature in a short-circuited

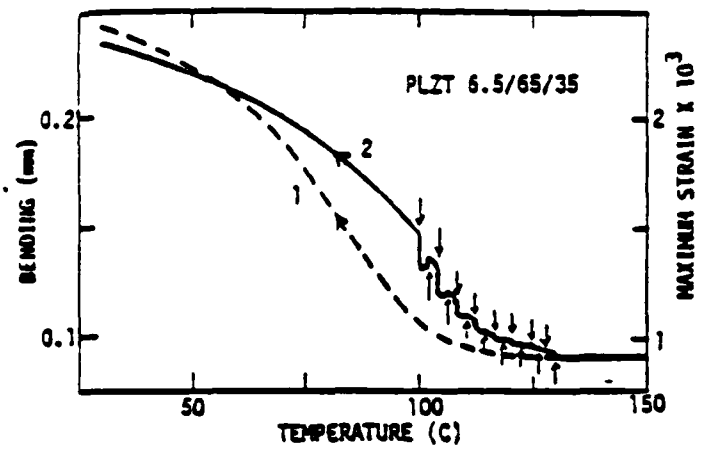

FIGURE 4. The effect of an alternating electric field on the bending produced mechanically as the sample is cooled to room temperature (curve 2). Curve 1 is the same as that in Figure 3. The arrows pointing up indicate the temperatures at which the electric field was switched on for curve 2, and the arrows pointing down the temperatures at which it was switched off.

condition. Figure 4 shows that when the sample temperature is closer to 100°C than to 130°C a substantial increase in bending occurs when the field is switched off, and a much lower decrease in bending occurs when it is switched on. There is thus a net increase in the effectiveness of the bending load in this temperature region. An experiment carried out at twice the above frequency for switching the field on and off did not produce any appreciable change in the net increase in bending.

We believe that this experiment provides a new kind of supportive evidence for the model described in the Introduction which postulates the existence of microdomains between T_p and T_c[3,4,5]. In the microdomains regime the material is "electrically soft" but not "mechanically soft," which means that when the external electric field is absent the bending load does not produce any significant amount of plastic bending. When the electric field is switched on, microdomains change to macrodomains and the material becomes mechanically soft also. The bending load now can produce greater plastic deformation. But the same electric field which is instrumental in making the material mechanically soft also opposes the bending which the load tends to produce. Therefore the net increase in bending is not large (it is even negative for temperatures near 100°C) when the electric field is on. However, when this field is switched off, the reappearance of microdomains and the loss of mechanical softness are not instantaneous. Instead there is a finite relaxation time. It is during this time (when the straightening effect of the electric field is missing because the field is zero) that the bending load is most effective in producing an extra amount of bending (Figure 4).

Since PLZT is a ferroelectric as well as a ferroelastic,it should be possible to produce the SME entirely with a suitably applied electric field. Experiments employing an interdigital set of electrodes on the lower face of the PLZT bar are under way in our laboratory.

ACKNOWLEDGMENT

This work was supported by the Army Research Office, Contract No. DAAG29-80-C-0008.

REFERENCES

1. H. Warlimont, Mat. Sci. and Engg. 25, 139 (1976).
2. A. H. Meitzler and H.M. O'Bryan, Jr., Appl. Phys. Lett. 19, 106 (1971).
3. A. H. Meitzler and H.M. O'Bryan, Jr., Proc. IEEE 61, 959 (1973).
4. K. Carl and K. Geisen, Proc. IEEE 61, 967 (1973).
5. E. T. Keve and A.D. Annis, Ferroelectrics 5, 77 (1973).
6. T. Kimura, R.E. Newnham and L.E. Cross, Phase Transitions (1981-in press).

Appendix 10

Shape-Memory Effect in PLZT Ferroelectric Ceramics

T. Kimura, R. E. Newnham and L. E. Cross

Phase Transitions, 1981, Vol. 2, pp. 113-130
0141-1594/81/0202-0113 $06.50/0

Printed in Great Britain

Shape-Memory Effect in PLZT Ferroelectric Ceramics

T. KIMURA, R. E. NEWNHAM and L. E. CROSS

Materials Research Laboratory, The Pennsylvania State University, University Park, Pennsylvania 16802, U.S.A.

(*Received April 30, 1981*)

The shape-memory effect in PLZT (Lead Lanthanum Zirconate Titanate) ceramics with composition $x/65/35$ ($4.0 \leq x \leq 8.0$) has been investigated using bending experiments and temperature cycling. Relationships between load and the degree of bending, together with their temperature dependence, have been determined, and characteristic temperatures associated with the onset and disappearance of the pseudo-plastic shape change are compared with the observed dielectric anomalies. Effects of mechanical stress and electric field on the shape-memory temperatures and the magnitude of strain have also been investigated. It is concluded that domain alignment and the temperature-dependence of spontaneous strain are important factors governing the shape-memory effect in ferroelectrics. Preferred-orientation effects have been confirmed by X-ray diffraction analysis.

1 INTRODUCTION

The recovery of a plastically deformed material to its original shape by heating is called the shape-memory effect. This effect has been extensively studied in metallic alloys and is generally associated with martensitic phase transformations (Warlimont, 1976; Delaey, Krishnan, Tas, and Warlimont, 1974). Phase transformations in ferroelectric materials are not martensitic, but Schmidt and Boczek (1978) observed apparently similar effects in PLZT ceramics. Details of the phenomena occurring in PLZT are not clear.

Applications for PLZT ceramics include a number of different optical devices (Haertling and Land, 1971; Maldonado and Meitzler, 1970, 1971; Maldonado and Anderson, 1971). The materials of interest are conventionally referred to in the $x/y/z$ notation, where x gives the atomic percentage of La and y/z is the Zr to Ti ratio. Attention has generally been concentrated

on materials of composition $x/65/35$. Those with $x > 4.5$ exhibit an interesting phenomenon called *penferroelectricity* (Meitzler and O'Bryan, 1973), *quasi-ferroelectricity* (Carl and Geisen, 1973) or $\beta \rightarrow \alpha$ *phase transformation* (Keve and Annis, 1973). PLZT specimens with $x = 8.0$ show relaxor behavior with a diffuse phase transition.

This paper describes the shape-memory effect in PLZT ceramics with La concentrations between 4.0 and 8.0 at. %. Because of their simplicity, bending experiments were used to investigate the shape change. The effects of stress and La content on the magnitude of bending strain, and on the memory effect were determined. The characteristic temperatures associated with the shape-memory effect were compared with the dielectric anomalies, and it was concluded that ferroelectric domains are the main cause of the shape-memory effect in ferroelectric ceramics.

2 EXPERIMENTAL

Five hot-pressed PLZT ceramic wafers with compositions $x/65/35$ ($x = 4.0$, 6.5, 7.0, 7.5 and 8.0) were obtained from Dr. William Harrison at Honeywell Inc. The wafers were cut and polished into rectangular bars of width 2 mm, thickness 0.35 mm and length 15 mm, and then annealed at 600°C for 15 h.

Bending experiments were used to measure the shape change. The specimen was positioned on two knife-edge supports separated by 12 mm, and surrounded by a small brass box. A heater placed under the box could raise the temperature up to 270°C, as measured by a thermocouple positioned near the sample. One end of a glass rod was placed at the center of the sample and the other end attached to a dilatometer probe. Movement of the probe was measured with a differential transformer. To apply load to the sample, lead weights were placed on a shelf attached to the glass rod.

The sample was heated to a selected temperature above the Curie temperature, and the load was then applied. The sample was then cooled to room temperature under constant load. At room temperature the load was removed (except for the 8.6 g weight of the measurement probe) and the sample was then reheated. During the reheating cycle, the glass rod and dilatometer probe maintained contact with the sample to measure the amount of bending.

Stress and strain were calculated assuming a circular arc. Since both stress and strain are functions of position throughout the cross-section of the bar, the calculated values are for the maximum stress and strain present on the outside surface of the bar.

Dielectric properties were measured at frequencies of 1, 10, 100 and 1000 kHz. The major face of the bar was electroded by Au-evaporation and poled with a DC field of 15 kV/cm at room temperature. Dielectric constant and

loss factor were measured by a capacitance bridge at a constant heating rate of 2°/mm.

The samples with x = 4.0 and 7.0% La (width 2 mm, thickness 1 mm and length 12 mm) were squeezed at 400 kg/cm^2 (equivalent to the bending load of 86 g) at 310°C and 800°C, respectively, and cooled to room temperature. Sample faces, perpendicular and parallel to the stress direction, were examined by X-ray diffraction using Ni-filtered CuKα radiation and compared with a diffraction pattern recorded before squeezing.

3 STRESS-STRAIN-TEMPERATURE RELATIONSHIPS

Figure 1 shows the typical behavior of the bending strain with temperature under several different loads. Application of a load at high temperature bent the sample bar elastically, and the bending returned to zero upon removal of the load. The magnitude of elastic bending agreed with the value calculated using the reported values of s_{11} (Schmidt and Boczek, 1978; O'Bryan, 1973). On cooling under load, the magnitude of bending did

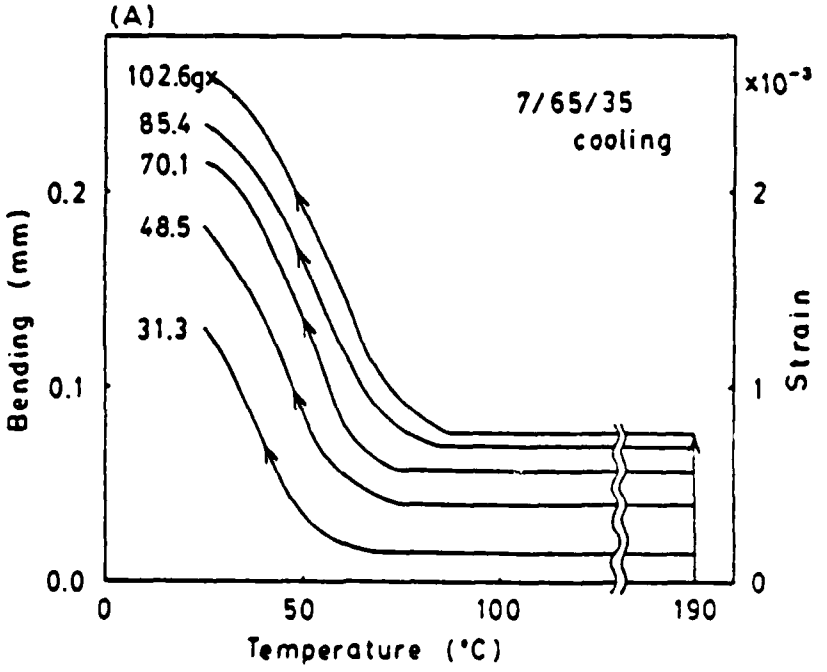

FIGURE 1(A) Bending behavior of a 7.0/65/3.5 ceramic as a function of temperature during cooling under several fixed loads. A load of 102.6 g caused fracture of the sample during cooling as indicated by X.

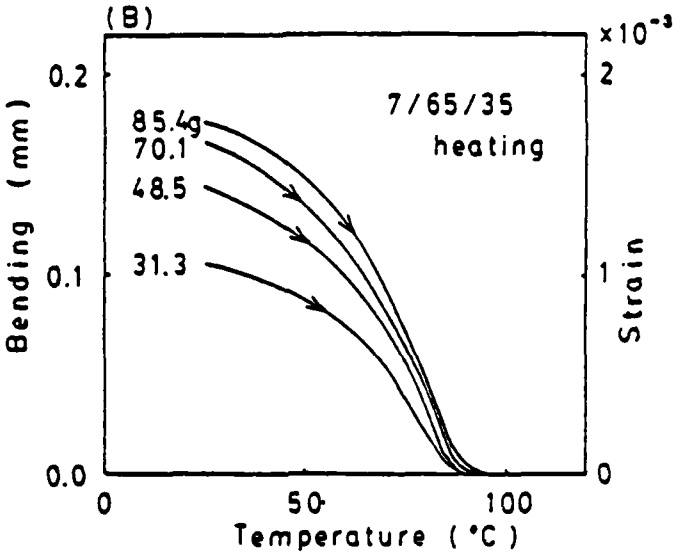

FIGURE 1(B) Bending behavior of a 7.0/65/35 ceramic during heating without load. The weights used to produce deformation during the preceding cooling cycle are given beside each curve.

not change appreciably down to a certain temperature T_s, at which bending began to increase rapidly, and continued increasing to room temperature. When the weight was removed at room temperature, there was a slight reduction in the amount of bending. The reduction in bending agreed with the value calculated from the s_{11} coefficient, indicating that this part of the strain was elastic. Reheating without load decreased the plastic portion of bending until it became zero at temperature T_f. The original shape was completely recovered by heating.

The elastic part of the bending increased linearly with the increase in load, but the plastic contribution tended to saturate. The amount of load also affected the characteristic temperature T_s. The initial deformation temperature T_s shifted to higher values under larger loads, but the shape-recovery temperature T_f did not depend noticeably on the size of load applied during cooling. Further increase in the load caused fracture of the sample during cooling, as indicated in Figure 1(A).

4 EFFECT OF La CONTENT ON THE STRAIN-TEMPERATURE RELATION

Figure 2 shows the effect of La content on the strain-temperature relation under various loads. Data showing maximum bending for each composition were selected; further increases in load caused fracture of the samples.

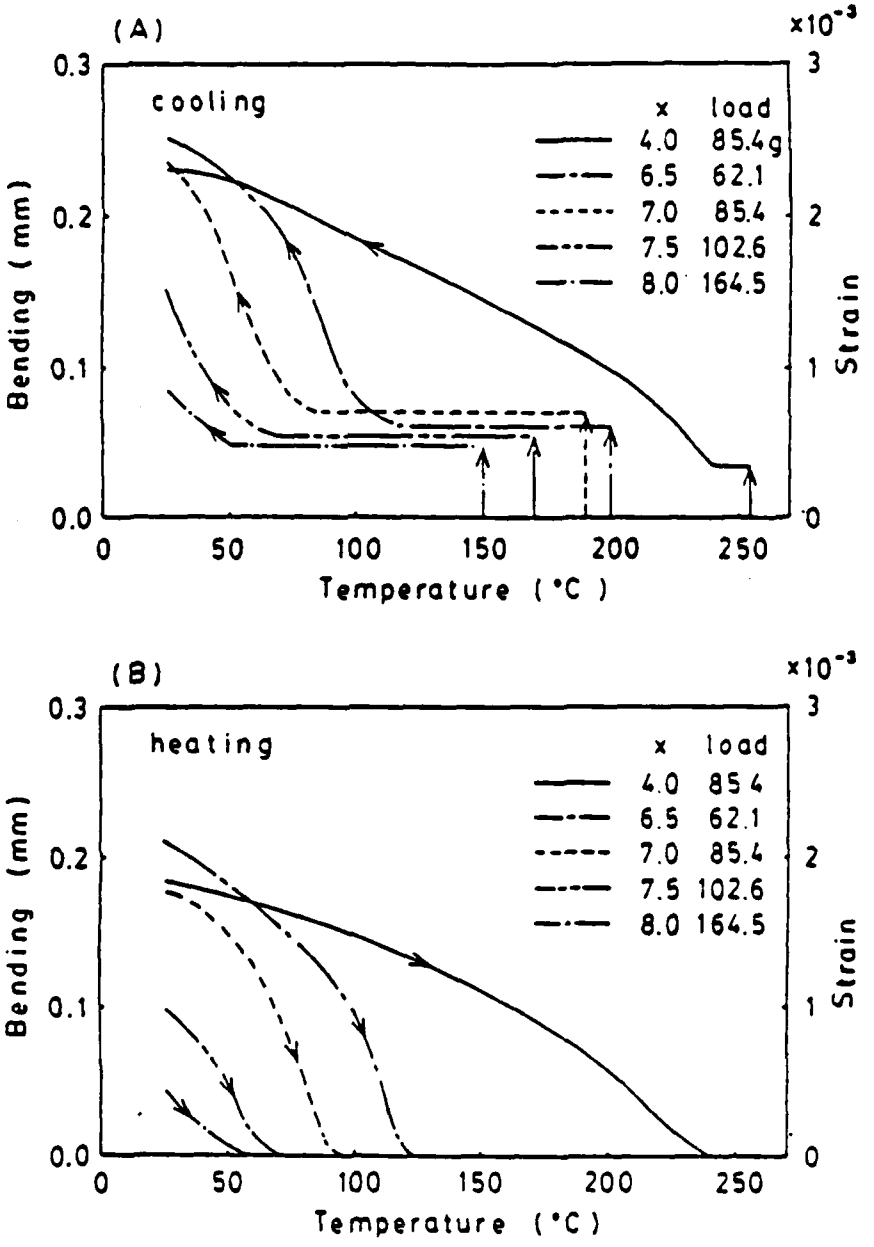

FIGURE 2 Effects of La content on the temperature-dependence of bending during (A) cooling under constant load and (B) heating without load.

Figure 3 shows the relations between temperatures T_s and T_f and the amount of load, as well as the load which caused fracture.

As judged from the amount of bending and dependence of T_s on load, the shape-memory behavior of the sample with $x = 4.0$ was different from that in the composition range $6.5 \leq x \leq 8.0$. For samples with $6.5 \leq x \leq 8.0$, those of higher La content showed less bending at room temperature as well as lower deformation temperatures T_s and restoration temperatures T_f. Larger loads were required to produce an equivalent bending in samples with high La content. The deformation temperature T_s was significantly lower than T_f. Furthermore, T_s increased appreciably with increasing load but T_f did not depend strongly on load. For the sample with $x = 4.0$, the characteristic temperatures T_s and T_f were the highest within the composition range examined, but the magnitude of bending at room temperature was about the same as the other samples. Furthermore, T_s and T_f were equal for the 4% sample and did not depend on the load applied.

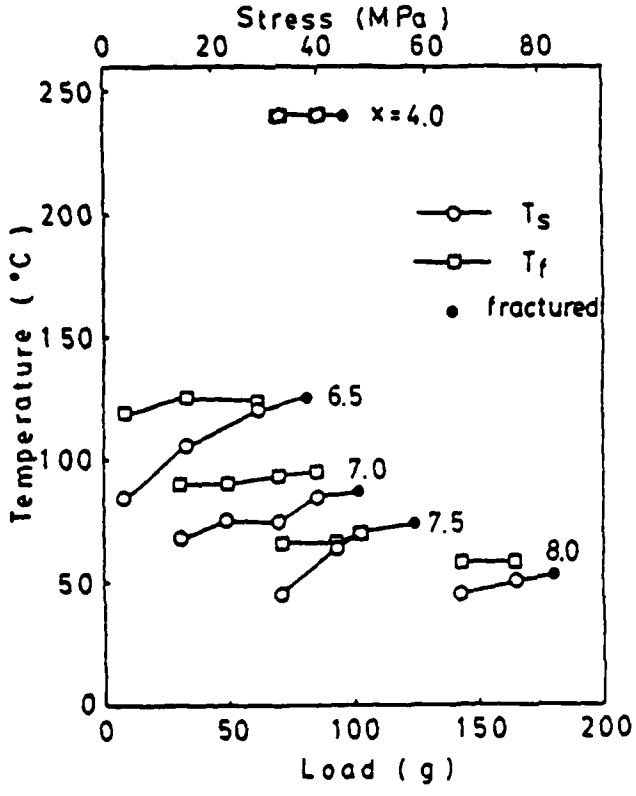

FIGURE 3 Relationships between characteristic temperatures T_s and T_f and the amount of load.

Another difference in the $x = 4.0$ sample was the behavior of bending during temperature-cycling under no load. After the samples were cooled under constant load, they were reheated to a certain temperature below T_f and then recooled without load. The bending increased as the temperature was lowered. For the $x = 4.0$ sample, the relation between bending and temperature was the same as that observed originally when cooled under stress, when the sample was reheated up to 10°C below T_f. Reheating above T_f and cooling without load caused no bending. In samples with $6.5 \leq x \leq 8.0$, the amount of bending observed during recooling was smaller than that of the initial cooling under load, and room-temperature bending was dependent on the temperature at which recooling was begun. For example in the case of the $x = 7.0$ sample deformed at 85.4 g ($T_f = 96$°C), recooling from 56°C reduced the room-temperature bending to 70% of the original value, and from 74°C the amount was 400%.

5 RELATION BETWEEN DIELECTRIC AND MECHANICAL PROPERTIES

The dielectric constant of poled samples with $6.5 \leq x \leq 8.0$ showed relaxor behavior in which the temperature of the dielectric maximum T_c depended on the measuring frequency. Furthermore there was a pre-maximum peak

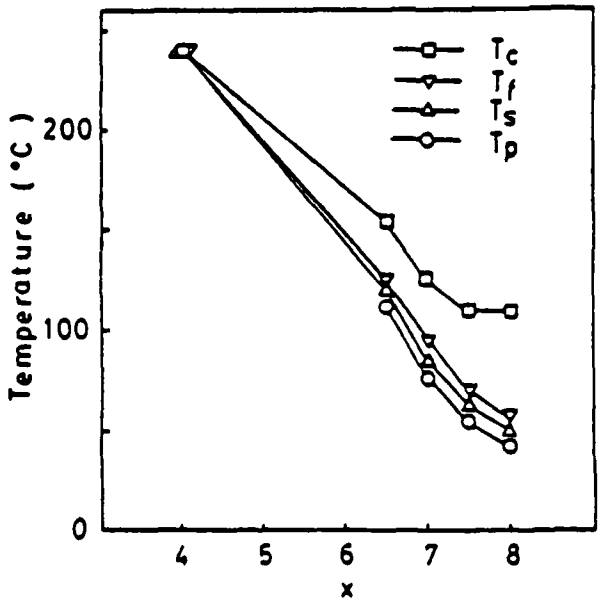

FIGURE 4 Curie temperature T_c, pre-maximum temperature T_p, deformation temperature T_s and restoration temperature T_f as a function of La content x.

associated with the disapperance of ferroelectric domains. The temperature of the pre-maximum peak T_p did not depend strongly on measuring frequency. In the case of $x = 4.0$, there was no pre-maximum peak and T_c did not depend on measuring frequency.

Figure 4 shows the relationship between La content and the characteristic temperatures T_c, T_p, T_s and T_f. The values of T_s and T_f were collected from the data shown in Fig. 2, and the T_c values correspond to those measured at 1 kHz. The T_s and T_f temperatures of the sample with $x = 4.0$ coincide with T_c, but those of the sample with $6.5 \leq x \leq 8.0$ lay between T_c and T_p. The dependence of T_s and T_f on La content more closely resembles that of T_p rather than T_c.

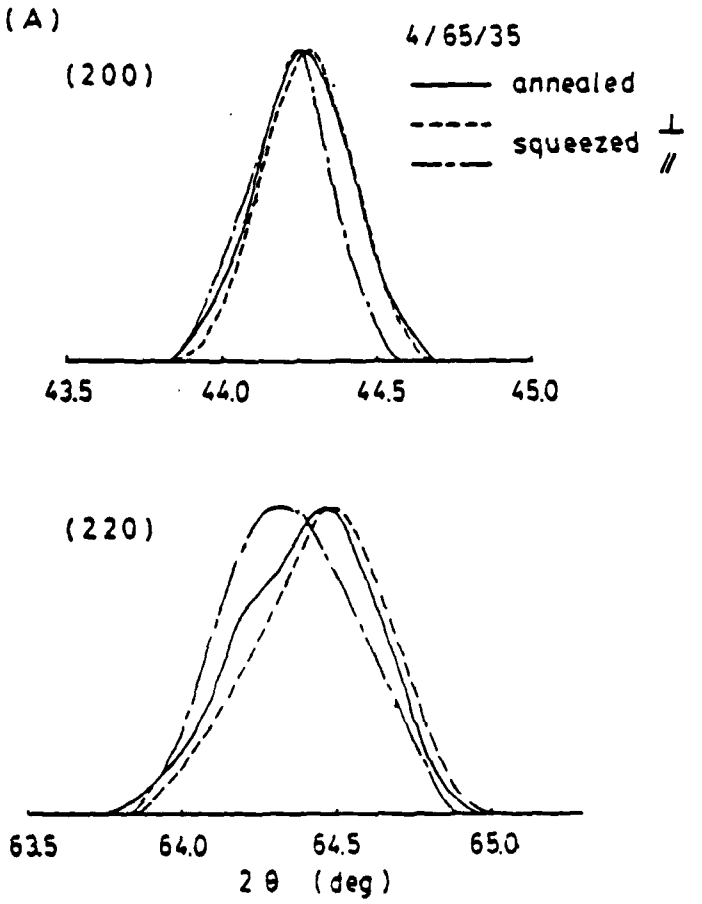

FIGURE 5 X-ray diffraction profiles of annealed (——) and compressed PLZT (------ face perpendicular, and —— - —— face parallel to stress direction) for (A) $x = 4.0$.

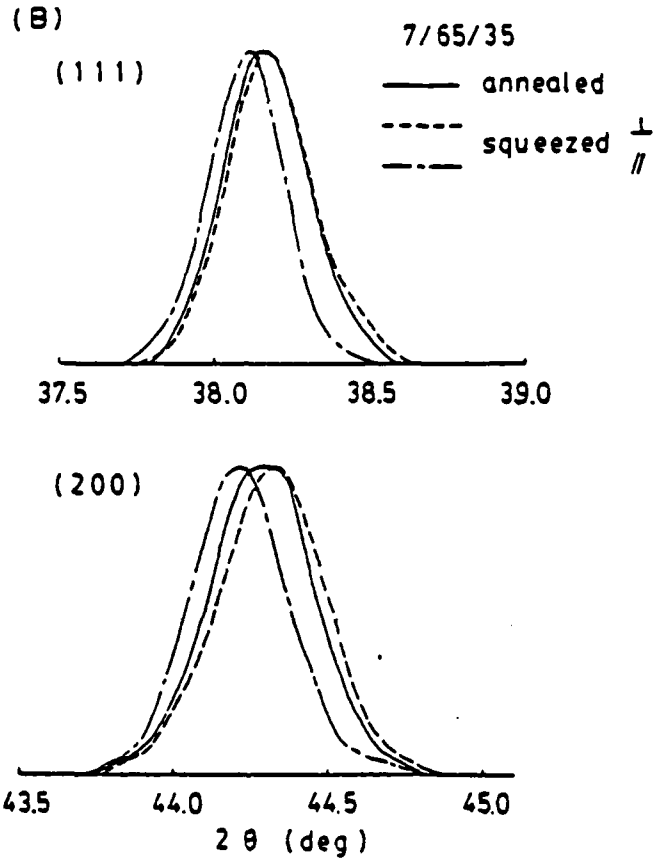

FIGURE 5 (contd.) for (B) $x = 7.0$.

6 X-RAY MEASUREMENT

Seven strong diffraction lines (110, 111, 200, 210, 211, 220 and 310) of annealed and compressed samples were examined. Figure 5 shows a few peak profiles and Table 1 lists the diffraction angles. The unit cell of the annealed samples was either rhombohedral ($x = 4.0$) with $a = 4.094$ Å and $\alpha = 89.76°$, or cubic ($x = 7.0$) with $a = 4.086$ Å, in good agreement with the reported structures and cell size (Keve and Bye, 1975; O'Bryan and Meitzler, 1972).

Peaks from the compressed samples shifted to higher values for faces cut perpendicular to the stress direction, and to lower angles for faces parallel to the stress. As expected for compression, the d-spacings of the faces oriented perpendicular to the stress direction were smaller than those of the faces

cut parallel to the stress. Peaks from the faces perpendicular to the stress were similar to those of the annealed sample.

Quantitative determination of phases present in the compressed samples was difficult because good high-angle diffraction data were not available. Because the largest differences in d-spacings between mutually perpendicular faces were between (220) and (200) for the $x = 4.0$ sample and between (200) and (111) for the $x = 7.0$ specimen, the structures were judged to be rhombohedral ($x = 7.0$).

7 DISCUSSION

For compositions with $x \leq 4.0$, the samples behave like normal ferroelectrics, but for those in the range $8 \geq x \geq 6.5$, domains are not observed on cooling through T_c, nor do they disappear at T_c on heating. Ordered domains in a poled ceramic disappear at T_p in this composition range. The close relationship between the shape-memory temperatures T_s and T_f, and T_c and T_p suggests that the domain process plays an important role in the shape-memory effect. Mechanical stress orders the domains at $T_c(x = 4.0)$ or at $T_p(6.5 \leq x \leq 8.0)$ during cooling, which results in a large pseudoplastic strain at room temperature. Heating eliminates the domains and restores the original shape.

X-ray diffraction measurements on the compressed samples (Figure 5 and Table I) gave the largest d-spacings from sample faces oriented parallel

TABLE I

Diffraction angles of annealed and compressed PLZT x/65/35 with $x = 4.0$ and 7.0

	Angle of peak maximum, 2θ (°)					
	$x = 4.0$			$x = 7.0$		
hkl	Annealed	Compressed ⊥	Compressed ∥	Annealed	Compressed ⊥	Compressed ∥
110	30.91	30.92	30.89	30.94	30.96	30.90
111	38.13	38.14	38.10	38.15	38.16	38.11
200	44.26	44.28	44.24	44.28	44.33	44.22
210	49.79	49.80	49.72	49.84	49.86	49.78
211	55.00	55.01	54.90	55.01	55.05	54.93
220	64.46	64.48	64.30	64.47	64.51	64.39
310	73.14	73.18	73.07	73.16	73.24	73.07

⊥ Faces perpendicular to stress.
∥ Faces parallel to stress.

to the stress direction. This means that the polar directions are preferentially aligned perpendicular to the compressional stress.

For samples with La content $6.5 \leq x \leq 8.0$, the deformation temperature T_s depends on load, but the restoration temperature T_f does not (Figure 3). Electrically, the discontinuity temperature in polarization shifts to higher values when the dc bias field increases (Keve and Annis, 1973). This abrupt change in polarization with temperature is associated with the domain phenomena occurring at T_p. This effect is analogous to the shift in T_s and T_f under mechanical stress. Since no mechanical stress was applied during heating, however, the restoration temperature T_f was not influenced by the stress applied during cooling. Apparently, mechanical stress has similar effects to an electric field in aligning domains. The anisotropic thermal expansion coefficients (O'Bryan and Meitzler, 1972) observed in hot-pressed PLZT ($x = 8.0$) further supports this view. Radial stresses developed during cooling in the hot-pressing procedure cause domain alignment below the Curie temperature. Thermal expansion coefficients parallel to the direction of the compressional stress are higher than in annealed material, while negative coefficients are observed in the direction of tensile stresses.

These facts show that the polar direction can be easily aligned by stress when the sample is cooled through the temperature at which the domains form. Tensile stress aligns the polar direction parallel to the stress direction, and compressive stress favors domains in the perpendicular direction.

The relationship between bending and temperature shown in Figures 1 and 2 differs from the results reported by Schmidt and Boczek (1978), especially with regard to the shape of the cooling curve and the magnitude of bending. They observed a large bending at high temperature, and an elastic compliance about 300 times larger than the value determined by resonance measurement. This discrepancy might be attributed to the method of supporting the sample. Schmidt and Boczek used a cantilever method, in which one end of the sample was fixed, but this results in a rather complicated stress state. In our experiment, the samples were freely held by two supports. Under these circumstances, the stress state at a supporting position is not as complicated. Since stress levels strongly affect the shape-memory effect, the discrepancy in the results may be attributable to the experimental method.

Schmidt and Boczek (1978) postulated, on the basis of their data, that the relaxor or diffuse phase transformation was essential to obtain the shape-memory effect in ferroelectrics. The PLZT sample with $x = 4.0$, however, is not a relaxor. The fact that this sample shows a shape-memory effect indicates that the relaxor behaviour is not an essential property. To confirm this idea, $BaTiO_3$ ceramic bar with the same shape and size as the PLZT samples was examined. Figure 6 shows the bending-temperature relation. Upon cooling from 180°C under constant stress, bending increased

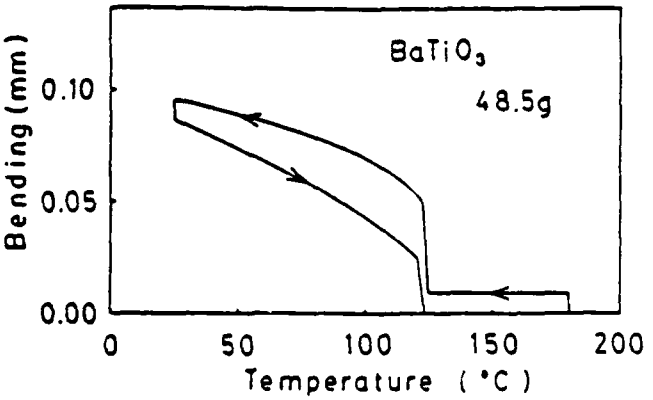

FIGURE 6 Temperature-dependence of bending of $BaTiO_3$.

abruptly between 125° and 122°C and more slowly below 122°C. When the sample was reheated after removing the load at room temperature, bending decreased gradually up to 121°C and then fell sharply to zero between 121° and 123°C. This abrupt change in shape near the Curie temperature (126°C) coincides with the discontinuity in the lattice parameters, and indicates that domain formation and disappearance are likely causes of the shape-memory effect in ferroelectrics.

The maximum room-temperature strain obtained in these experiments was 2.1×10^{-3} in the sample with $x = 6.5$. The stress field is complicated in the bending test and it is difficult to understand which of the stresses, tension or compression, govern the strain. However, the observed strain can be compared with electrically-induced strain. In the sample with $x = 7.0$, the strains parallel and perpendicular to the electric field at room temperature are 2.1×10^{-3} and 0.5×10^{-3}, respectively (Smith, 1973). In our experiment the plastic part of the strain at room temperature in such a sample was 1.8×10^{-3} (Figure 1), which is comparable to the strain parallel to the electric field. Table II lists the values calculated from the data in Table I. The strains were calculated by comparing the d-spacings between compressed and annealed samples. In both samples, the strains observed in the faces parallel to the stress direction were larger than those in perpendicular faces. In the compressed samples, the polar axes are nearly perpendicular to the stress direction as discussed previously. The large strains observed parallel to the stress direction coincide with the large strains measured parallel to the electric field.

Large strains under tensile stress have been observed in samples with $x = 1.3$ and 6.0 (Meitzler and O'Bryan, 1971). At room temperature, the maximum strain in the $x = 6.0$ sample was 2.5×10^{-3}, which is almost the same strain observed in the present experiments. A structural phase change

TABLE II

Differences of d-spacing between annealed and compressed samples

	$\frac{d \text{ compressed} - d \text{ annealed}}{d \text{ annealed}} \times 10^3$			
	$x = 4.0$		$x = 8.0$	
hkl	$\perp$	$\parallel$	$\perp$	$\parallel$
110	−0.3	0.7	−0.7	1.4
111	−0.2	0.8	−0.3	1.0
200	−0.4	0.4	−1.1	1.3
210	−0.2	1.3	−0.4	1.1
211	−0.2	1.7	−0.7	1.3
220	−0.3	2.2	−0.6	1.1
310	−0.5	0.9	−0.9	1.1

accompanied by a high degree of preferred orientation parallel to the direction of the applied tensile force is the cause of the large strains.

Figure 7 shows the temperature-dependence of the plastic part of the strain plotted with reduced temperature T/T_c and T, T_f. In the case of cooling under stress, the relationship between strain and the reduced temperature can be expressed by a single curve, except for the $x = 4.0$ sample. For the heating cycle, the relations for $x = 6.5$ and 7.0 coincide but others do not; all lie under the curve for $x = 6.5$ and 7.0. The behavior of the $x = 4.0$ ceramic might be attributed to differences in crystal structure. The structures of the compressed samples were rhombohedral ($x = 4.0$) and tetragonal or of mixed phases ($x = 7.0$). The single curve relating strain and the reduced temperature shown in Figure 7(A) would imply that the crystal structures of $6.5 \leq x \leq 8.0$ are the same. In perovskites, the strain associated with a tetragonal distortion is generally larger than that of a rhombohedral distortion. Inversion of the magnitude of strain between $x = 4.0$ and 6.5 might result from such a difference in crystal structure.

Disagreement of the relation between strain and reduced temperature in the heating cycle for samples with $6.5 \leq x \leq 8.0$ might be attributed to the temperature at which the load was removed. To confirm this conjecture, two additional experiments were undertaken. In the first experiment, the weight was removed at various temperatures during the cooling. Figure 8 shows the result for $x = 7.0$. When unloaded at high temperatures (but below T_c), the reduction in bending was larger than that observed at room temperature.

In the second experiment, the sample was loaded at room temperature and then heated. Room-temperature bending was almost the same as that observed when the cooled sample was unloaded at room temperature (Figure 1). Bending increased during heating up to a certain temperature, and then

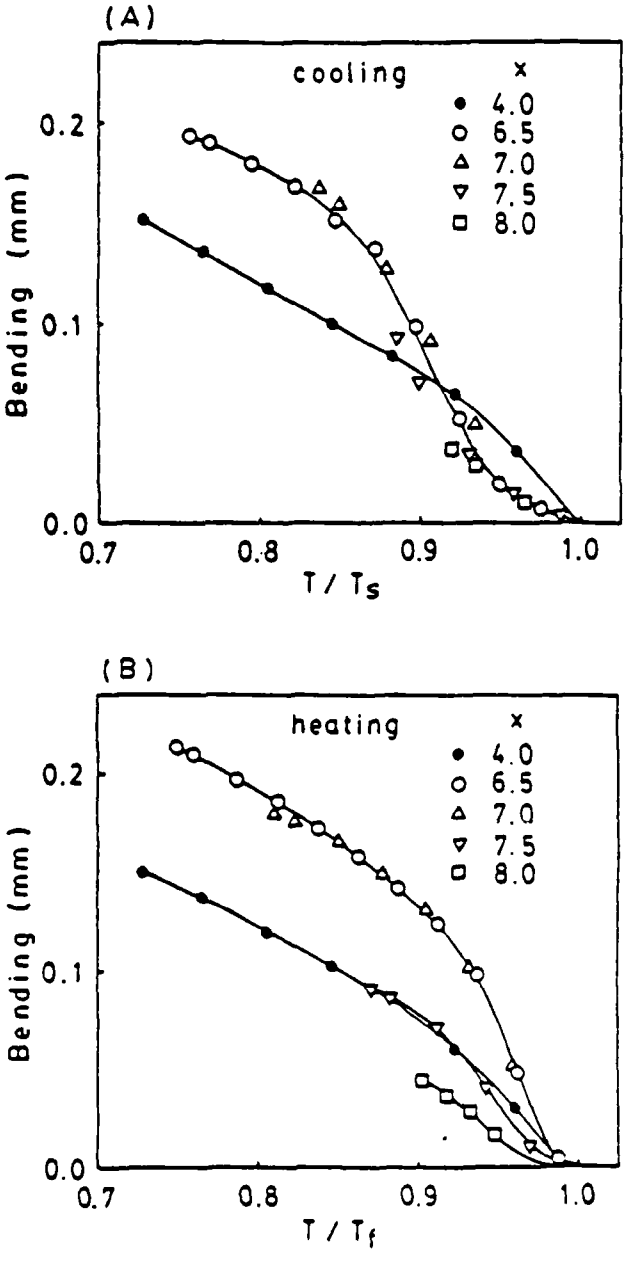

FIGURE 7 Relations between bending and reduced temperatures (A) T/T_s during cooling under constant load and (B) T/T_f during heating without load.

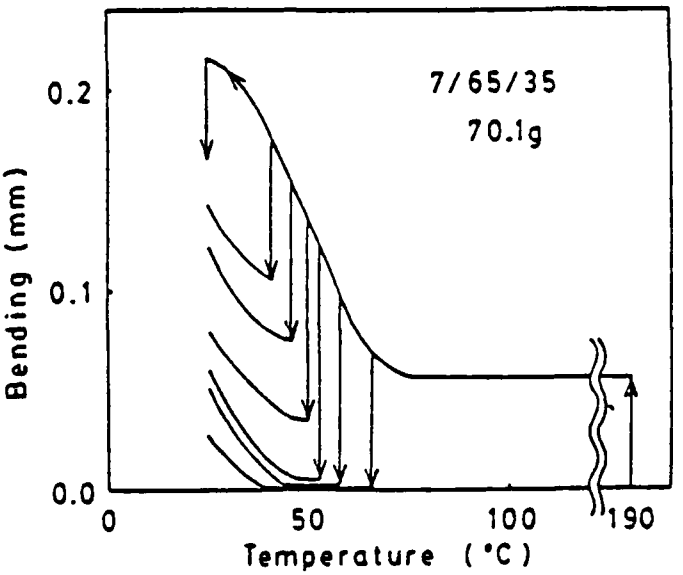

FIGURE 8 Reduction of bending by removal of the load at different temperatures in the sample 7.0/65/35.

decreased at higher temperatures, as shown in Figure 9. This result indicates that below T_p the stresses caused a phase transformation to a distorted structure with an aligned polar direction. The magnitude of the bending up to the temperature at which bending became a maximum is indicative of the ease of domain wall motion, i.e., the mechanical coercivity decreases with increasing temperature. Decrease in the bending at still higher temperature results from a reduction of the spontaneous strain.

Based on these two additional experiments, the following explanation appears feasible. The presence of mechanical stress forces domain alignment, so that a single curve expresses the relationship between strain and reduced temperature in the cooling cycle, as shown in Figure 7(A). Removal of the stress at room temperature releases the external constraint, and the internal stresses developed during cooling under stress tend to stabilize the structure. Since the difference between T_p and room temperature are large for $x = 6.5$ and 7.0, the domain walls cannot move, and the only reduction in bending during unloading is elastic in nature. For $x = 7.5$ and 8.0, on the other hand, T_p is low and some of the domains reorient to a more stable configuration during stress removal at room temperature. In other words, the mechanical relaxation time at room temperature decreases with increasing La content (Esaklul, Gerberich and Koepke, 1980). The reduction of bending accompanying unloading at room temperature has both elastic and domain

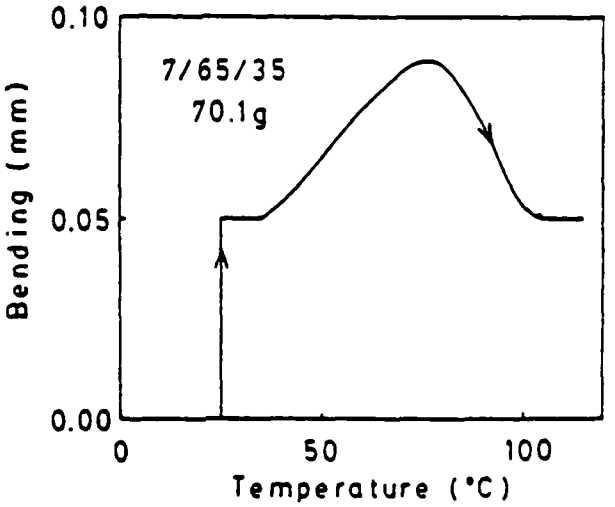

FIGURE 9 Temperature-dependence of bending during heating under constant load of 70.1 g.

contributions for $x = 7.5$ and 8.0, resulting in the different curves in Figure 7(B).

The anomalous behavior caused by temperature cycling without load can also be explained by this idea. For $x = 7.0$, heating to high temperatures just below T_f causes domain re-orientation, resulting in smaller strains when recooled to room temperature. But several cycles between room temperature and 10°C below T_f did not lead to appreciable domain re-orientation.

8 CONCLUSION

The strains associated with the shape-memory effect in ferroelectric ceramics can be explained as follows. Above T_c the crystallites are cubic, and domains form when the sample is cooled through the transition temperature under stress. Mechanical stress causes partial alignment of the polarization directions (but not the absolute sense). The degree of alignment is determined by the magnitude of the stress, as in the case of electrical poling. In the perovskite structures, the polar axis is longer than the other axes. Polar axes tend to align parallel to a tensile stress. Domains with polarization vectors perpendicular to the stress direction are favored for compressional stresses. The alignment in a ceramic is not complete, however, because of random grain orientation and becauses of internal stresses between neighboring grains. After the domain pattern is formed, further cooling has little

effect on the domain walls. But cooling increases the spontaneous strain of the distorted unit cell, and therefore the total strain increases as the temperature is decreased.

When the lattice parameters change discontinously at the ferroelectric transition temperature, an abrupt change in shape takes place, as in the case of $BaTiO_3$. When the lattice parameters change continuously, a gradual shape-change temperature-change is observed, as in the case of PLZT.

When stress is removed at room temperature, the total strain is reduced by an amount equivalent to the elastic contribution. If domain walls can move at room temperature, further reduction in total strain occurs by domain re-orientation as in the case of PLZT samples with $7.5 \leq x \leq 8.0$.

Upon heating without load, the decrease in spontaneous strain causes a gradual reduction in total strain. Domain re-orientation near the transition temperature contributes a further decrease in strain. Finally the spontaneous strain disappears at T_f, and the total strain goes to zero. In other words the shape-memory effect in ferroelectrics is caused by domain alignment together with the temperature-dependence of spontaneous strain.

Acknowledgements

This work was sponsored by the U.S. Army Research Office (DAAG29-80-C-0008). We also wish to thank Dr. William Harrison for supplying the samples, and Mr. James Laughner for his assistance with the experiments.

References

Carl, K. and K. Geisen (1973). Dielectric and optical properties of a quasi-ferroelectric PLZT ceramic. *Proc. IEEE*, 61, 967.

Delaey, L., R. V. Krishnan, H. Tas and H. Warlimont (1974). Thermoelasticity, pseudoelasticity and the memory effects associated with martensitic transformations. *J. Mater. Sci.*, 9, 1521, 1536, 1545.

Esaklul, K. A., W. W. Gerberich and B. G. Koepke (1980). Stress relaxation in PZT. *J. Amer. Ceram. Soc.*, 63, 25.

Haertling, G. H. and C. E. Land (1971). Hot-pressed (Pb, La) (Zr, Ti)O_3 ferroelectric ceramics for electrooptic applications. *J. Amer. Ceram. Soc.*, 54, 1.

Keve, E. T. and A. D. Annis (1973). Studies of phase transformations and properties of some PLZT ceramics. *Ferroelectrics*, 5, 77.

Keve, E. T. and K. L. Bye (1975). Phase identification and domain structure in PLZT ceramics. *J. Appl Phys.*, 46, 810.

Maldonado, J. R. and L. K. Anderson (1971). Strain-biased ferroelectric-photoconductor image storage, and display devices operated in a reflection mode. *IEEE Trans. Electron Devices*, 18, 774.

Maldonado, J. R. and A. H. Meitzler (1970). Ferroelectric ceramic light gates operated in a voltage-controlled mode. *IEEE Trans. Electron Devices*, 17, 148.

Maldonado, J. R. and A. H. Meitzler (1971). Strain-biased ferroelectric-photoconductor image storage and display devices. *Proc. IEEE*, 59, 368.

Meitzler, A. H. and H. M. O'Bryan, Jr., (1971). Ferroelastic behavior of PLZT ceramics when subjected to large tensile strains. *App. Phys. Letters*, 19, 106.

Meitzler, A. H. and H. M. O'Bryan, Jr. (1973). Polymorphism and penferroelectricity in PLZT ceramics. *Proc. IEEE*, 61, 959.

O'Bryan, Jr., H. M. and A. H. Meitzler (1972). Enhanced ordering of ferroelectric domains in PLZT ceramics. *Bull. Amer. Ceram. Soc.*, 51, 459.

O'Bryan, Jr., H. M. (1973). Phase relations in (Pb, La) $Zr_{0.65}Ti_{0.35}O_3$. *J. Amer. Ceram. Soc.*, 56, 385.

Schmidt, G. and I. Boczek (1978). Pseudoelasticity and shape memory of PLZT ceramic. *Phys. Stat. Sol.* (a) 50, K109.

Schulze, W. A., J. V. Biggers and L. E. Cross (1978). Aging of dielectric dispersion in PLZT relaxor ceramics. *J. Amer. Ceram. Soc.*, 61, 46.

Smith, W. D. (1973). Electrically-controlled secondary phase in PLZT ceramics. In L. E. Cross (Ed), *Phase Transitions*. Pergamon Press, New York, pp. 71.

Warlimont, H. (1976). Shape-memory effects. *Mater. Sci. Engineering*, 25, 139.

Appendix 11

Magnetoferroelectricity in Cr_2BeO_4

R. E. Newnham, J. J. Kramer, W. A. Schulze, and L. E. Cross

Magnetoferroelectricity in Cr_2BeO_4

R. E. Newnham, J. J. Kramer,[a] W. A. Schulze, and L. E. Cross

Materials Research Laboratory, Pennsylvania State University, University Park, Pennsylvania 16802
(Received 15 March 1978; accepted for publication 25 May 1978)

Chromium chrysoberyl undergoes a phase transformation from a paramagnetic state to a complex antiferromagnetic state at 28 K. The spiral spin structure of the antiferromagnetic state violates all the crystallographic symmetry elements, making Cr_2BeO_4 potentially ferroelectric. Chynoweth experiments conducted at low temperatures reveal a weak pyroelectric effect which disappears above 28 K. Cr_2BeO_4 ceramics can be poled electrically between 24 and 28 K, giving rise to remnant polarizations four to six orders of magnitude smaller than normal ferroelectrics. The pyroelectric coefficient and the remnant polarization reverse in sign with the poling field, but no anomalies in the electric permittivity or electric conductivity occur at the Néel point.

PACS numbers: 77.80.−e, 75.80.+q, 77.70.+a, 75.50.Ee

Recent research on ferroelectrics has led to a growing interest in the fundamental causes of ferroelectric phase transitions, focusing especially on soft modes, order parameters, and improper transitions. There has also been an increasing awareness of cross-coupled domain phenomena caused by electric, elastic, and magnetic interactions. Lithium ammonium tartrate, for instance, is a type of *elastoferroelectric* in which mechanical strain is the primary order parameter at the 98 K phase transition. Strain gives rise to ferroelectricity through piezoelectric coupling with the polarization.[1] The opposite effect occurs in sodium potassium tartrate (rochelle salt) where electric polarization is the primary order parameter. Domains can be switched with mechanical stress as well as with electric fields because of the small spontaneous strain resulting from piezoelectric coupling to the polarization. Since the ferroelastic effect has its origin in an electric instability, we refer to its as *electroferroelasticity*.

Four other cross-coupled effects arise when magnetic phenomena are included. There are a number of examples of *elastoferromagnetism* and *magnetoferroelasticity* and at least one good example of *electroferromagnetism*: nickel iodine boracite.[2] At room temperature, NiI boracite is cubic, point group $\bar{4}3m$. Below room temperature at 120 K, it undergoes a transition to an antiferromagnetic state as the Ni^{2+} moments align; at this stage, the material is an antiferromagnetic piezoelectric, but it is neither ferromagnetic nor ferroelectric. On further cooling, a second phase transition to an orthorhombic ferroelectric state takes place at 64 K. As the crystal structure develops a spontaneous polarization, the magnetic structure is also altered, destroying the balance of spins in the antiferromagnetic state and producing a weak ferromagnetism. The ferromagnetic effect is of electric origin and can be referred to as an *electroferromagnet*. We have described this effect in some detail because it is the opposite of a *magnetoferroelectric*, the subject of this investigation.

A magnetoferroelectric develops a reversible spontaneous electric polarization on passing through a magnetic phase transition. The one-dimensional model in Fig. 1 illustrates the principle of a magnetically induced ferroelectric. At high temperatures, the system is paramagnetic and nonpolar with the paramagnetic cations located on centers of symmetry. On cooling through the Néel point, the system becomes antiferromagnetic with spins aligned along the chain direction. The spins order in such a way that each magnetic ion has one neighbor with parallel spin and one with antiparallel spin. The inversion centers are destroyed by magnetic order, making the chain a polar axis. Small atomic movements take place because of the differences in interatomic forces between atom pairs with parallel spin and atom pairs with antiparallel spin.

If the cations move in the same direction, as in Fig. 1, an electric polarization is produced. The atomic displacements destroy the centers of symmetry and make the material pyroelectric, piezoelectric, and potentially ferroelectric. The expected polarization is small because most magnetic transitions show second-order behavior with very small magnetostrictive effects.

No magnetoferroelectrics are known at present, although three possibilities have been suggested.[3] Bismuth manganate ($BiMn_2O_5$), calcium manganate ($CaMn_2O_4$), and terbium chromite ($TbCrO_3$) show the required symmetry change. We have searched the magnetics literature and found more than 30 other potential magnetoferroelectrics. The compilations by Oles and co-workers[4] and by Connolly and Coperthaver[5] were helpful in this regard. Most of the potential magnetoferroelectrics are antiferromagnetic with low transition temperatures and complex magnetic struc-

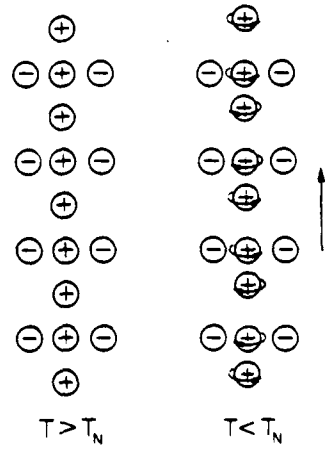

FIG. 1. Paramagnetic and antiferromagnetic states in a hypothetical magnetoferroelectric in which arrows indicate spin directions. Centers of symmetry are destroyed at the magnetic transition, converting the chain to a polar axis.

[a]On leave from the University of Delaware, Newark, Delaware 19702.

 0021-8979/78/4912-6088$01.10

tures, far more complicated than the model structure in Fig. 1. The material chosen for detailed investigation was chromium chrysoberyl, Cr_2BeO_4, one of the few good electrical insulators among the candidate compounds.

Cr_2BeO_4 is orthorhombic and isostructural with the minerals chrysoberyl (Al_2BeO_4) and forsterite (Mg_2SiO_4). The crystal structure consists of a close-packed lattice of oxygen ions with Cr^{3+} in octahedral sites and Be^{2+} in tetrahedral positions. At room temperature, Cr_2BeO_4 is paramagnetic and centrosymmetric and, therefore, nonpiezoelectric, nonpyroelectric, and nonferroelectric.

Low-temperature magnetic susceptibility measurements[6] show a cusp-shaped peak at 28 K characteristic of a paramagnetic-antiferromagnetic transition. The magnetic structure determined by neutron diffraction[7] at 4.5 K is a cycloidal spiral with a periodicity of about 65 Å, roughly 12 unit-cell lengths. Antiferromagnetic resonance experiments[8,9] confirmed the spiral structure and Néel temperature. The symmetry of the magnetic structure is triclinic, point group 1, making chromium chrysoberyl potentially magnetoferroelectric below 28 K.

Chromium chrysoberyl ceramics are prepared by calcining the coprecipitated metal-ion hydroxides. An intimate mixture was obtained by reacting mixed standard solutions of aluminum sulfate, chromium nitrate, and beryllium sulfate with ammonium hydroxide. The powder was dry pressed and then sintered at 1300 °C for 48 h to produce green-colored ceramics with resistivities greater than 10^7 Ω m. The crystal structure was confirmed by x-ray diffraction.

The properties of a magnetically induced ferroelectric are expected to differ radically from conventional ferroelectrics, since the atomic displacements are much smaller. Dielectric and piezoelectric coefficients are likely to be small, but domain walls should move easily, just as they do in most magnetic materials. In this case, however, domain-wall motion is controlled by electric fields rather than magnetic fields, and the resultant signal is electric charge rather than magnetic charge.

Five types of experiments were performed on polycrystalline Cr_2BeO_4: pyroelectric measurements, thermal depoling, pulse poling, complex permittivity measurements, and optical second-harmonic generation. The first three experiments gave evidence of ferroelectric behavior.

Electrical measurements were made on Cr_2BeO_4 ceramic disks 2.8 mm in diameter and 0.13 mm thick. The disks were electroded with evaporated gold and mounted on an alumina substrate in a TO-5 transistor can using conducting epoxy. Carbon black was coated on the upper gold electrode to absorb light. The TO-5 can was then mounted in a recessed copper holder and cooled with liquid helium in an Air Products LT-3-110 cold finger.

For the pyroelectric experiments, a buffer FET preamplifier positioned within the cold finger was used to minimize loading capacitance on the sample, thereby maintaining reasonable signal levels. Following the Chynoweth method,[10] the sample was irradiated by a chopped defocused

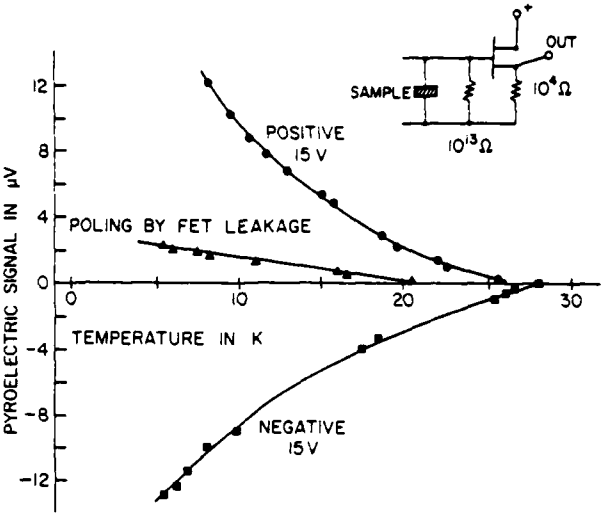

FIG. 2. Pyroelectric signal from Cr_2BeO_4 ceramics plotted as a function of temperatures.

1-mW He-Ne laser and the resulting pyroelectric signal detected with the aid of a lock-in amplifier.

For the initial pyroelectric measurements, the sample was poled with a field of 0.12 MV/m while cooling through the transition region. A signal was observed in the order of microvolts and was found to reverse in sign when poling was conducted with opposite polarity. If the supply voltage to the preamplifier was left on, a low level of poling was observed due to the leakage through the FET.

The level of pyroelectric signal as a function of temperature is illustrated in Fig. 2. Because of rapidly changing specific heat in this region, it is difficult to define the temperature change ΔT, but if a T^3 relation is assumed for specific heat, a more normal pyroelectric response is calculated.

Below about 24 K, the magnitude of the pyroelectric signal is reversible with temperature. When the temperature is raised above 24 K, however, the signal degrades and does not increase significantly with decreasing temperature. It appears that this is a transition region in which portions of the ceramic depole may only be repoled by an external bias.

Poling by any method other than cooling through the transition region under bias was only marginally successful. Small pyroelectric signals could be induced from a thermally depoled ceramic by poling with fields of 5 MV/m at 10 K. Attempts to reverse poling with up to 6 MV/m results in only very weak signals of opposite sign, showing that the coercive field increases rapidly below 24 K.

Calibration of the polarization levels observed in the pyroelectric experiments was achieved by thermal depoling. The absorbing surface of the sample was exposed to light from a 750-W projector lamp, and the resulting pyroelectric charge was collected with an integrating electrometer. When connected in a feedback mode, the system was capable of measuring charges less than 1 pC.

The polarization level is defined by the voltage applied as the sample was cooled through the transition region and by the discharge temperature. Once the polarization was in-

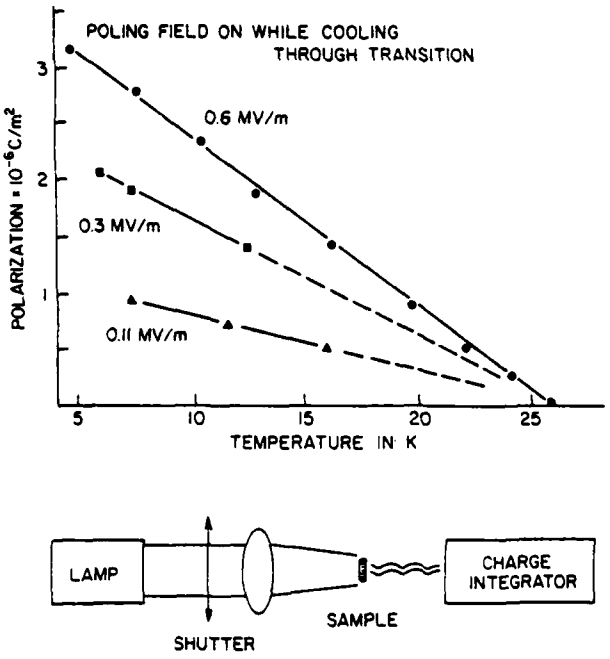

FIG. 3. Thermal depoling of Cr_2BeO_4 ceramics.

duced by the poling field, there appeared to be no degradation with temperature cycling below the transition region and with waiting periods up to 45 min. As shown in Fig. 3, Cr_2BeO_4 exhibits a linear dependence of polarization of the poling field and temperature. No saturation in polarization at low temperatures was observed in depoling experiments for poling fields ranging from 0.1 to 0.6 MV/m. Experiments at 7 K indicate a linear field dependence over 6 MV/m.

The temperature range in which maximum polarization is achieved for a given poling field lies between 24 and 28 K, in agreement with the pyroelectric experiments. Poling below 24 K led to only small polarizations.

Pulse poling was attempted utilizing differential integrators. A 10-ms voltage pulse was applied through an operational power supply to the sample and a linear capacitor of similar value. By observing the difference in these signals, small nonlinearities could be detected. Pulse poling lessens the effect of leakage current and sample heating that trouble a normal Sawyer-Tower measurement.

Pulse poling proved no more effective in reversing the polarization below the transition region than did the steady application of a field used in the pyroelectric experiment, even through much higher fields were applied. Field levels up to 8 MV/m were applied in 10-ms pulses, but polarizations of less than 1 μC/m² could be induced, and these were not achieved consistently.

The complex permittivity of Cr_2BeO_4 was measured as a function of temperature at several frequencies and under different bias fields, but nothing unusual was observed. Capacitance and tanδ were measured at 1, 10, 100 kHz, and 1 MHz using an automatic bridge. A three-terminal configuration connecting the cold-finger housing and the TO-5 can to the guard held the stray capacitance to about 0.3 pF. The resistivity increased on cooling from room temperature to liquid-helium temperature, but the capacitance remained at 4.0 ± 0.1 pF over the entire range. There were no anomalies at the Néel temperature of Cr_2BeO_4. Bias fields as large as 1.5 MV/m had no effect on the results. The measurements were repeated at high ac fields using a transformer ratio bridge operating at 100 Hz, 1 kHz, and 10 kHz. No change in ϵ or tanδ was observed in fields as large as 0.7 kV/m.

Chromium chrysoberyl and about 20 other potential magnetoferroelectrics were also tested for acentricity by optical second-harmonic generation, but with negative results. Our apparatus is similar in design to the SHG powder experiment described by Kurtz and Perry.[11] Second-harmonic signals as small as 0.001 times that of a comparable quartz specimen could be detected, but none were observed, either above or below the Néel points. The sensitivity of the experiment was hampered by absorption (all the specimens were colored) and by spurious light originating from a plasma in the evacuated low-temperature sample chamber. In any case, there was no evidence for acentricity from the SHG experiments.

In summary, when poled electrically, chromium chrysoberyl shows a pyroelectric effect in its antiferromagnetic state. The sign of the pyroelectric coefficients changes when the bias field is reversed. The reversible spontaneous polarization in the magnetoferroelectric state is approximately a million times smaller than that of $BaTiO_3$.

The influence of a magnetic phase transition on the spontaneous polarization of a pyroelectric has been described in a recent publication by Glass and co-workers.[12] Barium nickel fluoride ($BaNiF_4$) is a normal ferroelectric with a spontaneous polarization of 0.07 C/m², but at low temperatures, the nickel spins align antiferromagnetically causing a pronounced anomaly in the dynamic pyroelectric signal. The magnetic contribution to the spontaneous polarization is 0.9 mC/m², about two orders of magnitude smaller than P_s, and is proportional to the magnetic specific heat.

The reversible spontaneous polarization in Cr_2BeO_4 is approximately a thousand times smaller than the magnetic contribution to the spontaneous polarization of $BaNiF_4$ and about a hundred times smaller than the polarization predicted theoretically.[13] Goshen and co-workers also predicted[13] that the changes in electric susceptibility accompanying a magnetically induced ferroelectric transition would be too small to measure. This is consistent with the permittivity measurements on Cr_2BeO_4.

Magnetoferroelectrics are a type of improper ferroelectric, like gadolinium molybdate, in which polarization is not the order parameter driving the transformation. Because of the weakness in coupling between magnetic and electric effects, magnetoferroelectrics might be termed the ultimate impropriety.

ACKNOWLEDGMENTS

This work was sponsored by the Army Office of Research and Development (DAA 29-76-G-0145). We also wish to thank our colleagues at the Materials Research Laboratory for their advice and assistance.

[1]A Sawada, M. Udagawa, and T. Nakamura, Phys. Rev. Lett. **39**, 829 (1977).
[2]H. Ascher, H. Rieder, H. Schmid, and H. Stössel, J. Appl. Phys. **37**, 1404 (1966).
[3]S. Goshen, D. Mukamel, H. Shaked, and S. Shtrikman, J. Appl. Phys. **40**, 1590 (1969).
[4]A. Oles, F. Kajzar, M. Kucab, and W. Sikora, *Magnetic Structures Determined by Neutron Diffraction* (Panstwowe Wydawnictwo Naukowe, Warsaw, 1976).
[5]T.F. Connolly and E.D. Copenhaver, *Solid State Physics Literature Guides* (Plenum, New York 1972), Vol. 5.
[6]R.P. Santoro and R.E. Newnham, J. Am. Ceram. Soc. **47**, 491 (1964).
[7]D.E. Cox, B.C. Frazer, R.E. Newnham, and R.P. Santoro, J. Appl. Phy **40**, 1124 (1969).
[8]J.H. Ranicar and P R. Elliston, Phys. Lett. A **25**, 720 (1967).
[9]P.R. Elliston and G.J. Troup, Proc. Phys. Soc. (London) **92**, 1040 (196
[10]A.G. Chynoweth, J. Appl. Phys. **27**, 78 (1956).
[11]S.K. Kurtz and T.T. Perry, J. Appl. Phys. **39**, 3798 (1968).
[12]A.M. Glass, M.E. Lines, M. Eibschutz, F.S.L. Hsu, and H.J. Guggenheim, Comments Phys. **2**, 103 (1977).
[13]S. Goshen, D. Mukamel, H. Shaked, and S. Shtrikman, Phys. Rev. B **2** 4679 (1970).

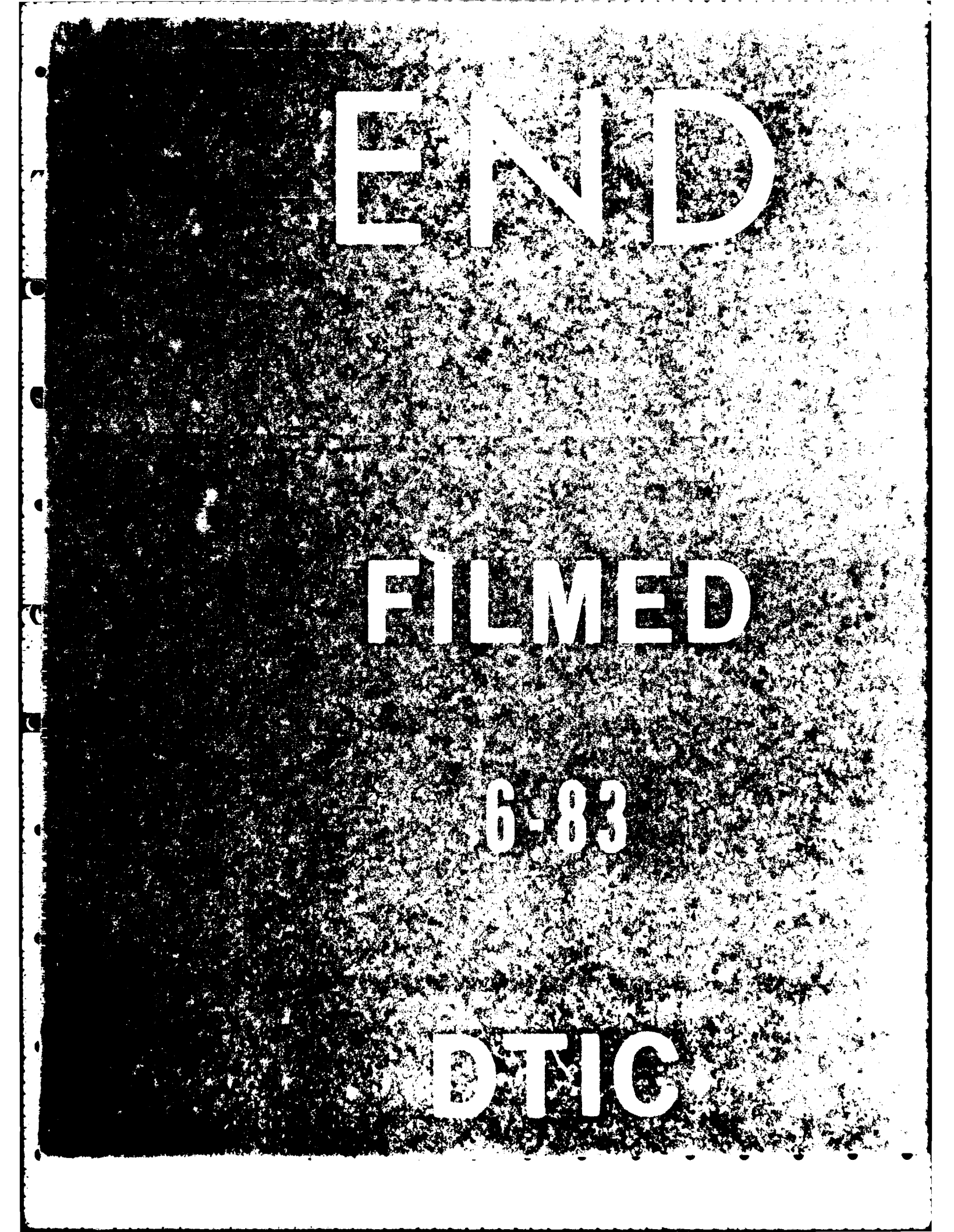
END
FILMED
6-83
DTIC